MOLECULAR STUDIES OF THE BIOLOGICAL AND

CATALYTIC ACTIVITIES OF RIBONUCLEASES

by

Peter A. Leland

A dissertation submitted in partial fulfillment

of the requirements for the degree of

Doctor of Philosophy

(Biochemistry)

at the

UNIVERSITY OF WISCONSIN–MADISON

2000

A dissertation entitled

Molecular Studies of the Biological and
Catalytic Activities of Ribonucleases

submitted to the Graduate School of the

University of Wisconsin-Madison

in partial fulfillment of the requirements for the

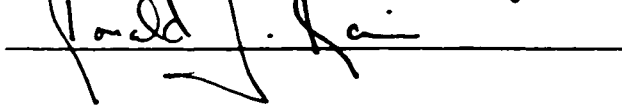degree of Doctor of Philosophy

by

Peter Andrew Leland

Date of Final Oral Examination: May 30, 2000

Month & Year Degree to be awarded: **December**　　　**May**　　　**August** 2000

* *

Approval Signatures of Dissertation Readers:　　**Signature, Dean of Graduate School**

Abstract

Bovine pancreatic ribonuclease A (RNase A) catalyzes cleavage of RNA. Homologs of RNase A effect diverse biological phenomena. Onconase™ (ONC), an amphibian ribonuclease, is a potent toxin to cancer cells. Angiogenin (ANG), a ribonuclease present in human plasma, promotes angiogenesis. The cytotoxic activity of ONC and the angiogenic activity of ANG depend on the enzymes' ribonucleolytic activity. This Dissertation describes factors that alter the ribonucleolytic activities, and consequently, the biological activities of ONC and ANG. Chapters Two and Three show that Ribonuclease Inhibitor (RI), a ubiquitous cytosolic protein, distinguishes ONC and other cytotoxic ribonucleases from their nontoxic homologs. Chapter Four shows that high conformational stability helps to preserve the catalytic activity of ONC within the cytosol and thereby contributes to its cytotoxicity. Chapter Five describes solution conditions, including pH and [Na^+], that affect the catalytic activity of ANG. Definition of the factors that influence ribonucleolytic activity offers insight into the molecular mechanisms ribonuclease biology.

Cytotoxic ribonucleases enter the cytosol, where they degrade RNA and cause cell death. RI binds to members of the RNase A superfamily with inhibition constants that span 10 orders of magnitude. RI plays an integral role in defining ribonuclease cytotoxicity. RNase A is not cytotoxic and binds RI with high affinity. ONC, in contrast, binds RI with low affinity. To disrupt the RI – RNase A interaction, RNase A residues that contact RI were replaced with arginine or aspartate. Replacing Gly88 with arginine or aspartate yields variants of

RNase A that retain catalytic activity in the presence of RI and are cytotoxic to a human cancer grown in culture.

Like RNase A, human pancreatic ribonuclease can be made cytotoxic by specifically decreasing its susceptibility to RI. ERDD hpRNase, which is the L86E/N88R/G89D/R91D variant, is shown to have 10^3-fold less affinity for RI than does wild-type hpRNase. Moreover, ERDD hpRNase is toxic to a human cancer grown in culture. Replacing Arg4 and Val118 of ERDD hpRNase with cysteine residues to form a fifth disulfide bond increases conformational stability, decreases affinity for RI, and (most significantly) increases cytotoxicity of the ERDD hpRNase variant. Because ERDD hpRNase is derived from a human protein, it is unlikely to cause an immune reaction if used as a cancer chemotherapeutic.

The conformational stability of ONC is remarkable—the midpoint of its thermal denaturation curve is 90 °C. ONC and its amphibian homologs have a C-terminal disulfide bond, which is absent in RNase A. Replacing this cystine with a pair of alanine residues decreases significantly the conformational stability of ONC. In addition, deletion of the C-terminal disulfide bond diminishes significantly the cytotoxicity of ONC.

The biological activity of ANG is dependent on its ribonucleolytic activity, which is several orders of magnitude lower than that of RNase A. Efficient heterologous production of ANG is achieved by replacing two sequences of rare codons with codons favored by *Escherichia coli*. Catalysis by ANG is dependent on the length of its substrates. When a substrate is extended from two nucleotides to four or six nucleotides, values of k_{cat}/K_M increase 5- or 12-fold, respectively. The ANG pH–rate profile is a classic bell-shaped curve,

with $pK_1 = 5.0$ and $pK_2 = 7.0$. Finally, the ribonucleolytic activity of ANG is sensitive to salt concentration—a 10-fold decrease in [Na^+] causes a 170-fold increase in the value of k_{cat}/K_M. Likewise, ANG binding to a tetranucleotide substrate analog is dependent on [Na^+]. These data provide a systematic evaluation of substrate binding and catalysis by ANG.

Acknowledgements

Although my name alone appears on the title page, this Dissertation is the product of many talented individuals. The students, technicians, and postdoctoral fellows in the Raines laboratory create an outstanding environment in which to conduct scientific research and are themselves outstanding sources of assistance. In particular, Dr. L. Wayne Schultz helped to design the cytotoxic ribonuclease A variants described in Chapter One. Dr. Byung-Moon Kim helped to create some of the ribonuclease variants described in Chapter Two, Chapter Three, and Chapter Four. Chiwook Park made significant contributions to the analysis of the angiogenin pH–rate and salt–rate profiles presented in Chapter 5. Kristine E. Staniszewski is a gifted undergraduate student, with whom I had the privilege to work with for the past two years. Ms. Staniszewski helped to collect data that appears in Chapter Three and Chapter Four. Tony A. Klink, Kenneth J. Woycechowsky, Marcia C. Haigis, Cara L. Jekins, Bradley R. Kelemen, Richele L. Abel, and Kimberly A. Dickson have willingly served as editors of this Dissertation.

Ronald T. Raines has served as an excellent advisor during my tenure in the Raines lab. His efforts guaranteed that the necessary resources – both physical and intellectual – were always available.

Finally, I thank my family for continually supporting my education. I must also thank my wife, Jill. Without her constant presence and her laughter, this work would not have been possible.

Table of Contents

Chapter Six

List of Figures

List of Tables

List of Abbreviations

A .... anisotropy

AcOH .... acetic acid

ANG .... human angiogenin

BisTris .... Bis[2-hydroxyethyl]iminotris[hydroxymethyl]methane

BS-RNase .... bovine seminal ribonuclease

CD .... circular dichroism

DEPC .... diethylpyrocarbonate

DTT .... dithiothreitol

EDTA .... ethylenediaminetetraacetic acid

F .... fluorescence

HEPES .... N-[2-hydroxyethyl]piperazine-N'-[4-butanesulfonic acid]

hpRNase .... human pancreatic ribonuclease

hRI .... human ribonuclease inhibitor

IPTG isopropyl-1-thio-β-D-galactopyranoside

MES .... 2-[N-morpholino]ethanesulphonic acid

*M*r .... relative molecular mass

OD .... optical density

ONC .... onconase

PBS .... Dulbecco's phosphate-buffered saline

PCR .... polymerase chain reaction

PMSF .... phenylmethanesulfonylfluoride

poly(C)..poly(cytidylic acid)

poly(U) ....poly(uridylic acid)

pRI ....porcine ribonuclease inhibitor

RI ....ribonuclease inhibitor

RNase A..bovine pancreatic ribonuclease A

SDS–PAGE ....sodium dodecyl sulfate–polyacrylamide gel electrophoresis

TB..terrific broth

Tris..tris(hydroxymethyl)aminomethane

T_m..midpoint of the thermal denaturation curve

UV ....ultraviolet

6-FAM 6-carboxyfluorescein

6-TAMRA 6-carboxytetramethylaminorhodamine

Chapter One

Introduction

Portions of this chapter will form a review solicited by *Chemistry & Biology*:

Leland, P. A., and Raines, R. T. (2000) Cancer chemotherapy: ribonucleases to the rescue. *Chemistry & Biology*.

Prelude. Bovine pancreatic Ribonuclease A (RNase A; EC 3.1.27.5) was perhaps the most studied enzyme of the 20th century. RNase A is the defining member of a superfamily of secretory enzymes that operate at the crossroads of transcription and translation by catalyzing RNA cleavage (Raines, 1998). Remarkably, homologs of RNase A use this singular enzymatic activity to effect diverse biological phenomena. Angiogenin is a plasma enzyme that promotes the growth of new blood vessels (Riordan, 1997). Onconase™ (ONC), an amphibian protein, is toxic to tumor cells *in vitro* and *in vivo* (Youle & D'Alessio, 1997).

The ensuing introduction reviews natural and engineered cytotoxic ribonucleases, as well as angiogenin. Chapter Two describes the role of the cytosolic ribonuclease inhibitor protein in defining ribonuclease cytotoxicity. In Chapter Three, hypotheses developed in Chapter Two are used to create a cytotoxic variant of human pancreatic ribonuclease. Chapter Four examines the contributions of a *C*-terminal disulfide bond to the conformational stability, ribonucleolytic activity, and cytotoxic activity of ONC. Together, Chapters Two, Three and Four offer a molecular description of the mechanisms of ribonuclease cytotoxicity and provide direction for engineering ribonucleases with specific and useful cytotoxic activity. Chapter Five describes an efficient system for the heterologous production of ANG in *E. coli* and characterizes in detail substrate binding and turnover by this ribonuclease. These results provide the foundation necessary to build a complete description of the molecular mechanism of angiogenesis by ANG.

Ribonuclease A. RNase A is secreted in large quantities by the bovine pancreas. Presumably, high concentrations of RNase A are necessary to digest the large amount of RNA produced by microorganisms residing in the rumen (Barnard, 1969). The *in vivo*

function of RNase A is likely enhanced by two exceptional features of the enzyme—high

catalytic activity and high conformational stability.

RNase A catalyzes the cleavage of the P–O$^{5'}$ bond of RNA 3' to pyrimidine nucleotides

(Raines, 1998; Raines, 1999). Catalysis occurs in two discrete steps: (A) fast

transphosphorylation to yield a 2',3'-cyclic phosphodiester, and (B) slow hydrolysis of the

cyclic phosphodiester to form a 3' phosphomonoester (Figure 1.1). RNase A is one of the

most efficient catalysts known—its k_{cat}/K_M values can reach 10^9 M^{-1}s^{-1} [1](Park & Raines,

2000b).

The tertiary structure of RNase A resembles a kidney (Figure 1.3) (Wlodawer *et al.*,

1988). The predominant elements of secondary structure include two antiparallel β-sheets

and three α-helices. The RNase A tertiary structure is stabilized by four disulfide bonds that

involve all eight of its cysteine residues (Figure 1.3). The RNase A tertiary structure is stable,

remaining intact in half of the molecules at 62 °C (Klink *et al.*, 2000). Moreover,

denaturation of RNase A is fully reversible (Anfinsen, 1973).

Ribonuclease Inhibitor. Remarkably, the most potent known inhibitor of RNase A, a

secreted enzyme, is a *cytosolic* protein. Ribonuclease inhibitor (RI) is a 50-kDa protein that

constitutes ≤0.01% of cytosolic protein in most mammalian cells (Lee & Vallee, 1993;

Hofsteenge, 1997). Homologous ribonuclease inhibitor proteins from porcine (pRI) and

human (hRI) have been described in detail. Both inhibitors contain 15 sequential leucine-rich

β–α repeats arranged in the shape of a horseshoe (Kobe & Deisenhofer, 1993). In addition,

---

[1] Values of k_{cat}/K_m reach 10^9 M^{-1}s^{-1} when RNase A catalysis is measured with a fluorogenic tetranucleotide substrate and Na$^+$ concentrations less than 0.02 M. Figure 5.3 includes data for RNase A catalyzed cleavage of this tetranucleotide substrate at several [Na$^+$]. Values of k_{cat}/K_m for RNase A catalyzed cleavage of polynucleotide substrates at [Na$^+$] ≥0.10 M are approximately 10^6 M^{-1}sec^{-1}, as described in Table 2.1.

pRI and hRI contain 30 and 32 cysteine residues, respectively. Oxidation of the ribonuclease inhibitor proteins is rapid and highly cooperative. When oxidized, the inhibitor does not bind to RNase A and is degraded rapidly by cellular proteases (Blázuez *et al.*, 1996).

pRI and hRI form a 1:1, noncovalent complex with RNase A (Figure 1.4). The K_d value for the pRI•RNase A complex is 6.7×10^{-14} M (Vicentini *et al.*, 1990). At 4.4×10^{-14} M, the K_d value for the hRI•RNase A complex is essentially indistinguishable from that of the pRI•RNase A complex (Lee *et al.*, 1989). In the crystalline pRI•RNase A complex, the RNase A active-site is centered on the inhibitor's *C*-terminus (Kobe & Deisenhofer, 1995; Kobe & Deisenhofer, 1996). Seven of the twelve RNase A residues that contribute to substrate binding or turnover participate in intermolecular contacts with the inhibitor. The four disulfide bonds of RNase A and the 30 reduced cysteine residues of pRI are preserved in the complex.

RI is a potent inhibitor of other mammalian pancreatic-type ribonucleases, including angiogenin and human pancreatic ribonuclease (Lee *et al.*, 1989; Boix *et al.*, 1996; Papageorgiou *et al.*, 1997). The action of RI is, however, class specific. RIs from amphibia and aves do not inhibit mammalian pancreatic-type ribonucleases (Roth, 1962).

The biological function of RI has yet to be defined rigorously (Hofsteenge, 1997). It is possible that this inhibitor preserves cellular RNA should a secretory ribonuclease inadvertently enter the cytosol. Simultaneously, RI may regulate the biological actions of ribonucleases such as angiogenin. Regardless of its function, the pronounced redox sensitivity of RI suggests an elegant means to control their *in vivo* action.

Onconase^{TM}. ONC is a 12-kDa homolog of RNase A present in the oocytes and early embryos of *Rana Pipiens* (Northern leopard frog) (Youle & D'Alessio, 1997; Irie *et al.*,

1998). ONC was discovered based on its pronounced antitumor activity and was immediately

recognized as a promising cancer chemotherapeutic agent (Darzynkiewicz *et al.*, 1988).

The amino acid sequence of ONC is approximately 30% identical to that of RNase A

(Figure 1.2) (Ardelt *et al.*, 1991). The tertiary structure of ONC is also similar to that of

RNase A (Figure 1.3) (Mosimann *et al.*, 1994). The prominent elements of secondary

structure described for RNase A are preserved in ONC, however, each is diminished in size.

Additionally, the surface loops in ONC differ dramatically from their RNase A counterparts.

The ONC tertiary structure is crosslinked by four disulfide bonds, three of which are

conserved in RNase A (Figure 1.3). The T_m of ONC is 90 °C, nearly 30 °C higher than that of

RNase A (Leland *et al.*, 1998). Unlike in RNase A, the *N*-terminus of ONC is blocked by a

pyroglutamyl residue, which is formed by the spontaneous cyclization of an *N*-terminal

glutamine residue.

Like RNase A, ONC catalyzes cleavage of the $P-O^{5'}$ bond of RNA 3' to pyrimidine

nucleotides. The principal catalytic residues of RNase A are conserved in ONC (Figure 1.2),

implying that RNase A and ONC catalyze RNA cleavage by identical mechanisms. Yet, the

catalytic activity of ONC is reported to be from one to five orders of magnitude lower than

that of RNase A (Ardelt *et al.*, 1991; Boix *et al.*, 1996; Leland *et al.*, 1998). In marked

contrast to RNase A, the catalytic activity of ONC is largely unaffected by RI. The value of

K_i for the interaction between RI and ONC is estimated at $\geq 10^{-6}$ M, a value more than 10^7-

fold greater than that measured for the RI•RNase A complex (Boix *et al.*, 1996).

ONC was first described as a cytostatic agent that arrests the cell cycle in the G1 phase

(Darzynkiewicz *et al.*, 1988; Juan *et al.*, 1998). Later, it was shown that ONC is also a

cytotoxic molecule (Wu *et al.*, 1993). The *in vitro* IC_{50} value for ONC cytotoxicity depends

on the type of cancer cell, but is commonly near 10^{-7} M. Proliferating cells are more susceptible to ONC than are quiescent cells (Smith *et al.*, 1999). Correspondingly, agents that increase the rate of cell proliferation potentiate ONC cytotoxicity and agents that decrease the rate of cell proliferation reduce ONC cytotoxicity. The IC_{50} values are lowered significantly when ONC is administered in combination with small-molecule chemotherapeutic agents, including tamoxifen, trifluoroperazine, cisplatin, lovostatin, and vincristine (Mikulski *et al.*, 1990b; Mikulski *et al.*, 1992; Rybak *et al.*, 1996). In addition to its anti-cancer activity, ONC has intriguing anti-viral properties. At 10^{-8} M, ONC inhibits HIV-1 replication in chronically infected human cells by degrading viral RNA (Youle *et al.*, 1994; Saxena *et al.*, 1996). Significantly, a 10^{-8} M dose of ONC does not kill the virally infected cell.

ONC is an effective chemotherapeutic agent in an animal model. In one study, tumor cells were injected into the intraperitoneal cavity of mice and treatment with ONC was initiated 24 h later (Mikulski *et al.*, 1990a). All treatment schedules increased significantly the median time to death, compared to that of untreated animals. Weekly injections of 40 μg/mouse yielded the greatest number of long-term survivors. In this test group, 6 of 18 mice survived for >220 days with no evidence for onset of disease. The most consistent side effect of ONC was weight loss, which increased in severity with the frequency and the size of the dose.

ONC has been tested in Phase I and Phase II human clinical trials for treatment of numerous solid tumors, including lung and pancreatic cancers (Mikulski *et al.*, 1993; Mikulski *et al.*, 1995). In these trials, ONC appeared to have a favorable impact on the median survival time of the patients. Despite being a foreign protein, ONC is well tolerated

by patients. Renal toxicity is dose limiting, but is reversible on discontinuation of treatment.

More recently ONC, in combination with tamoxifen, was tested in a Phase III trial for

treatment of patients with advanced pancreatic adenocarcinoma. This trial was discontinued

in 1998 because ONC did not offer a significant advantage compared to Gemzar® [2'-deoxy-

2'.2'-difluorocytidine monohydrochoride (β-isomer)]. The outcome of a Phase III trial for

treatment of malignant mesothelioma (an asbestos-related lung cancer) has yet to be made

public.

Rana catesbeiana and Rana japonica ribonucleases. ONC is not unique. Ribonucleases

with chemical and biological properties remarkably similar to those of ONC have been

isolated from the oocytes of *Rana catesbeiana* (bullfrog) and *Rana japonica* (Japanese rice

paddy frog) (Youle & D'Alessio, 1997; Irie *et al.*, 1998). The *R. catesbeiana* and *R. japonica*

ribonucleases share approximately 50% amino acid sequence identity with ONC (Figure 1.2)

(Titani *et al.*, 1987; Lewis *et al.*, 1989; Kamiya *et al.*, 1990). The solution structure of the

R. catesbeiana resembles the crystalline structure of ONC (Figure 1.3). Each of the four

disulfide bonds in *R. catesbeiana* have a counterpart in ONC (Figure 1.3). Also like ONC,

R. catesbeiana has unusually high conformational stability—its T_m is >75 °C. The tertiary

structure of the *R. japonica* ribonuclease has not been described. Still, the *R. japonica*

ribonuclease does retain the eight cysteine residues of ONC (Figure 1.2) and has high

conformational stability. The *R. catesbeiana* and *R. japonica* ribonucleases catalyze cleavage

of the P–O$^{5'}$ bond of RNA 3' to pyrimidine nucleotides. Significantly, the ribonucleolytic

activity of the *R. catesbeiana* ribonuclease is not inhibited by hRI (Nitta *et al.*, 1993). The

effect of hRI on the *R. japonica* ribonuclease is unknown.

The *R. catesbeiana* and the *R. japonica* ribonucleases are cytotoxic to various cancer cells *in vitro* with IC_{50} values of 10^{-7}–10^{-6} M. (Nitta *et al.*, 1994; Liao *et al.*, 1996). To study the therapeutic potential of the *R. catesbeiana* ribonuclease in an animal model, tumor cells were injected into intraperitoneal cavity of mice on day 0 (Nitta *et al.*, 1994). Daily intraperitoneal injections of the *R. catesbeiana* ribonuclease (0.5–2.0 mg/kg, initiated on day 1 and continued through day 10) increased significantly survival of the tumor-bearing mice compared to control animals. A single, high dose of the ribonuclease (10 mg/kg) given on day one was markedly less effective in prolonging survival. Similar to ONC, treatment with the *R. catesbeiana* ribonuclease caused weight loss in the test animals.

Molecular Mechanisms of Ribonuclease Cytotoxicity. As cytotoxins, ribonucleases are administered extracellularly. Yet, cytotoxic ribonucleases kill cancer cells by hydrolyzing RNA—a cytosolic molecule. Indeed, wild-type ribonucleolytic activity is necessary for the full cytotoxic activity of ONC (Wu *et al.*, 1993; Wu *et al.*, 1995; Boix *et al.*, 1996; Newton *et al.*, 1997) and the *R. catesbeiana* ribonuclease (Huang *et al.*, 1998). Although rRNA is degraded in cultured cells treated with ONC (Wu *et al.*, 1993), tRNA is degraded preferentially in a reticulocyte lysate (Lin *et al.*, 1994; Boix *et al.*, 1996). Nevertheless, it appears that cytotoxic ribonucleases cause cell death by destroying RNA. Because RI inhibits neither ONC nor the *R. catesbeiana* ribonuclease, the cell is left without means to prevent the destruction.

At present, it is unclear how an extracellular protein (with disulfide bonds) reaches the cytosol in a catalytically competent form. Limited, but intriguing preliminary data does suggest a route for cytotoxic ribonucleases.

The first requisite step in ribonuclease cytotoxicity is an interaction between the ribonuclease and the plasma membrane of the target cell (Figure 1.5). ONC binds to specific sites on the plasma membrane of cultured glioma cells with K_d values of 6.2×10^{-8} M and 2.5×10^{-7} M (Wu *et al.*, 1993). The receptors have not been identified. In addition, it is unclear if these receptors are intrinsic to glioma cells, or if ONC binds to other cancer cells by using the same interactions.

The cytotoxic ribonucleases from *R. catesbeiana* and *R. japonica* also bind specifically to the plasma membrane of cancer cells. Indeed, these enzymes were first identified as sialic acid-binding lectins that specifically agglutinate cancer cells (Sakakibara *et al.*, 1979; Nitta *et al.*, 1987; Okabe *et al.*, 1991). Interestingly, ONC does not cause tumor cell agglutination (Ardelt *et al.*, 1991). Cancer cell agglutination by the *R. catesbeiana* and the *R. japonica* ribonucleases is inhibited by sialoglycoproteins and gangliosides but is not blocked by monomeric sialic acid (Sakakibara *et al.*, 1979; Nitta *et al.*, 1987). Agglutination is also inhibited by nucleotides, indicating that the active-site residues contribute to at least one of the binding sites (Okabe *et al.*, 1991). Finally, pretreatment with sialidase protects tumor cells from both agglutination and cytotoxicity by the *R. catesbeiana* ribonuclease (Nitta *et al.*, 1987; Nitta *et al.*, 1994). Thus, it is likely that the same receptor renders cancer cells susceptible to agglutination and cytotoxicity by the *R. catesbeiana* and *R. japonica* ribonucleases.

Many research groups have manipulated the interactions between ribonucleases and the plasma membrane to create cytotoxic ribonucleases. RNase A, ONC, and their homologs have been linked to protein ligands that target them to the plasma membrane (Youle *et al.*, 1993; Rybak & Newton, 1999). The IC_{50} values for the toxicity of the targeted ribonucleases

to cancer cells approach nM. These fusion proteins are markedly less toxic to cells that do not express receptors for the targeting epitope.

RI susceptibility has been quantitated for few of the ribonuclease fusion proteins. In one notable exception (Suzuki *et al.*, 1999), transferrin was coupled to residue 89 of human pancreatic ribonuclease. Analogous to the G88R substitution in RNase A, transferrin sterically prevented RI from binding. In addition, transferrin targeted the conjugate to the surface of cells expressing the transferrin receptor. In the presence of retinoic acid (a small molecule that disrupts the Golgi apparatus), the ribonuclease–transferrin conjugate is toxic to cancer cells with an IC_{50} value of 2 nM.

Other ribonuclease fusions may be cytotoxic despite being sensitive to RI (Newton *et al.*, 1996). The targeting domain of the fusion enables receptor-mediated entry of the ribonuclease into the cell, which in turn may enhance accumulation of ribonucleolytic activity in the cytosol. If the cytosolic concentration is sufficiently high, the ribonuclease fusions may titrate RI, leaving ribonucleolytic activity unchecked in the cytosol. In this respect. ONC may be a double-edged sword—being internalized by a receptor-dependent process and not being inhibited by RI.

After binding to a plasma membrane receptor, ONC appears to reach the cytosol via endocytosis and subsequent retrograde transport through the secretory pathway (Figure 1.5). Metabolic inhibitors that block ATP synthesis also block ONC cytotoxicity (Wu *et al.*, 1993). This result is consistent with the hypothesis that ONC enters the cell by endocytosis, an energy-dependent process. Like retinoic acid, monensin is a small molecule that disrupts the Golgi apparatus. Both retinoic acid and monensin potentiate ONC cytotoxicity (Wu *et al.*, 1995), indicating that ONC is able to reach the cytosol more efficiently in cells with a

damaged a Golgi apparatus. It appears, however, that retinoic acid changes the intracellular routing of ONC. Brefeldin A stops both forward and retrograde vesicular transport between the endoplasmic reticulum and the Golgi apparatus. This drug blocks retinoic acid potentiation of ONC cytotoxicity, but does not affect ONC cytotoxicity in the absence of retinoic acid (Wu et al., 1995).

Cytotoxic ribonucleases face a topological problem. Regardless of their path through the cell, they must cross a lipid bilayer to reach the cytosol. The location and mechanism of bilayer transversal is unknown. Unlike many bacterial toxins, which have catalytic and translocation domains (Pelham et al., 1992; Montecucco et al., 1994), ONC and the other pancreatic-type ribonucleases are single-domain proteins. Moreover, these ribonucleases are highly charged proteins and contain multiple disulfide bonds. Thus, it seems unlikely that they could cross a lipid bilayer directly. In addition, it is unlikely that the cytotoxic ribonucleases cross the bilayer in a reduced and denatured state. Although the pancreatic-type ribonucleases refold readily, the reducing environment of the cytosol would disfavor oxidation of cysteines to reform the disulfide bonds. Because only very few molecules of a cytotoxic ribonuclease are required to kill a cell (Saxena et al., 1991), delineating the transbilayer movement of ribonucleases remains a formidable challenge.

Therapeutic Index of Cytotoxic Ribonucleases. In cell culture systems, animal models, and human trials the cytotoxic ribonucleases are far more toxic to cancerous cells than to non-cancerous cells. The basis for the therapeutic index of the cytotoxic ribonucleases is unknown. Changes to the plasma membrane—perhaps upregulation of a receptor—may increase the susceptibility of cancerous cells to cytotoxic ribonucleases. Indeed, the density of sialic acid-rich gangliosides is elevated in some types of cancers (Fredman, 1993; Lavie *et*

al., 1996). Alternatively, the cellular routing of ribonucleases may differ between cancerous

cells and their normal counterparts. Finally, due to their accelerated growth rate, cancerous

cells may be more sensitive to the integrity of their RNA than are non-cancerous cells.

Angiogenin. The unusual biological activities of ribonucleases are not limited to

cytotoxicity. Indeed, angiogenin (ANG), a 14.1-kDa homolog of RNase A present in human

plasma, causes angiogenesis, which is defined as the growth of new blood vessels from an

existing capillary network (Riordan, 1997). Angiogenesis is prevalent during development

and other physiological events such as ovulation. Pathological conditions that signal the

onset of angiogenesis include wounding, select immune reactions, and tumor formation

(Folkman & Klagsbrun, 1987). At present, the role of ANG in physiological and/or

pathological angiogenesis is unknown.

ANG and RNase A share 35% amino acid sequence identity (Figure 1.6) (Kurachi *et al.,* 1985;

Strydom *et al.,* 1985). ANG retains three of the four disulfide bonds present in RNase A

(Figure 1.7). The tertiary structures of ANG and RNase A can be superimposed with an overall rms

deviation of 2.26 Å (Figure 1.7) (Acharya *et al.,* 1994; Leonidas *et al.,* 1999).

The triad of residues most important for catalysis by RNase A (His12, Lys41, His119) are

conserved in ANG as His13, Lys40, and His114 (Figure 1.6). The ribonucleolytic activity of ANG is

reported to be 10^4- to 10^6-fold lower than that of RNase A, but nevertheless, is necessary for

angiogenic activity (Shapiro *et al.,* 1989; Shapiro & Vallee, 1989). Remarkably, the value of K_d for

the RI•ANG complex (K_d = 7.1 × 10^{-16} M) is lower than that of the RI•RNase A complex

(K_d = 4.4 × 10^{-14} M). (Lee *et al.,* 1989; Lee & Vallee, 1989; Papageorgiou *et al.,* 1997).

Significantly, RI is also a potent inhibitor of the biological activity of ANG in model systems

(Polakowski *et al.,* 1993).

Two features, in addition to ribonucleolytic activity, appear to be requisite for the biological activity of ANG. Residues 60-68 of ANG form a surface loop that mediates specific binding to endothelial cells (Figure 1.6) The plasma membrane receptor is unknown. Modification of residues 60-68 by proteolysis or by site-directed mutagenesis yields variants with severely diminished angiogenic activity (Hu et al., 1991), suggesting that the interaction between ANG and the cell membrane is necessary for angiogenesis.

ANG is endocytosed by subconfluent endothelial cells and is rapidly translocated to the nucleus. Because the nuclear import machinery is cytosolic, ANG must cross a lipid bilayer after endocytosis. Like that of the cytotoxic ribonucleases, the mechanism of transbilayer movement by ANG is unknown. Residues 31–35 (Arg-Arg-Arg-Gly-Leu) comprise the nuclear localization signal in ANG (Figure 1.6) (Moroianu & Riordan, 1994a). Significantly, the nuclear localization signal is buried in the RI•ANG complex (Papageorgiou et al., 1997). The R33A variant of ANG is not translocated to the nucleus and is not angiogenic (Moroianu & Riordan, 1994b), demonstrating that nuclear translocation is critical for that biological activity of ANG.

The molecular mechanisms of angiogenesis by ANG are unknown. It is intriguing that ANG and the cytotoxic ribonucleases have common features—specific interaction with the plasma membrane of a target cell, internalization and retrograde transport to the cytosol, and ribonucleolytic activity. But unlike the cytotoxic ribonucleases, ANG is extremely sensitive to inhibition by RI and is ultimately translocated to the nucleus of a target cell.

Prospectus. Both the cytotoxic ribonucleases and ANG represent novel therapeutics. A complete description of the molecular mechanisms of ribonuclease cytotoxicity, including the basis for the favorable therapeutic index, should facilitate their use as a cancer

chemotherapeutics. Likewise, definition of the molecular mechanisms of ANG may reveal

new methods to treat diseases caused by abnormal angiogenesis.

Figure 1.1   Mechanisms for RNA the transphosphorylation and hydrolysis reactions

catalyzed by pancreatic-type ribonucleases.

In reactions catalyzed by ribonuclease A, "B" is His-12 and "A" is His-119.
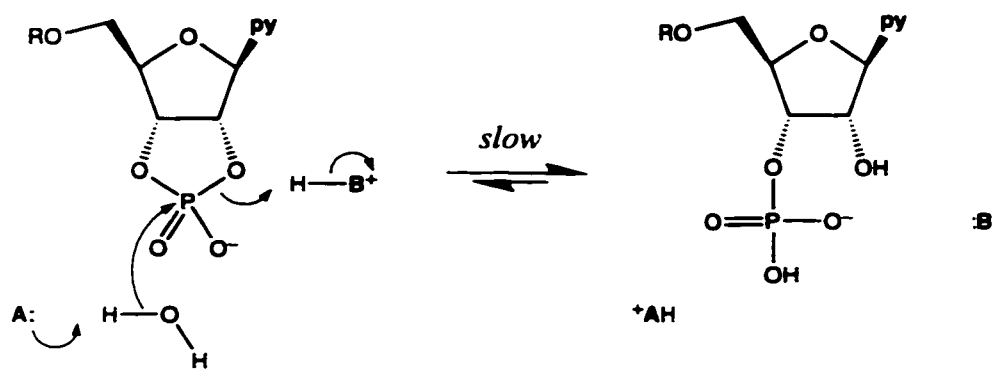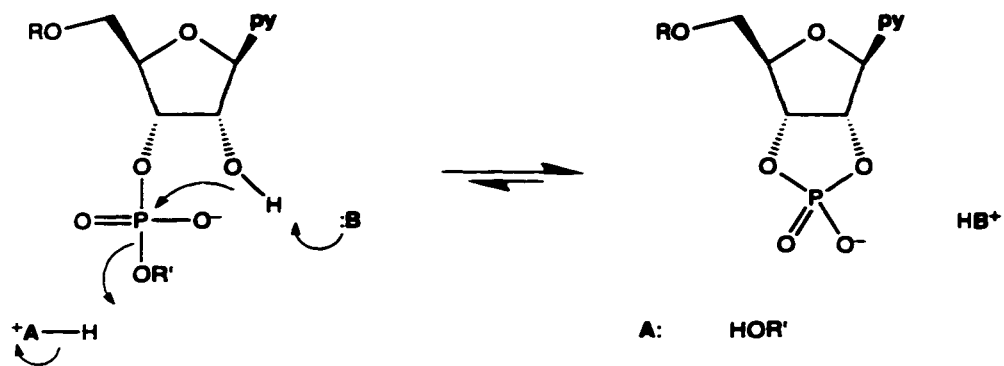
Figure 1.2   Amino acid sequences of bovine pancreatic ribonuclease A and three

cytotoxic homologs.

Sequences are aligned based on results obtained from the PILEUP program

(Genetics Computer Group—Version 10; Madison, WI) with a Gap Creation

Penalty of 8 and a Gap Extension Penalty of 2. Residues are numbered

according to ribonuclease A. Ribonuclease A residues that contact

ribonuclease inhibitor in the RI•RNase A complex are white on black. Boxes

are drawn around conserved residues. The three residues most important for

catalysis by ribonuclease A (His12, Lys41, His119), and the corresponding

residues in the cytotoxic homologs, are highlighted in blue. Cysteine residues

are highlighted in yellow.

```
                1              10                   20                  30                    40
RNase A          K E T A A A K F E R Q H M D S S T S A A S S S N Y C N Q M M - K S R N L T K D R C K P
Onconase         - - <E D W L T F Q K K H I T N T - - - - P I I N - C D N I M S T N L F - - - - H C K D
Rana catesbeiana - - <E N W A T F Q Q K H I I N T - - - - S S P N - C N T I M D N N I Y I V G G Q C K R
Rana japonica    - - <E N W A K F Q E K H I P N T - - - - S N I N - C N T I M D K S I Y I V G G Q C K E

                               50                   60                  70                    80
RNase A          V N T F V H E S L A D V Q A V C S Q K N V A C K N G Q T N C Y Q S Y S T M S I T D C R I
Onconase         K N T F I Y S R P E P V K A I C K G I I A S K N V L T T S E F Y - - - - - - - L S D C - -
Rana catesbeiana V N T F I I S S A T T V K A I C T G V - I N M N V L S T T R F Q - - - - - - - L N T C T R
Rana japonica    R N T F I I S S A T T V K A I C S G A S T N R N V L S T T R F Q - - - - - - - L N T C I R

                          90                 100                 110                   120     124
RNase A          T G S S K Y P N C A Y K T T Q A N K H I I V A C E G N P Y V P V H Q A S V - - - -
Onconase         - N V T S R P - C K Y K L K K S T N K F C V T C E N Q - - A P V F - V G V G S C -
Rana catesbeiana T S I T P R P - C P Y S S R T E T N Y I C V K C E N Q - - Y P V F - A G I G R C P
Rana japonica    S A T A P R P - C P Y N S R T E T N V I C V K C E N R - - L P V F - A G I G R C -
```
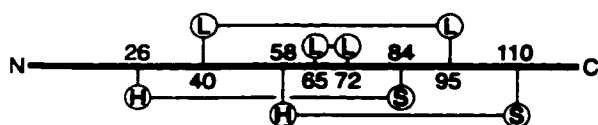
Figure 1.3   Structures of ribonuclease A, onconase, and the *Rana catesbeiana*

ribonuclease.

(A) Connectivity of the disulfide bonds in ribonuclease A, onconase, and the

Rana catesbeiana ribonuclease. The secondary structural context of the half-

cystines is indicated by H (helix), S (sheet), or L (loop). (B) Tertiary

structures of ribonuclease A, onconase, and the *Rana catesbeiana*

ribonuclease. Ribbon diagrams were created with the programs MOLSCRIPT

(Kraulis, 1991) and RASTER3D (Merritt & Murphy, 1994) using coordinates

derived from x-ray (Wlodawer *et al.*, 1988; Mosimann *et al.*, 1994) or NMR

analysis (Chang *et al.*, 1998).

Ribonuclease A
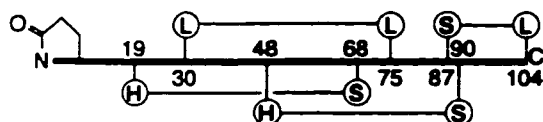
Onconase™
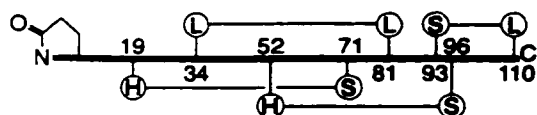
Rana catesbeiana Ribonuclease

Figure 1.4   Structure of the complex between porcine ribonuclease inhibitor (red) and

ribonuclease A (blue).

Ribbon diagrams were created with the programs MOLSCRIPT (Kraulis,

1991) and RASTER3D (Merritt & Murphy, 1994) by using coordinates derived

from x-ray analysis (Kobe & Deisenhofer, 1995).

RI
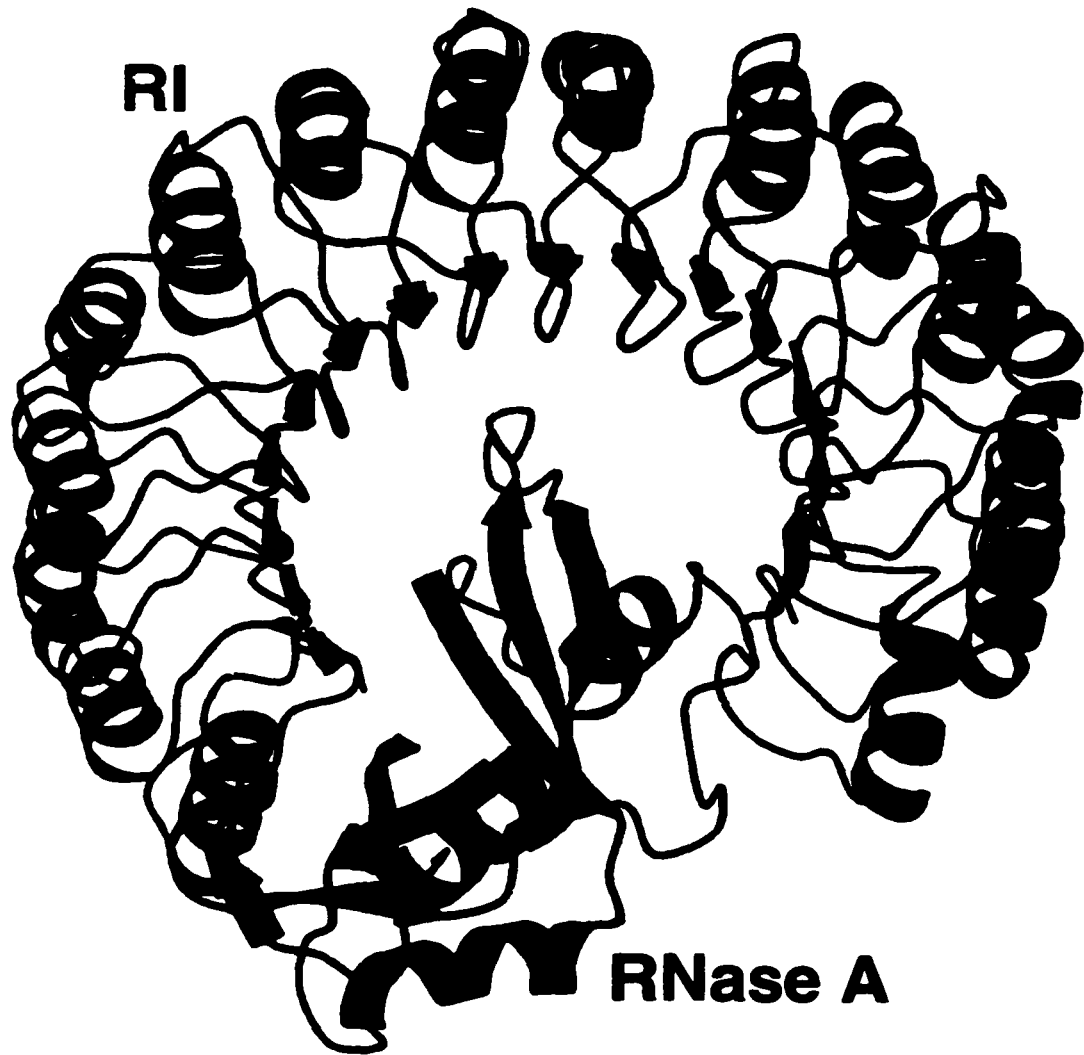
RNase A

Figure 1.5   Putative cellular routing of cytotoxic pancreatic-type ribonucleases.

(I) The ribonuclease first interacts with the surface of the target cell. Onconase

and the *Rana catesbeiana* and *Rana japonica* ribonucleases appear to bind

receptors on the plasma membrane. (II) The ribonuclease is internalized by

endocytosis and then travels retrograde through the Golgi apparatus. The

ribonuclease must cross a lipid bilayer to reach the cytosol. (III) In the cytosol,

ribonucleases interact with ribonuclease inhibitor. Ribonucleases that bind

tightly to ribonuclease inhibitor are inhibited. Ribonucleases that evade

ribonuclease inhibitor catalyze cleavage of cellular RNA and thereby cause

cell death.

I
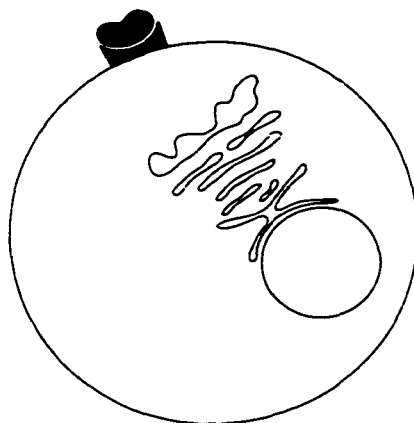
II
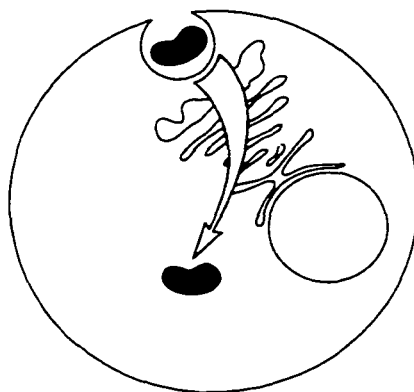
III
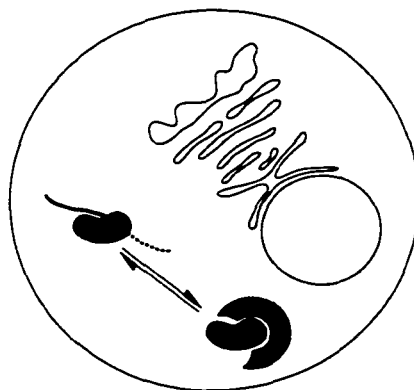
Figure 1.6   Amino acid sequences of ribonuclease A and human angiogenin.

The sequences are aligned by comparison of the structures of the crystalline

enzymes. Residues are numbered according to ribonuclease A. Residues that

contact ribonuclease inhibitor in the RI•RNase A complex or the RI•ANG

complex are white on black. Boxes are drawn around conserved residues.

Cysteine residues are highlighted in yellow. The nuclear localization signal in

angiogenin is highlighted in blue. The receptor recognition loop in angiogenin

is highlighted in green.

	1	10	20	30	40
RNase A *(Bos taurus)*	- K E T A A A K F E R Q H M D S S T S A A S S S N Y C N Q M M K S R N L T K D R C K P V N T
Angiogenin (human)	Q D N S R Y T H F L T Q H Y D - A K P Q G R D D R Y C E S I M R R R T - G I C K R I N T

	50	60	70	80
RNase A *(Bos taurus)*	F V H E S L A D V Q A V C S Q K N V A C K N G Q T - - N C Y Q - - - - - S Y S T M S I T D C
Angiogenin (human)	F I H G N K R S I K A I C - - E N - - - K N G - - - - N P H R E N L R I S K S S F Q V T T C

	90	100	110	120	124
RNase A *(Bos taurus)*	R E T G S S K - - Y P N C A Y K T T Q A N K H I I V A C E G N P Y V P V H F D A S V - - - -
Angiogenin (human)	K L H G G S P - - W P P C Q Y R A T A G F R N V V V A C E N G - - L P V H L D Q S I F R R P

26

Figure 1.7   Structures of ribonuclease A and angiogenin.

(A) Connectivity of the disulfide bonds in ribonuclease A and human

angiogenin. The secondary structural context of the half-cystines is indicated

by H (helix), S (sheet), or L (loop). (B) Tertiary structures of ribonuclease A,

and angiogenin. Ribbon diagrams were created with the programs

MOLSCRIPT (Kraulis, 1991) and RASTER3D (Merritt & Murphy, 1994) using

coordinates derived from x-ray analysis (Wlodawer *et al.*, 1988; Acharya *et*

al., 1995).
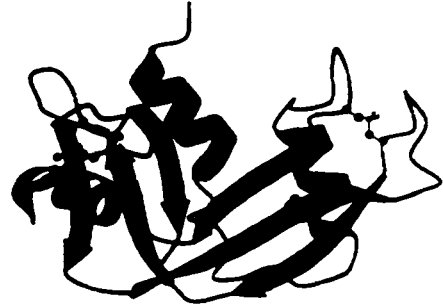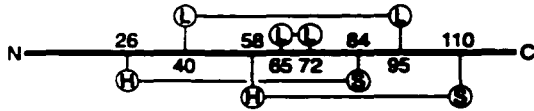
Ribonuclease A
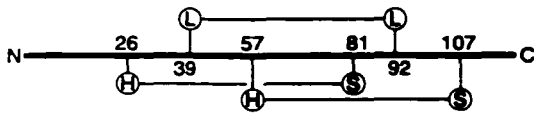
Angiogenin

Chapter Two

Ribonuclease A Variants with Potent Cytotoxic Activity

2.1 Abstract

Select members of the bovine pancreatic ribonuclease A (RNase A) superfamily are potent cytotoxins. These cytotoxic ribonucleases enter the cytosol, where they degrade cellular RNA and cause cell death. Ribonuclease inhibitor (RI), a cytosolic protein, binds to members of the RNase A superfamily with inhibition constants that span 10 orders of magnitude. Here, we show that the affinity of a ribonuclease for RI plays an integral role in defining the potency of a cytotoxic ribonuclease. RNase A is not cytotoxic and binds RI with high affinity. Onconase (ONC), a cytotoxic RNase A homolog, binds RI with low affinity. To disrupt the RI – RNase A interaction, three RNase A residues (Asp38, Gly88, and Ala109) that form multiple contacts with RI were replaced with arginine. Replacing Asp38 and Ala109 with an arginine residue has no effect on the RI – RNase interaction. In addition, these variants are not cytotoxic. In contrast, replacing Gly88 with an arginine residue yields a ribonuclease (G88R RNase A) that retains catalytic activity in the presence of RI and is cytotoxic to a transformed cell line. Replacing Gly88 with aspartate also yields a ribonuclease (G88D RNase A) with a decreased affinity for RI and cytotoxic activity. The cytotoxic potency of ONC, G88R RNase A, and G88D RNase A correlate with RI evasion. We conclude that ribonucleases that retain catalytic activity in the presence of RI are cytotoxins. This finding portends the development of a new class of chemotherapeutic agents based on pancreatic ribonucleases.

2.2 Introduction

Bovine pancreatic ribonuclease A (RNase A; EC 3.1.27.5) catalyzes the cleavage of RNA (Raines. 1998). Select homologs of RNase A use this enzymatic activity to effect diverse biological phenomena. Angiogenin (ANG) promotes the growth of new blood vessels (Riordan, 1997). Bovine seminal ribonuclease (BS-RNase) displays immunosuppressive. embryotoxic, aspermatogenic, and antitumor activities (D'Alessio *et al.*, 1997). Onconase (ONC). a ribonuclease from the oocytes and early embryos of the Northern leopard frog (*Rana pipiens*), is a potent toxin to several transformed cell lines (Youle & D'Alessio, 1997). Significantly. the biological activities of ANG, BS-RNase, and ONC are strictly dependent on their ribonucleolytic activity. Though an efficient catalyst of RNA cleavage, RNase A does not display any pronounced biological action.

Members of the RNase A superfamily have divergent amino acid sequences but similar tertiary structures. The amino acid sequences of BS-RNase A and RNase A, which are from the same species. are 80% identical (Suzuki *et al.*, 1987). ONC and human ANG, however, share only 30% and 33% amino acid identity with RNase A (Fett *et al.*, 1985; Ardelt *et al.*, 1991). The majority of nonconserved residues are in surface loops, which appear to play a significant role in the special biological activities of ANG, BS-RNase, and ONC (Kim *et al.*, 1995c; Raines *et al.*, 1995). The three-dimensional structure of the pancreatic-type ribonucleases is comprised of a central 4-stranded anti-parallel β-sheet, flanked by two α-helices. The active site is located in a cleft defined by a third, N-terminal α-helix and one edge of the β-sheet. This tertiary structure is stabilized by 3 or 4 disulfide bonds.

Ribonuclease inhibitor (RI) is a 50-kDa protein that constitutes ~0.01% of the cytosolic

protein in mammalian cells (Blackburn & Moore, 1982; Lee & Vallee, 1993; Hofsteenge,

1997). Mammalian RIs are highly conserved. For example, porcine RI (pRI) and human RI

(hRI) share 77% amino acid sequence identity, with no insertions or deletions except for a 4-

residue extension on the N-terminus of hRI. Both inhibitors contain 15 leucine-rich, $\beta - \alpha$

repeat units arranged symmetrically in a horseshoe. The β-strands form a solvent-exposed β-

sheet that defines the inner circumference of RI. The α-helices define the outer surface of the

inhibitor (Kobe & Deisenhofer, 1993). RI forms a 1:1, noncovalent complex with target

ribonucleases, including RNase A (Lee et al., 1989; Vicentini et al., 1990) and ANG (Lee et

al., 1989). Values of the inhibition constant (K_i) are in the fM range. The unusually low K_i

values are a consequence of an association rate constant (k_{on}) close to the diffusion limit and

a dissociation rate constant (k_{off}) near 10^{-7} s^{-1} (Lee et al., 1989; Lee & Vallee, 1989; Vicentini

et al., 1990).

Atomic details of RI – ribonuclease interactions are apparent from the three-dimensional

structures of the crystalline pRI•RNase A and hRI•ANG complexes (Kabsch, 1988; Kobe &

Deisenhofer, 1995; Kobe & Deisenhofer, 1996; Papageorgiou et al., 1997). To a first

approximation, the two structures are similar. In both, one-third of the ribonuclease rests

within the RI horseshoe and the remainder extends out of the plane defined by the inhibitor

(Figure 2.1). This arrangement centers each enzyme's active site on the C-terminus of the

inhibitor. The intermolecular contacts in the RI•ribonuclease complexes differ significantly,

but this heterogenety is due largely to the low sequence identity between RNase A and ANG.

The inhibitory activity of RI is manifested in the cytosol. This location provides the

reducing environment that is necessary to maintain RI activity. Mammalian RIs contain 30 or

32 reduced cysteine residues (Kawanomoto *et al.*, 1992). Oxidation of a single cysteine residue causes rapid oxidation of the remaining cysteine residues and consequent inactivation of RI (Blázuez *et al.*, 1996). All known RI ligands, including RNase A, are secreted ribonucleases. This observation and the cytosolic localization of RI supports the hypothesis that the inhibitor functions to preserve the integrity of cellular RNA should a secretory ribonuclease inadvertently reach the cytosol (Lee & Vallee, 1993; Wu *et al.*, 1993; Hofsteenge, 1997).

The protection offered to cells by RI is limited. The cytotoxic activities of BS-RNase and ONC appear to be a consequence of their abilities to escape inactivation by RI. BS-RNase is isolated as a homodimer, covalently linked by two disulfide bonds. As a dimer, BS-RNase is not inhibited by RI and is cytotoxic. RI becomes a potent inhibitor when BS-RNase is reduced to its monomeric form (Murthy & Sirdeshmukh, 1992; Cafaro *et al.*, 1995; Kim *et al.*, 1995b; Murthy *et al.*, 1996). Though monomeric, ONC also evades tight binding by RI (Boix *et al.*, 1996). ONC retains the elements of tertiary structure that characterize pancreatic-type ribonucleases, but its surface loops are truncated severely compared to their counterparts in RNase A and ANG. Further, the majority of RNase A and ANG residues that contact RI are replaced by dissimilar residues in ONC.

We have investigated directly the relationship between RI inhibition of ribonucleases and ribonuclease cytotoxicity. Specifically, we reasoned that RNase A could be endowed with a cytotoxic activity by specifically decreasing its susceptibility to inactivation by RI. We created two RI-evasive RNase A variants by incorporating amino acid residues that introduce steric and electrostatic strain into the RI•RNase A complex. As anticipated, these variants are

toxic to a transformed cell line. Our data indicate that ribonuclease cytotoxicity is a direct

consequence of an enzyme's ability to overcome inhibition by RI.

2.3 Experimental Procedures

Materials. *Escherichia coli* strain BL21(DE3) and the pET22b(+) expression vector were

from Novagen (Madison, WI). K-562 cells were from the American Type Culture Collection

(Rockville. MD). Enzymes used for DNA manipulation were from Promega (Madison, WI)

or New England Biolabs (Beverly, MA). Ribosomal RNA (16S and 23S) was from

Boehringer Mannheim (Indianapolis, IN). Poly(C) was from Midland Reagent (Midland,

TX). [Methyl-^{3}H]thymidine (6.7 Ci/mmol) was from DuPont NEN (Boston, MA). All other

chemicals and reagents were of commercial reagent grade or better, and were used without

further purification.

DNA oligonucleotides for DNA sequencing and site-directed mutagenesis were from

Integrated DNA Technologies (Coralville, IA). Reagents for DNA sequencing, including

AmpliTaq DNA polymerase, FS, were from Applied Biosystems (Foster City, CA). DNA

was sequenced by using an Applied Biosystems Automated DNA Sequencer at the university

Biotechnology Center.

Terrific broth (TB) medium contained (in 1 L) Bacto tryptone (12 g; Difco; Detroit, MI),

Bacto yeast extract (24 g; Difco), glycerol (4 mL), KH_2PO_4 (2.31 g), and K_2HPO_4 (12.54 g).

TB medium was prepared in distilled, deionized water and autoclaved. RPMI 1640 medium,

fetal bovine serum, and penicillin-streptomycin were from Life Technologies (Gaithersburg,

MD). PBS contained (in 1 L) KCl (0.20 g), KH$_2$PO$_4$ (0.20 g), NaCl (8.0 g), and Na$_2$HPO$_4$•7H$_2$O (2.16 g).

Ultraviolet absorbance measurements were made on a Cary Model 3 spectrophotometer (Varian; Palo Alto, CA) equipped with a Cary temperature controller. Circular dichroism (CD) spectra were collected on an Aviv Model 62A DS circular dichroism spectrophotometer (Lakewood, NJ) equipped with an Aviv temperature controller.

Design of Ribonuclease Variants. Our goal was to alter RNase A so as to perturb (only) its interaction with RI. We selected target residues in RNase A based on the following criteria. First, the residue must either form a hydrogen bond with RI or make van der Waals contacts (<4 Å) with RI, as defined in the structure of the crystalline pRI•RNase A complex [Figure 2.1; (Kobe & Deisenhofer, 1995; Kobe & Deisenhofer, 1996)]. Due to the high sequence identity between pRI and hRI, it is likely that such contacts are preserved in the hRI•RNase A complex. Second, the target residues must not be in the RNase A active site. Ribonucleolytic activity is requisite for ribonuclease cytotoxicity (Ardelt *et al.*, 1991; Kim *et al.*, 1995a). Consequently, any amino acid change that diminishes catalytic activity is likely to also reduce cytotoxicity. Third, the target residues must be solvent exposed and confined to the surface loops of RNase A. Substitutions in the enzymic core could decrease the stability of the native three-dimensional structure. From this analysis, three RNase A target residues were selected (Figure 2.1):

- **Asp38** forms a salt bridge with Arg453 of pRI. In addition, Asp38 makes van der Waals contacts with Ile455 of pRI.

- **Gly88** lies within a hydrophobic region of pRI defined by Trp257, Trp259 and

  Trp314 (Figure 2.1). Gly88 makes one atom-to-atom contact with Trp257 and

  six atom-to-atom contacts with Trp259.

- **Ala109** contributes to a hydrophobic pocket that is occupied by Tyr433 of pRI.

  The residues make two atom-to-atom contacts in the pRI•RNase A crystal

  structure.

Initially, we replaced target residues in RNase A with arginine to yield D38R RNase A,

G88R RNase A, and A109R RNase A. The arginine side chain is the second largest (van der

Waals volume: 148 Å^3) and most polar of all amino acid side chains (Radzicka &

Wolfenden, 1988). Its δ-guanido group is hydrated extensively when exposed to solvent, and

this hydration shell increases significantly the effective size of the side chain. Thus, to form

the inhibitor•enzyme complex, RI must accommodate the polarity and size of the arginine

side chain. In an attempt to perturb further the interaction with RI, we combined the changes

in single variants to yield two double variants: D38R/G88R RNase A and

G88R/A109R RNase A.

We also replaced Gly88 with an aspartate residue to yield G88D RNase A. The aspartate

side chain is the second most polar amino acid side chain (Radzicka & Wolfenden, 1988).

Like the δ-guanido group of arginine, the β-carboxylate group of aspartate is hydrated

extensively when solvent exposed. In contrast to arginine, the aspartate side chain is anionic

and small (van der Waals volume: 91 Å^3).

Finally, we replaced Trp264 of hRI with an alanine residue. As first proposed by Crick

(Crick, 1952), receptor − ligand interactions can resemble 'knobs-into-holes'. Trp264 is

homologous to Trp259 of pRI, and is in the hydrophobic pocket that surrounds Gly88 in the

RI•RNase A complex (Figure 2.1). By making the W264A variant of hRI, we created a

'hole' that could better accommodate an RNase A variant with a 'knob' at position 88. The

relative ability of W264A hRI to inhibit G88R RNase A and G88D RNase A could thus

provide new information on the RI•RNase A complex.

Production of Ribonucleases. Plasmid pBXR (delCardayré *et al.*, 1995) directs the

expression of RNase A in *E. coli.* Oligonucleotide-mediated site-directed mutagenesis

(Kunkel *et al.*, 1987) of plasmid pBXR was used to replace Asp38, Gly88, and Ala109 with

arginine residues, and to replace Gly88 with an aspartate residue.

A cDNA that codes for Met(−1)/M23L ONC was a generous gift of R. J. Youle (Boix *et*

al., 1996). This cDNA was modified to produce ONC that is identical to the native protein

isolated from frog. The ONC cDNA was amplified with the PCR such that the product has a

5' blunt end and a 3' *Sal*I site downstream from the termination codon. The PCR product was

inserted into pET22B(+) using the *Msc*I and *Sal*I sites. Site-directed mutagenesis was used to

restore the methionine residue at position 23. The resulting plasmid, pONC, carries a cDNA

coding for the wild-type ONC in frame with the pelB signal sequence.

The RNase A variants and ONC were produced and purified by methods described

previously (Kim & Raines, 1993a), with the following modifications. A culture of *E. coli*

strain BL21(DE3), transformed with the appropriate plasmid, was grown to an OD of 1.6 −

2.0 at 600 nm in TB medium. Expression was induced by the addition (to 0.5 mM) of IPTG,

and cells were collected 3 − 4 h after induction. Following cell lysis with a French pressure

cell, inclusion bodies were recovered by centrifugation and resuspended in a solution of 20

mM Tris-HCl buffer, pH 8.0, containing guanidine-HCl (7 M), DTT (10 mM), and EDTA

(10 mM). The inclusion bodies were solubilized and denatured by stirring at room

temperature under $N_2(g)$ for 2 h. The protein solution was then diluted 10-fold with 20 mM

AcOH, centrifuged to remove precipitant, and dialyzed overnight versus 20 mM AcOH.

Material that precipitated during dialysis was removed by centrifugation. Refolding of

RNase A and ONC was initiated by diluting the supernatant rapidly to a protein

concentration of ~0.5 mg/ml in 0.10 M Tris-AcOH buffer, pH 8.0, containing NaCl (0.10 M),

reduced glutathione (3.0 mM), and oxidized glutathione (0.6 mM). D38R RNase A,

G88R RNase A, G88D RNase A, A109R RNase A, D38R/G88R RNase A, and

G88R/A109R RNase A were refolded by rapid dilution to a protein concentration of

~0.25 mg/mL in 0.10 M Tris-AcOH buffer, pH 8.0, containing L-arginine (0.5 M; to prevent

protein aggregation), reduced glutathione (3.0 mM), and oxidized glutathione (0.6 mM) at 10

°C. Samples were concentrated by ultrafiltration with a YM10 membrane (10,000 M_r cut-off;

Amicon: Beverly, MA) and applied to a Superdex G-75 gel filtration FPLC column

(Pharmacia: Uppsala, Sweden) in 50 mM sodium acetate buffer, pH 5.0, containing NaCl

(0.10 M) and NaN_3 (0.02% w/v). Protein from the major peak was collected, concentrated by

ultrafiltration, dialyzed versus 50 mM HEPES-HCl buffer, pH 8.0, and applied to a Mono S

cation exchange FPLC column (Pharmacia). Ribonucleases were eluted from the column

with a linear gradient of NaCl (0.2 − 0.4 M) in 50 mM HEPES-HCl buffer, pH 8.0. Protein

concentrations were determined by UV spectroscopy using with extinction coefficients of ε_{278}

= 0.72 mg ml^{-1} cm^{-1} for RNase A (Sela *et al.*, 1957) and its variants and ε_{280} = 0.87 mg ml^{-1}

cm^{-1} for ONC. The extinction coefficient for ONC was calculated with the method of Pace

and coworkers (Pace *et al.*, 1995).

Production of Ribonuclease Inhibitor. A cDNA that codes for hRI was a generous gift of

Promega (Madison, WI). This cDNA was inserted into the pET22b(+) expression vector

between the *EcoRI* and *SphI* sites to give plasmid pET–RI. Oligonucleotide-mediated site-directed mutagenesis (Kunkel *et al.*, 1987) of plasmid pET–RI was used to replace Trp264 with an alanine residue. A culture of *E. coli* strain BL21(DE3), transformed with the appropriate plasmid, was grown in TB medium to *OD* of 1.0 at 600 nm. Expression was then induced by the addition (to 0.5 mM) of IPTG. After an additional 4 h of growth, cells were collected by centrifugation and resuspended in 10 mM potassium phosphate buffer, pH 7.5, containing NaCl (0.15 M), EDTA (1 mM), PMSF (1 mM), and DTT (10 mM). Cells were lysed by two passes through a French pressure cell. Insoluble debris was removed by centrifugation. The remaining steps of the purification, including RNase A–affinity chromatography, were performed as described (Blackburn, 1979; Lee *et al.*, 1989). Following elution from the RNase A–affinity column, the hRI was transferred by ultrafiltration to 0.10 M MES-NaOH buffer, pH 6.0, containing NaCl (0.10 M), and DTT (10 mM). The resulting solution was stored in a sealed vial at 4 °C. The molar concentration of active wild-type hRI or W264A hRI was measured by titration against a known concentration of RNase A (Neumann & Hofsteenge, 1994), with remaining ribonucleolytic activity monitored using poly(C) as a substrate (*vide infra*).

Conformational Stability Assays. Because cytotoxicity is assessed by prolonged incubation of ribonucleases at physiological temperature, it is important to establish that the RNase A variants retain adequate conformational stability. Conformational stabilities of the variants were measured by monitoring the change in absorbance at 287 nm (A_{287}) with increasing temperature (Eberhardt *et al.*, 1996). The temperature of the ribonuclease solutions (0.1 – 0.2 mg/ml in PBS) was increased from 25 °C to 80 °C in 1-°C increments. The A_{287} was recorded following a 6-min equilibration at each temperature.

Attempting to measure the conformational stability of ONC with UV spectroscopy

yielded uninterpretable thermal denaturation curves. Consequently, the conformational

stability of ONC was determined by using CD spectroscopy to monitor the change in molar

ellipticity at 204 nM ($[\Theta]_{204}$)with increasing temperature. The temperature of an ONC

solution (0.2 mg/ml in PBS) was increased from 50 °C to 104 °C in 2-°C increments. The

$[\Theta]_{204}$ was recorded following a 2.5-min equilibration at each temperature.

UV and CD data were fitted to a two-state model for denaturation, and these fits were

used to determine values of T_m.

Ribonuclease Inhibitor Binding Assays. The RNase A variants were screened initially for

ribonucleolytic activity in the presence of hRI using an agarose gel-based assay (Wu *et al.*,

1993; Matousek *et al.*, 1997). Briefly, 10 ng of ribonuclease was added to a reaction mixture

containing 50 mM Tris-HCl buffer, pH 7.4, containing DTT (10 mM), 16S- and 23S-rRNA

(4 µg), and recombinant wild-type hRI (0, 20, or 40 units, where one unit of hRI is defined as

the amount of hRI required to inhibit the ribonucleolytic activity of 5 ng of RNase A by

50%). Each mixture (10 µL) was incubated for 10 min at 37 °C. The assays were then

stopped by the addition of 2 µL of loading buffer [which was 10 mM Tris-HCl buffer, pH

7.5, containing EDTA (50 mM), glycerol (30% v/v), xylene cyanol FF (0.25% w/v), and

bromphenol blue (0.25% w/v)] and subjected to electrophoresis through a NuSieve agarose

gel (1.5% w/v) containing ethidium bromide (0.4 µg/mL). This same assay was performed

with W254A hRI (20 units).

Values of K_i for the hRI•G88R RNase A and the hRI•G88D RNase A interactions were

determined by measuring the steady-state rate of poly(C) cleavage in the presence of hRI.

Reactions were performed at 25 °C in MES-NaOH buffer, pH 6.0, containing NaCl (0.10 M),

enzyme (50 pM) and poly(C) (61 – 69 μM). Eight hRI concentrations (25 pM – 2.5 nM) were

used to determine the value of $K_i' = K_i(1 + S/K_m)$, the apparent inhibition constant for the

hRI•G88R RNase A complex. Seven hRI concentrations (49 pM – 0.49 nM) were used to

determine the value of K_i' for the hRI•G88D RNase A complex. Values of K_i' were calculated

by fitting steady-state rates to an equation that describes tight-binding inhibitors (Stone &

Hofsteenge. 1986):

$$v_s = \left(\frac{v_o}{2E_t}\right)\left\{\left[\left(K_i' + x - E_t\right)^2 + 4K_i'E_t\right]^{1/2} - \left(K_i' + x - E_t\right)\right\} \tag{2.1}$$

where v_o is the rate of poly(C) cleavage in the absence of RI, v_s is the steady-state rate. x is

the concentration of active hRI, and E_t is the concentration of ribonuclease.

Steady-State Kinetics Assays. Polymeric RNA is hypochromic. The ability of a

ribonuclease to catalyze the cleavage of poly(C) ($\varepsilon = 6200$ $M^{-1}cm^{-1}$ per nucleotide at 268 nm)

was monitored by the increase in UV absorption ($\Delta\varepsilon = 2380$ $M^{-1}cm^{-1}$ at 250 nm) (delCardayré

& Raines, 1994). Assays were performed at 25 °C in 0.10 M MES-NaOH buffer, pH 6.0,

containing NaCl (0.10 M), poly(C) (5 μM to 1.5 mM), and enzyme (2.5 nM for an RNase A

variant: 1.5 μM for ONC). Initial velocity data were used to calculate values of k_{cat} and k_{cat}/K_m

with the program HYPERO (Cleland, 1979).

Cytotoxicity Assays. Cytotoxicity assays were conducted with K-562 cells, which are

from a continuous human erythroleukemia line. K-562 cells were maintained at 37 °C in a

humidified atmosphere containing CO_2 (g; 5% v/v). Culture medium was RPMI 1640

supplemented with fetal bovine serum (10% v/v), penicillin (100 units/mL), and

streptomycin (100 µg/ml). Cytotoxicity was evaluated by measuring [methyl-^{3}H]thymidine

incorporation into newly synthesized DNA, as described previously (Kim et al., 1995b; Kim

et al., 1995c; Kim et al., 1995a; Matousek et al., 1997). Briefly, aliquots (95 µL) of cultured

K-562 cells (5 × 10^4 cells/mL) were placed in a microtiterplate, and sterile solutions (5 µL) of

ribonucleases in PBS were added to the aliquots. (Concentrated ribonuclease solutions were

sterilized by passage through a 0.45 micron acetate membrane syringe-tip filter. UV

spectroscopy was used to confirm that filtration did not change significantly the

concentration of the ribonuclease solutions.) Cells were incubated in the presence of

ribonucleases for 44 h, followed by a 4-h pulse with [methyl-^{3}H]thymidine (0.20 µCi per

well). Cells were then harvested onto glass fiber filters using a PHD cell harvester

(Cambridge Technology; Watertown, MA) and lysed by the passage of several mL of water

through the filters. DNA and other cellular macromolecules are retained by the filter; small

molecules, including unincorporated label, pass through the filters. After washing extensively

with water, the filters were dried with methanol and counted using a liquid scintillation

counter. Results from the cytotoxicity assays were expressed as the percentage of [methyl-

^{3}H]thymidine incorporated into the DNA of PBS-treated control cells. Data represent the

average of triplicate samples within an individual assay. All cytotoxicity assays were

repeated at least three times.

To assess the nature of cell death caused by the cytotoxic ribonucleases, K-562 cells

(1 × 10^5 cells/mL) were incubated with RNase A (50 µM), ONC (10 µM), or G88R RNase A

(50 µM) for 48 h, recovered by centrifugation, resuspended in 50 µL of PBS, and stained

with DAPI (4′,6-diamidino-2-phenylindole, dihydrochloride; 0.02 µg/µL final

concentration). DAPI appears to bind preferentially to adenine, thymine clusters in the minor groove of DNA. Samples were added to a microscope slide and visualized with a Zeiss Axioskop fluorescence microscope equipped with a digital camera.

2.4 Results

Ribonucleases and Ribonuclease Inhibitor. RNase A, the RNase A variants, and ONC were produced in *E. coli*. Following purification, each ribonuclease migrated as a single species of the appropriate M_r during SDS-PAGE (data not shown), indicating that the pelB signal sequence had been removed by endogenous *E. coli* proteases. Wild-type RNase A, G88R RNase A, and G88D RNase A had identical CD spectra (data not shown), suggesting that they had a similar tertiary structure. Previous studies had demonstrated that our purification scheme effectively removes all endotoxin from ribonuclease preparations (Raines *et al.*, 1995). The isolated yields for all ribonucleases were 5 – 50 mg per L of *E. coli* culture.

ONC isolated from frog oocytes has an N-terminal pyroglutamyl residue that contributes to the structure of its active site (Mosimann *et al.*, 1994). This N-terminal pyroglutamyl residue is produced by the spontaneous cyclization of an N-terminal glutamine residue. If ONC is produced with an N-terminal methionine residue [Met(−1)], then Gln1 cannot to cyclize to form a pyroglutamate. The resulting protein [Met(−1) ONC] retains only 2% of the ribonucleolytic activity of ONC and is ineffective as a cytotoxin, despite being folded properly (Mikulski *et al.*, 1993). To overcome this limitation, a cDNA that codes for ONC was fused in frame with the pelB signal sequence. As listed in Table 2.1, catalysis of poly(C) cleavage by this recombinant ONC occurred with steady-state kinetic parameters nearly

identical to those reported for ONC isolated from frog oocytes (Boix *et al.*, 1996). This result

suggests that, following removal of the pelB signal sequence, Gln1 did cyclize to form a

pyroglutamyl residue and that the ONC described herein is identical to ONC from frog

oocytes.

Wild-type hRI and W264A hRI were produced in *E. coli*. Following purification, each

hRI migrated as a single species of the appropriate M_r during SDS–PAGE (data not shown).

The inhibitory activities of the purified hRIs was quantitated by titrating a sample of

RNase A with the inhibitor and recording remaining enzymatic activity. The isolated yields

for the two hRIs were ~1.2 mg (2.6 nmol) per 4 L of *E. coli* culture.

Conformational Stability. To effect a cytotoxic response, either in cell culture or *in vivo*,

a ribonuclease must retain its native conformation for an extended time at physiological

temperature. The RNase A amino acid substitutions described herein were designed to

weaken the interaction between RNase A and RI without compromising the enzyme's

conformational stability. As listed in Table 2.1, T_m values of all single variants were within 5

°C of RNase A. Consequently, a shift to physiological temperature would cause

inconsequential changes to the enzymes' tertiary structures.

Surprisingly, the T_m of ONC was determined to be 90 °C. The remarkable conformational

stability of ONC is potentially due to a disulfide bond (Cys87 – Cys104) that tethers the *C*-

terminus to a middle strand of the antiparallel β-sheet (Mosimann *et al.*, 1994). High thermal

stability had been reported for other members of the RNase A superfamily—a ribonuclease

from the liver of *R. catesbeiana* and ribonucleases from the oocytes of *R. catesbeiana* and *R.

japonica* (Okabe *et al.*, 1991). Like ONC, each of these ribonucleases has a *C*-terminal

disulfide bond. Moreover, the ribonuclease from *R. catesbeiana* oocytes is toxic to several

transformed cell lines (Liao *et al.*, 1996)

Binding to Ribonuclease Inhibitor. An agarose gel-based assay was used to screen for

inhibition of the RNase A variants by hRI. As shown in Figure 2.2, RNase A was highly

sensitive to the effects of hRI. In the absence of hRI, RNase A cleaved rRNA efficiently,

producing a faint smear of low M_r molecules. Addition of excess hRI protected the rRNA

completely. D38R RNase A and A109R RNase A showed patterns nearly identical to that of

RNase A, indicating that these variants, despite the arginine substitutions, remained highly

sensitive to hRI. Thus, it appears that RNase A, hRI, or the RI•RNase A complex is able to

accommodate an arginine residue at positions 38 or 109, and still preserve contacts that are

necessary for tight binding.

In the absence of hRI, G88R RNase A and G88D RNase A displayed enzymatic activity

comparable to that of RNase A. In contrast to the native enzyme, addition of excess hRI to

reactions containing the Gly88 variants did not inhibit the cleavage of rRNA. Thus, replacing

Gly88 with an arginine or aspartate residue reduced significantly the susceptibility of

RNase A to hRI-mediated inactivation. The additional arginine residue in the double variants,

D38R/G88R RNase A and G88R/A109R RNase A, did not enhance resistance to hRI (data

not shown). Based on these results, subsequent characterization of the RNase A variants

focused on G88R RNase A and G88D RNase A.

In the absence of hRI, ONC catalyzed rRNA cleavage. But, the cleavage products were

of higher M_r than were those produced by RNase A. This result is consistent with ONC

having a lower specific catalytic activity than does RNase A. Like G88R RNase A and G88D

RNase A, ONC catalyzed rRNA cleavage despite the presence of excess of hRI. Thus, ONC,

G88R RNase A, and G88D RNase A are far less sensitive to the inhibitory activity of hRI

than is RNase A. As listed in Table 2.2, the inhibition of G88R RNase A by hRI had

$K_i = 0.41$ nM. RI inhibition of G88D RNase A was more pronounced, with $K_i = 0.052$ nM.

These values are 10^4-fold and 10^3-fold greater, respectively, than that for the pRI•RNase A

interaction.

To explore further the interactions between hRI and RNase A near Gly88, we created a

variant of hRI in which Trp264 is replaced by an alanine residue to yield W264A hRI. As

shown in Figure 2.2, wild-type hRI and W264A hRI inhibit the ribonucleolytic activity of

wild-type RNase A to a similar extent. W264A hRI is, however, a much more potent

inhibitor of G88R RNase A and G88D RNase A than is wild-type hRI. Apparently, RNase A

and G88R and G88D variants bind to hRI in a similar orientation. Replacing Trp264 with an

alanine residue creates a pocket that is able to accommodate the sidechain of an arginine or

aspartate residue, thereby relieving the steric strain that weakens binding to wild-type hRI.

Thus, the behavior of residue 88 of RNase A and residue 264 of RI is consistent with the

'knobs-into-holes' model of receptor – ligand interaction (Crick, 1952).

Steady-State Kinetics. Several studies had shown that the biological activities of

ribonucleases, including ONC cytotoxicity, rely on the enzymes' catalytic activity (Wu *et al.*,

1993; Kim *et al.*, 1995a). The results of the agarose gel-based assays showed that all of the

ribonucleases were active catalysts (Figure 2.2), and that G88R RNase A, G88D RNase A,

and ONC evaded inhibition by hRI. We evaluated the ribonucleolytic activity of these latter

enzymes in detail.

G88R RNase A and G88D RNase A were found to be efficient catalysts of RNA

cleavage (Table 2.1). Their k_{cat} values did not deviate significantly from that of RNase A, and

their k_{cat}/K_m values were lower by only twofold. These high levels of ribonucleolytic activity indicate that the active-site structures and catalytic mechanisms of the RNase A variants were similar to those of RNase A. Moreover, because G88R RNase A and G88D RNase A are thermally stable, the enzymes likely maintain a high level of ribonucleolytic activity at physiological temperature.

ONC was found to be a relatively inefficient catalyst of RNA cleavage. The values of k_{cat} and k_{cat}/K_m for ONC were 10^4-fold lower than those of RNase A (Table 2.1). This lower catalytic activity is due, in part, to differences in substrate preference. When assayed for the cleavage of a polymeric substrate, ONC shows a 25-fold preference for poly(U) over poly(C) (Boix *et al.*, 1996). RNase A activity, however, is maximal when assayed for the cleavage of poly(C) (Sorrentino & Libonati, 1994).

Cytotoxicity. Our hypothesis is that overcoming inhibition by RI is central to ribonuclease cytotoxicity. Accordingly, the increased K_i values for G88R RNase A and G88D RNase A interactions should be manifested as a cytotoxic activity. The ability of G88R RNase A and G88D RNase A to kill mammalian cells was assessed by measuring [methyl-^{3}H]thymidine incorporation into cellular DNA following a 44-h incubation with the ribonucleases. As shown in Figure 2.3 and listed in Table 2.2, ONC is a potent cytotoxin with $IC_{50} \cong 0.5$ μM. This value is similar to that reported by Youle and coworkers, who measured [^{35}S]methionine incorporation into cellular proteins to assess ONC toxicity to K-562 cells (Newton *et al.*, 1994). Like ONC, G88R RNase A has a pronounced effect on K-562 cell viability. The IC_{50} value of G88R RNase A ($IC_{50} \cong 7$ μM) was ~10-fold greater than that of ONC. The additional arginine residue in D38R/G88R RNase A and G88R/A109R RNase A did not enhance the cytotoxic potency of G88R RNase A (data not shown). Like the G88R enzyme,

G88D RNase A inhibited K-562 cell viability, with an IC_{50} value (IC_{50} = 30 μM) that was

~5-fold greater than that of G88R RNase A. At concentrations used in this assay, RNase A

had no measurable effect on K-562 cell viability. The IC_{50} values determined for ONC,

G88R RNase A, and G88D RNase A varied by ≤30% in three distinct assays (data not

shown).

To assess the nature of cell death caused by the cytotoxic ribonucleases, K-562 cells were

treated with RNase A, G88R RNase A, or ONC and then visualized by light and fluorescence

microscopy (Figure 2.4). The appearance of cells treated with RNase A was indistinguishable

from cells treated with PBS (data not shown), confirming the results of the cytotoxicity

assays. In contrast, K-562 cells treated with G88R RNase A or ONC showed characteristics

consistent with the induction of apoptosis, including condensation and fragmentation of their

nuclei.

2.5 Discussion

Attributes of a Cytotoxic Ribonuclease. A ribonuclease must have several properties to be

cytotoxic. First, its three-dimensional structure must be stable at physiological temperature.

Otherwise, the ribonuclease would be an inactive catalyst as well as a target for proteolysis.

The values of T_m for G88R RNase A, G88D RNase A, and ONC indicate that each of these

enzymes retains its native structure during the course of a cytotoxicity assay (Table 2.1).

Second, a ribonuclease must be an active catalyst. Cytotoxic ribonucleases effect cell

death by catalyzing the cleavage of cellular RNA (Wu *et al.*, 1993; Mastronicola *et al.*, 1995;

Wu *et al.*, 1995). G88R RNase A and G88D RNase A are equally efficient catalysts of RNA

cleavage (Table 2.1). Yet, G88R RNase A is a significantly more potent cytotoxin than is

G88D RNase A. Moreover, both RNase A variants are more efficient catalysts than is ONC.

Yet, ONC is more cytotoxic than is either G88R RNase A or G88D RNase A. This result

indicates that ribonucleolytic activity alone is not responsible for the different cytotoxic

potencies of ribonucleases.

Third, a ribonuclease must evade RI. As the inhibition constant (K_i) for a ribonuclease

decreases, the IC_{50} value for cytotoxicity increases (Table 2.2). Should a tight-binding

ribonuclease such as RNase A reach the cytosol, it would be inactivated rapidly by

endogenous RI. In contrast, cytotoxic ribonucleases, such as ONC, G88R RNase A and

G88D RNase A, resist inactivation by RI. These ribonucleases then catalyze the degradation

of cellular RNA, ultimately causing cell death.

An important conclusion from our data is that wild-type RNase A has all of the properties

necessary to be cytotoxic, except for resistance to RI. In other words, ONC is not

unique—other monomeric homologs of RNase A can be endowed with potent cytotoxic

activity. Other data support this conclusion. For example, monomeric BS-RNase, which is

80% identical to RNase A, is not cytotoxic. Carboxymethylation of Cys31 in monomeric

C32S BS-RNase (to give MCM31) or Cys32 in monomeric C31S BS-RNase (to give

MCM32) diminishes affinity for RI (Matousek *et al.*, 1997). Moreover, MCM31 and

MCM32 are aspermatogenic to mice. In contrast to the aspermatogenic activity of dimeric

BS-RNase, that of MCM31 and MCM32 is directed only at spermatogenic layers.

Intratesticular injection of MCM31 or MCM32 affects neither the diameter of seminiferous

tubules nor the weight of testes. Also in contrast to wild-type BS-RNase, MCM31 and

MCM32 are not toxic to other cell types. These data are consistent with the affinity of

MCM31 and MCM32 for RI being diminished only slightly. The cellular concentration of RI

is tissue-specific (Lee & Vallee, 1993). One explanation for the toxicity of MCM31 and

MCM32 for spermatogenic layers is that spermatogenic layers do not contain enough RI to

inactivate invading MCM31 and MCM32. We suspect that the susceptibility of a cell to a

cytotoxic ribonuclease is related to its RI level.

Replacing residues 1 – 9 of human pancreatic ribonuclease with the corresponding

residues of ONC decreases the K_i of RI by 28-fold (Boix et al., 1996). In the presence of

retinoic acid, this hybrid ribonuclease is toxic to U251 cells. Under the same conditions,

human pancreatic ribonuclease does not affect cell viability. These results add further support

to the proposal that ribonuclease susceptibility to RI defines the cytotoxic potential of a

ribonuclease.

The cytotoxic potency of a ribonuclease correlates with the presence of ribonucleolytic

activity to the cytosol. RI constitutes ~0.01% of the cytosolic protein in a typical mammalian

cell (Blackburn & Moore, 1982; Lee & Vallee, 1993). Using this value and data on the

volume and composition of the cytosol (Lodish et al., 1995), we estimate that the cytosolic

concentration of RI is near 10^{-6} M. Thus, any ribonuclease with $K_i > 10^{-6}$ M would be largely

free (not bound by RI) in the cytosol. The K_i value of ONC is in that range (Boix et al.,

1996), but those of G88R RNase A and G88D RNase A are not (Table 2.2). The RNase A

variants could compensate for being more susceptible to RI by being better catalysts of RNA

degradation (Table 2.1). Alternatively, K-562 cells could have an unusually low

concentration of RI. As a consequence, the K_i values for G88R RNase A and G88D RNase A

could approach the RI concentration. Nonetheless, the concentration of cytosolic RI in K-562

cells is sufficient to fully protect these cells from high doses of RNase A (Figure 2.3).

Mechanism of Cytotoxicity. To act as a cytotoxin, a ribonuclease must reach cellular

RNA. Once in proximity to the RNA, the ribonuclease must catalyze RNA cleavage. The

destruction of cellular RNA appears to result ultimately in apoptosis (Liao *et al.*, 1996;

Piccoli *et al.*, 1999). At a minimum, gaining access to RNA must involve crossing a cellular

membrane. The route taken by cytotoxic ribonucleases to cellular RNA appears to be

indirect, perhaps involving internalization in an endosome, retrograde transport through the

Golgi apparatus to the endoplasmic reticulum (ER), and translocation from the ER to the

cytosol (Ardelt *et al.*, 1991; Wu *et al.*, 1993; Kim *et al.*, 1995b; Mastronicola *et al.*, 1995;

Wu *et al.*, 1995).

Changing the flux through any step in the pathway to cellular RNA could influence the

potency of a ribonuclease. For example, BS-RNase variants, ANG, and human pancreatic

ribonuclease are toxic to 9L (rat glioma) cells in the presence of retinoic acid (Wu *et al.*,

1995). In the absence of the drug, these ribonucleases do not affect cell viability. Retinoic

acid enhances cytosolic accumulation of a ribonuclease by disrupting the integrity of the

Golgi apparatus. Endogenous RI is overwhelmed, leaving the cell without a means to protect

its RNA. Further, ANG is toxic to lymphocytes despite being highly susceptible to inhibition

by RI (Lee *et al.*, 1989; Matousek *et al.*, 1992; Matousek *et al.*, 1995). ANG has a surface

loop that functions as a ligand for a cell-surface receptor, allowing the enzyme to enter cells

via receptor-mediated endocytosis (Harper & Vallee, 1989; Raines *et al.*, 1995). A rapid

influx of ANG could overwhelm cellular RI, leaving the lymphocyte without protection from

the lethal effects of cytosolic ribonucleolytic activity. These results do not contradict the

conclusion that RI mediates ribonuclease cytotoxicity. Rather, each mechanism—evading RI

or overwhelming RI—effects the delivery of a lethal enzymatic activity.

Prospectus. Ribonucleases have much potential as chemotherapeutics. For example, ONC is presently undergoing Phase III human clinical trials for the treatment of malignant mesothelioma. Here, we have used rational design to weaken the interaction between RI and RNase A. The consequence of the amino acid substitutions at Gly88 is a pronounced cytotoxicity to a human leukemic cell line. Because RNase A is a mammalian protein and ONC is amphibian protein, a chemotherapeutic based on RNase A is likely to be less immunogenic and thus more efficacious than is ONC. Finally, appropriate substitutions to the surface loop containing residue 88 in human pancreatic ribonuclease could endow that enzyme with potent cytotoxicity.

2.6 Acknowledgements

Table 2.1 Ribonuclease conformational stabilities and steady-state kinetic

parameters for catalysis of poly(C) cleavage

Ribonuclease	T_m (°C)[a]	k_{cat} (s^{-1})	k_{cat}/K_m (10^6 M^{-1}s^{-1})
RNase A	63	507 ± 15±	5.7 ± 0.5[b]
D38R RNase A	59	ND[c]	ND
G88R RNase A	60	790 ± 20	2.9 ± 0.3
G88D RNase A	64	370 ± 10	3.2 ± 0.2
A109R RNase A	64	ND	ND
ONC	90	0.20 ± 0.01	0.0014 ± 0.0001

[a] T_m values (±2 °C) of RNase A and RNase A variants in PBS

were determined by UV spectroscopy. The T_m value (±2 °C)

of ONC in PBS was determined by CD spectroscopy.

[b] From ref (Fisher *et al.*, 1998b).

[c] Not determined.

Table 2.2 Ribonuclease inhibition constants by ribonuclease inhibitor and

IC_{50} values for K-562 cell toxicity

| Ribonuclease	K_i (pM)	IC_{50} (μM)
RNase A	0.067[a]; 0.044[b]	–
G88D RNase A	52	30
G88R RNase A	410	7
ONC	>1 × 10^6 [c]	0.5

[a] For pRI•RNase A (Vicentini *et al.*, 1990).

[b] For hRI•RNase A, calculated from values of k_{on} and k_{off} (Lee

et al., 1989).

[c] The value of K_i for ONC is from ref (Boix *et al.*, 1996) and is

an estimate based on the IC_{50} for inhibition.

Figure 2.1   Molecular interactions between porcine ribonuclease inhibitor (red) and

ribonuclease A (blue).

This figure was created with the programs MOLSCRIPT (Kraulis, 1991) and

RASTER3D (Merritt & Murphy, 1994) using atomic coordinates derived by

X-ray diffraction analysis (Kobe & Deisenhofer, 1995). (A) Three-

dimensional structure of the crystalline pRI•RNase A complex. The indicated

residues were replaced in RNase A variants. (B) Close-up of the contacts

between RI and RNase A near Gly88 of RNase A. The views in A and B are

from opposite sides of the pRI•RNase A complex. Trp259 of pRI corresponds

to Trp264 of hRI.
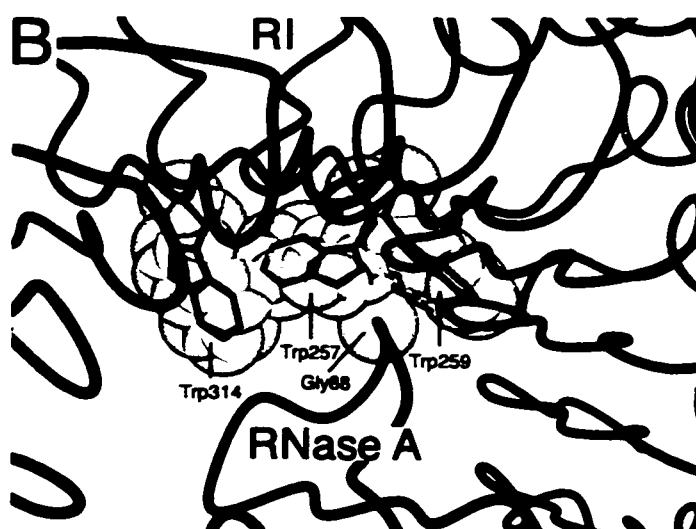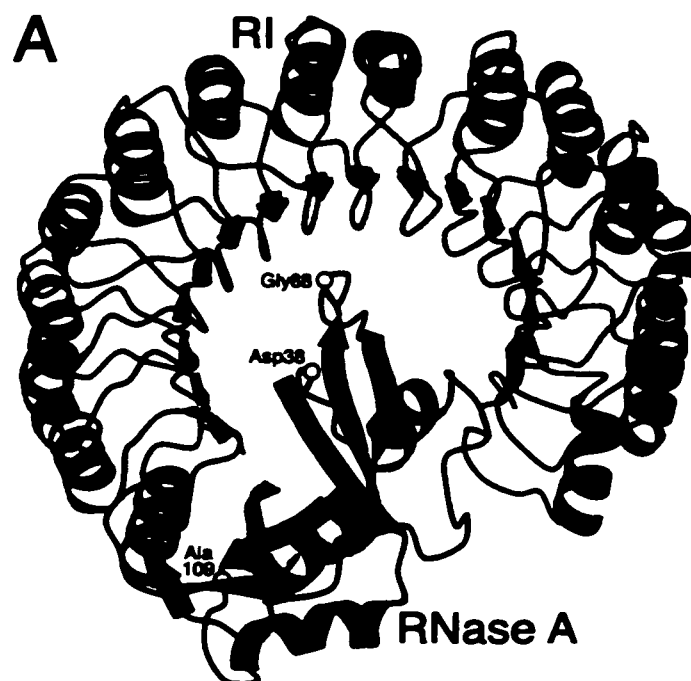
Figure 2.2   Agarose gel-based assay for ribonuclease inhibition by ribonuclease inhibitor.

Inhibition was assessed by visualizing the ribonuclease-catalyzed degradation

of 16S- and 23S-rRNA in the absence or presence of excess hRI. Because the

gel was run for only a short period of time, the 16S- and 23S-rRNAs are not

well resolved. "–" designates experiments that lacked ribonuclease or hRI (or

both). (A) Inhibition of a ribonuclease (0 or 10 ng) by wild-type hRI (0, 20, or

40 units). (B) Inhibition of RNase A varying at residue 88 (0 or 10 ng) by

wild-type hRI or W264A hRI (0 or 20 units).

Ribonuclease	–	RNase A			D38R			G88R			A109R			ONC			G88D		
Units of hRI	0	0	20	40	0	20	40	0	20	40	0	20	40	0	20	40	0	20	40

A

hRI		–			Wild-Type			W264A		
Residue 88 of RNase A	–	G	R	D	–	G	R	D	–	G	R	D

B
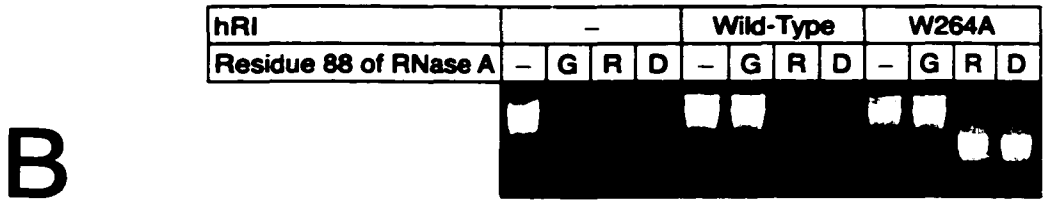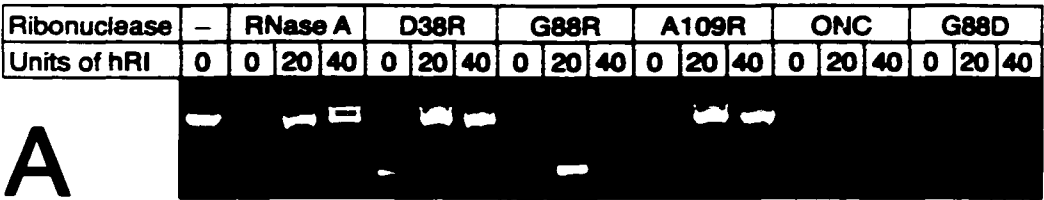
Figure 2.3   Effect of ribonucleases on the proliferation in culture of K-562 cells.

Proliferation was measured by incorporation of methyl-[^{3}H]thymidine into

cellular DNA following a 44-h incubation with the ribonucleases. Values

reported are the mean from three cultures and are expressed as a percentage of

the control, which is the mean from cultures lacking exogenous ribonuclease.

The standard error of each value is <11%.
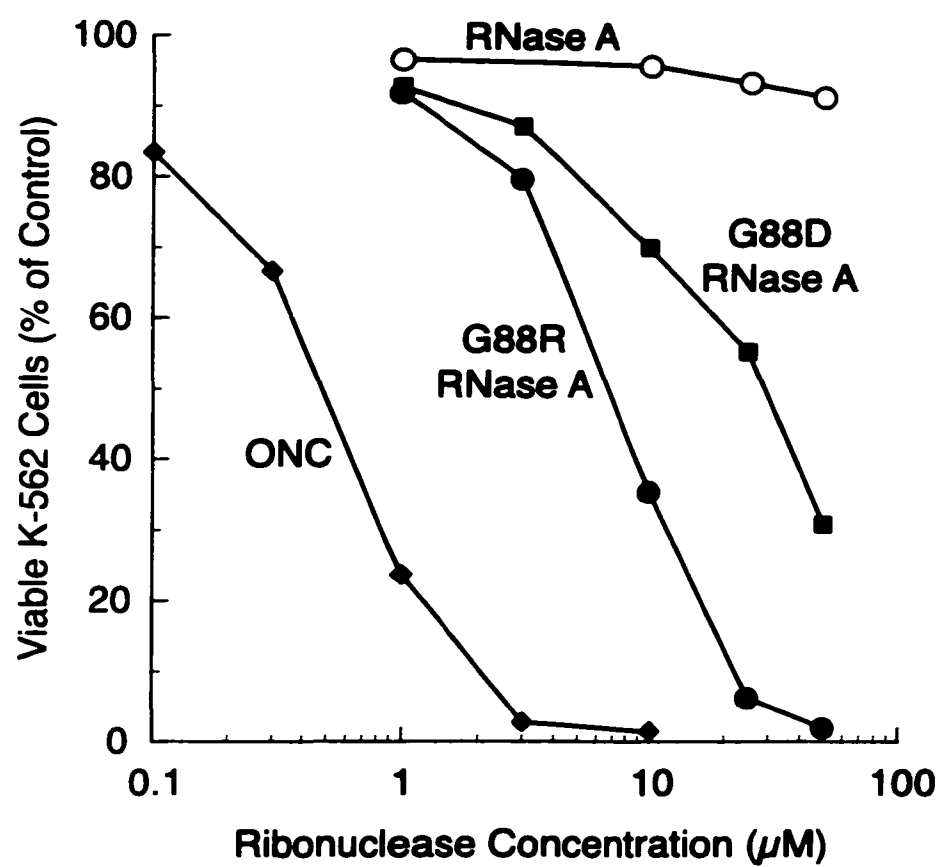
Figure 2.4   Visualization of K-562 cells treated with Ribonuclease A, Onconase, and

G88R Ribonuclease A.

K-562 cells (1×10^5 cells/mL) were incubated with Ribonuclease A (50 μM),

Onconase (10 μM), or G88R Ribonuclease A (50 μM) for 48 h, recovered by

centrifugation, stained with DAPI (4′,6-diamidino-2-phenylindole,

dihydrochloride; 0.02 μg/μL in PBS) and plated on a microscope slide.

Samples were visualized with both light microscopy (top) and fluorescence

microscopy (bottom).
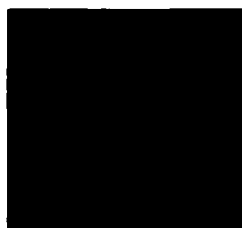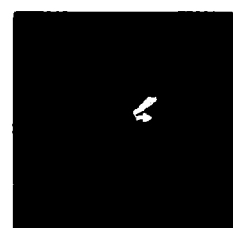
RNase A   Onconase   G88R RNase A

Chapter Three

Endowing Human Pancreatic Ribonuclease

with Cytotoxic Activity

This chapter is in preparation for submission to *Cancer Research* as:

3.1 Abstract

Human pancreatic ribonuclease (hpRNase or RNase 1) is homologous to bovine

pancreatic ribonuclease A (RNase A). Both enzymes are efficient catalysts of RNA cleavage,

but neither is cytotoxic. Here, ERDD hpRNase, which is the L86E/N88R/G89D/R91D

variant, is shown to have conformational stability and ribonucleolytic activity similar to that

of the wild-type enzyme, but 10^3-fold less affinity for the endogenous cytosolic ribonuclease

inhibitor protein (RI). In addition, ERDD hpRNase is toxic to a human erythroleukemia cell

line. Lys41 is a key active-site residue of hpRNase. The K41R substitution decreases further

the affinity for RI, but also decreases conformational stability and ribonucleolytic activity

and has little effect on the cytotoxicity of ERDD hpRNase. Replacing Arg4 and Val118 with

cysteine residues to form a fifth disulfide bond in ERDD hpRNase increases conformational

stability, has little effect on ribonucleolytic activity, decreases affinity for RI, and (most

significantly) increases cytotoxicity. Thus, hpRNase variants with high conformational

stability, high ribonucleolytic activity, and low affinity for RI are toxic to cancer cells. This

finding has significant implications for human cancer chemotherapy.

3.2 Introduction

Bovine pancreatic ribonuclease A (RNase A; EC 3.1.27.5) was perhaps the most studied

enzyme of the 20th century (Raines, 1998; Raines, 1999). In contrast, its human counterpart,

human pancreatic ribonuclease (hpRNase), has attracted significantly less attention

(Sorrentino. 1998). The amino acid sequences of hpRNase and RNase A are 70% identical

(Figure 3.1). There are no insertions or deletions, save a four amino-acid C-terminal

extension on hpRNase. RNase A residues that contribute to the active-site (*P1* subsite) are

strictly conserved in hpRNase. In addition, RNase A residues that define other phosphoryl

group binding sites [*P(-1)*, *P0*, and *P2*] and the nucleobase binding sites (*B1* and *B2*) are

conserved in hpRNase. Finally, the four disulfide bonds present in RNase A are also present

in hpRNase. Atomic coordinates of native hpRNase have yet to be deposited in the protein

data bank. Still, the similar amino acid sequences of RNase A and hpRNase suggest that the

enzymes have similar three-dimensional structures.

Select ribonucleases are toxic to cancer cells. Bovine seminal ribonuclease (BS-RNase), a

dimeric homolog of RNase A, is a potent anti-tumor agent (D'Alessio *et al.*, 1997). Like BS-

RNase. Onconase™ (ONC), a ribonuclease isolated from the Northern Leopard frog, is

selectively toxic to cancer cells and is now in Phase III human clinical trials as a cancer

chemotherapeutic (Youle & D'Alessio, 1997). The basis for the favorable therapeutic index

of ribonucleases is unknown.

To act as a cytotoxin, a ribonuclease must associate with the target cell plasma

membrane, be internalized, and undergo translocation to the cytosol. In the cytosol,

ribonucleases encounter ribonuclease inhibitor (RI), a 50-kDa protein common to most

mammalian cell types (Hofsteenge, 1997). BS-RNase and ONC are not inhibited by RI

(Murthy & Sirdeshmukh, 1992; Wu *et al.*, 1993; Kim *et al.*, 1995b; Hofsteenge, 1997). As a

consequence, these ribonucleases catalyze the cleavage of cellular RNA and thereby cause

cell death. Unlike BS-RNase and ONC, hpRNase is highly susceptible to inhibition by RI

(Murthy & Sirdeshmukh, 1992; Boix *et al.*, 1996; Suzuki *et al.*, 1999). We suspected that this

inhibition prevents hpRNase from catalyzing cellular RNA cleavage and acting as a

cytotoxin.

Other workers have described efforts to bestow hpRNase and RNase A with cytotoxic

activity. D'Alessio and colleagues have described an artificial RNase A dimer and an

artificial hpRNase dimer, each with a quaternary structure resembling that of BS-RNase (Di

Donato *et al.*, 1994; Piccoli *et al.*, 1999). The quaternary structure of the hpRNase dimers

likely prevents binding by RI, allowing the ribonuclease to cleave cellular RNA and thereby

kill cells. Monomers of hpRNase and RNase A have been conjugated to peptides, proteins,

and antibodies to enhance uptake by target cells (Rybak *et al.*, 1991; Newton *et al.*, 1992;

Psarras *et al.*, 1998; Futami *et al.*, 1999; Suwa *et al.*, 1999). A large influx of a ribonuclease

conjugate, mediated by the targeting epitope, likely overwhelms cellular stores of RI, leaving

ribonucleolytic activity unchecked in the cytosol. This circumstance ultimately results in cell

death. Youle and colleagues have chemically conjugated transferrin to hpRNase residue 89

(Suzuki *et al.*, 1999). At this position, transferrin serves as both a steric block to prevent RI

binding and an epitope that affords the conjugate receptor-mediated entry into cells. In the

presence of 10 µM all-*trans* retinoic acid, the transferrin–hpRNase conjugate is cytotoxic.

Unfortunately, both artificial dimers and ribonuclease conjugates require *in vitro* processing

following initial purification or are readily isolated only as multiple isoforms. These

limitations complicate their use as chemotherapeutic agents and prevent their use in gene

therapy protocols.

Recently, we described a monomeric variant of RNase A in which Gly88 was replaced

with an arginine residue [G88R RNase A (Leland *et al.*, 1998)]. The G88R RNase A variant

retains conformational stability and ribonucleolytic activity comparable to that of RNase A

but is 10^4-fold less susceptible to inhibition by RI. In addition, G88R RNase A is toxic to

human erythroleukemia cells, despite lacking an exogenous targeting epitope. Finally,

G88R RNase A was readily isolated as a single, defined species that did not require any

processing after purification from an *Escherichia coli* culture.

Here, we have applied the concepts developed with G88R RNase A to hpRNase. We

describe amino acid substitutions in an hpRNase surface loop that preserve conformational

stability and ribonucleolytic activity but relieve inhibition by RI. In addition, we describe

other amino acid substitutions in hpRNase that affect further inhibition by RI, as well

conformational stability and ribonucleolytic activity. Finally, we report on the cytotoxicity of

each hpRNase variant. We find that monomeric hpRNase can be transformed into a potent

cytotoxin with only limited amino acid substitutions. This finding has significant

implications for human cancer chemotherapy.

3.3 Experimental Procedures

Materials. *Escherichia coli* strain DH5α was from Life Technologies (Gaithersburg,

MD). *E. coli* strain BL21(DE3) and the pET22b(+) expression vector were from Novagen

(Madison, WI). ONC was prepared as described (Leland *et al.*, 1998). Enzymes used for

DNA manipulation were from Promega (Madison, WI) or New England Biolabs (Beverly,

MA). RI was from Promega. The fluorogenic ribonuclease substrate [6-FAM–dArU(dA)$_2$–6-

TAMRA; (Kelemen *et al.*, 1999)] was from Integrated DNA Technologies (Coralville, IA).

K-562 cells were from the American Type Culture Collection (Manassas, VA). Ribosomal

RNA (16S and 23S) was from Boehringer Mannheim (Mannheim, Germany). Poly(cytidylic

acid) [polyC] was from Midland Certified Reagents (Midland, TX). [*methyl*-^{3}H]Thymidine

was from DuPont/NEN (Boston, MA). Terrific broth (TB) contained (in 1 L) Bacto tryptone

(12 g), Bacto yeast extract (24 g), glycerol (4 mL), KH$_2$PO$_4$ (2.31 g), and K$_2$HPO$_4$ (12.54 g).

Phosphate buffered-saline (PBS) contained (in 1 L) KCl (0.20 g), KH$_2$PO$_4$ (0.20 g), NaCl

(8.0 g), and Na$_2$HPO$_4$•7H$_2$O (2.16 g). All other chemicals and reagents were of commercial

grade or better and were used without further purification.

DNA oligonucleotides for PCR, site-specific mutagenesis, and DNA sequencing were from

Integrated DNA Technologies. PCR reagents were from Clontech (Palo Alto, Ca). DNA was

sequenced with a BigDye cycle sequencing kit (Perkin Elmer, Norwalk, CT) and an

ABI 377XL Automated DNA Sequencer at the University of Wisconsin Biotechnology

Center.

Instruments. A QuantaMaster 1 Photon Counting Fluorometer equipped with sample

stirring (Photon Technology International, South Brunswick, NJ) was used for the

fluorescence-based assays of ribonucleolytic activity and RI inhibition. A Cary Model 3

spectrophotometer or a Cary 50 Bio spectrophotometer was used for UV absorbance

measurements (Varian, Palo Alto, CA).

Design of hpRNase variants. Our goal was to engineer variants of hpRNase that are

cytotoxic. First, we replaced amino acid residues in hpRNase to reduce the affinity for RI.

Second, we replaced an active-site residue to reduce further the affinity for RI but at the expense of ribonucleolytic activity. Third, we incorporated a nonnative disulfide bond into hpRNase to enhance conformational stability. Our design was intentionally restricted to monomeric hpRNase variants containing only the 20 natural amino acids. This restriction facilitates the ease of production of the variants in *E. coli*. Further, a cytotoxic hpRNase variant so restricted may be incorporated directly into a gene therapy regimen. The three types of amino acid changes are described below.

RNase A residues 85–94 comprise a solvent-exposed surface loop flanked by half-cystine residues. In the structure of the crystalline RI•RNase A complex, this loop makes many contacts with RI (Kobe & Deisenhofer, 1995; Kobe & Deisenhofer, 1996). Substitution of RNase A residue Gly88 with arginine (G88R RNase A) lessens inhibition by RI due to steric and electrostatic strain introduced to the RI•RNase A complex (Leland *et al.*, 1998). Because the structure of the RI•hpRNase complex is unknown, we used the RI•RNase A complex as a model. hpRNase and RNase A are 70% identical (Figure 3.1). Thus, they likely participate in similar intermolecular contacts with RI. First, we created the N88R variant of hpRNase. This substitution was intended to introduce steric and electrostatic strain into the RI•hpRNase complex. Yet, N88R hpRNase binds to RI with high affinity (data not shown). Consequently, we resorted to multiple substitutions, as detailed in Table 3.1. The L86E substitution was added to make the hpRNase amino acid sequence on both sides of Cys84 identical to that of RNase A. Our hope was that this change would likewise equate the three-dimensional structures near Cys84. The G89D and R91D substitutions were made to introduce additional steric and electrostatic strain into the RI•hpRNase complex. Hereafter, the variant that contains the L86E, N88R, G89D, and R91D substitutions is referred to as ERDD hpRNase.

RNase A residue Lys41 is part of the enzymic active site (*P1* subsite). Previous work with variant and semisynthetic enzymes revealed that the role of Lys41 in RNase A catalysis is to donate a hydrogen bond to the rate-limiting transition state (Messmore *et al.*, 1995). Arginine can substitute for Lys41 in RNase A catalysis, albeit with a 10^2-fold reduction in catalytic activity (Trautwein *et al.*, 1991; Messmore *et al.*, 1995). Lys41 makes van der Waals contacts with RI residues Tyr430 and Asp431 in the crystalline RI•RNase A complex (Kobe & Deisenhofer, 1995; Kobe & Deisenhofer, 1996). Adding the K41R substitution to G88R RNase A reduces the affinity for RI by 20-fold (Bretscher *et al.*, 2000). Moreover, K41R/G88R RNase A is 3-fold more toxic to K-562 cells than is G88R RNase A (Bretscher *et al.*, 2000). Based on amino acid sequence alignment (Figure 3.1), it is likely that hpRNase residue Lys41 plays the same role in catalysis as does Lys41 of RNase A. Further, it is probable that Lys41 of hpRNase participates in intermolecular contacts with RI that are similar to those in the RI•RNase A complex. Thus, we added the K41R substitution to ERDD hpRNase to observe the impact of a decreased susceptibility to inactivation by RI but a loss of catalytic activity on the cytotoxic activity of ERDD hpRNase.

The cytotoxic activity of a ribonuclease correlates with its conformational stability (Klink & Raines, 2000). Hence, we incorporated a nonnative disulfide bond into ERDD hpRNase to increase its stability and thereby its cytotoxicity. Previously, we described an RNase A variant in which Ala4 and Val118 are each replaced with cysteine (Klink & Raines, 2000). These cysteine residues form a disulfide bond that increases the conformational stability of RNase A. Addition of the Cys4–Cys118 disulfide bond to hpRNase could cause a subtle reorientation of neighboring residues. This potential change in conformation could disturb key intermolecular contacts between the hpRNase variant and RI. We suspected that the

increased conformational stability and the reduced affinity for RI would enhance the

cytotoxic activity of the hpRNase variants. The hpRNase variant that includes the

Cys4–Cys118 disulfide bond is designated with the prefix: 'S–S'.

Production and purification of hpRNase and its variants. A synthetic cDNA that codes

for Met(-1) hpRNase was the generous gift of R. J. Youle (Wu *et al.*, 1995). This cDNA was

excised from pET11D and inserted into pET22B(+) by using the *Bam*HI and *Xba*I sites. The

resulting plasmid was termed pHP-RNase.

The cDNAs coding for the hpRNase variants were made by site-directed mutagenesis and

PCR-based mutagenesis of pHP-RNase. hpRNase residues Lys41, Leu86, Asn88, Gly89, and

Arg91 were replaced using site-directed mutagenesis. Oligonucleotide PL28

(5′-CGAAAGTGT TAAC<u>AGGCCT</u>GCAACGACCA-3′) was used to replace the AAA

codon of Lys41 with an AGG codon of arginine (reverse complement in bold).

Oligonucleotide PL28 also incorporates a translationally silent *Stu*I site (underlined).

Oligonucleotide BMK15

(5′-GTAAGCGCAGTTCGGGTAATCAGAATC<u>ACGCGT</u>TTCACGGCAGTCAGTGAT

ATG-3′) incorporates four codon changes. This oligonucleotide replaces (1) the CUG codon

of Leu86 with a GAA codon of glutamate, (2) the AAC codon of Asn88 with a CGU codon

of arginine, (3) the GGU codon of Gly89 with a GAU codon of aspartate, and (4) the CGU

codon of Arg91 with a GAU codon of aspartate (reverse complement of new codons are

indicated by bold type). In addition, oligonucleotide BMK15 incorporates a translationally

silent *Mlu*I site (underlined). hpRNase residues Arg4 and Val118 were replaced with cysteine

using PCR-based mutagenesis. Oligonucleotide PL29

(5′-GGAGATATA*CATA TG*AAAGAATCT <u>TGCGCA</u>AAAAAAATCCCAGCG-3′) replaces

the CGU codon of Arg4 with a UGC of codon cysteine (bold) and incorporates

translationally silent *Fsp*I (underlined) and *Nde*I (italics) sites. Oligonucleotide PL30a

(5'-TC*GGATC*CCTACTAAGAGTCTTCAAC<u>GCTAGC</u>GTCGAA ATGACACGG-3')

replaces the GUU codon of Val118 with a UGU codon of cysteine (reverse complement in

bold) and incorporates translationally silent *Nhe*I (underlined) and *Bam*HI (italics) sites. The

PCR product was band purified, treated with restriction endonucleases *Nde*I and *Bam*HI, and

inserted into a pET22b(+) fragment prepared with the same restriction endonucleases. The

nucleotide sequence of all hpRNase variants was confirmed with dye-terminator cycle

sequencing.

hpRNase, its variants, and ONC were produced and purified by using methods described

previously (Leland *et al.*, 1998). Briefly, *E. coli* strain BL21(DE3) was transformed with the

appropriate plasmid and grown in TB to an OD_{600} of 2.0. Protein expression was induced by

addition of isopropyl-1-thio-β-D-galactopyranoside to 0.5 mM. Cells were then harvested by

centrifugation and lysed with a French pressure cell. Inclusion bodies were recovered by

centrifugation, then reduced and denatured with a 20 mM Tris-HCl buffer, pH 8.0,

containing guanidine-HCl (7 M), DTT (10 mM), and EDTA (10 mM). Proteins were

oxidatively folded by drop-wise addition into 0.1 M Tris-HCl buffer (pH 8.0) containing L-

Arg (0.5 M), reduced glutathione (3.0 mM), and oxidized glutathione (0.6 mM) at 10 °C.

Following a 15-h incubation, the solution was adjusted to pH < 7.0 and concentrated by

ultrafiltration. Concentrated samples were applied to a Superdex G-75 gel filtration FPLC

column (Pharmacia) equilibrated in 50 mM sodium acetate buffer (pH 5.0) containing NaCl

(0.1 M) and NaN$_3$ (0.02% w/v). Protein from the major peak was collected and applied to a

Mono S cation-exchange FPLC column (Pharmacia). hpRNase and its variants were eluted

with a linear gradient of NaCl (0.3–0.6 M) in 50 mM sodium acetate buffer (pH 5.0). The

concentration of hpRNase and its variants was determined by UV spectroscopy using an

extinction coefficient of ε_{280} = 0.53 mL mg⁻¹ cm⁻¹, which was calculated by using the method

of Gill and von Hippel (Gill & von Hippel, 1989). The extinction coefficient for hpRNase

differed by less than 1% when calculated by using the method of Pace and coworkers (Pace

et al., 1995). Both methods predict that addition of a disulfide bond to hpRNase will change

the extinction coefficient by less than 3%. Hence, the same extinction coefficient was used

for all hpRNase variants. The concentration of ONC was determined by UV spectroscopy

using an extinction coefficient of ε_{280} = 0.87 mL mg⁻¹ cm⁻¹ (Leland et al., 1998).

Conformational stability assay. The conformational stability of hpRNase and its variants

was measured by recording the change in absorbance at 287 nm with increasing temperature

(Klink et al., 2000). The temperature of the ribonuclease solution (0.1–0.2 mg/mL) in PBS

was increased continually from 20–80 °C at 0.2 °C per min. The A_{287} was recorded at 1-°C

intervals and fitted to a two-state model for denaturation, where the temperature at the

midpoint of the transition is the T_m.

Steady-state kinetics assay. Steady-state kinetic parameters for hpRNase and its variants

were determined with a fluorogenic substrate for ribonucleases [6-FAM–dArU(dA)₂–6-

TAMRA] (Kelemen et al., 1999). This substrate consists of a single ribonucleotide

embedded within three deoxyribonucleotides. The 5′ end of the substrate is labeled with 6-

carboxyfluorescein (6-FAM) and the 3′ end is labeled with 6-carboxytetramethylrhodamine

(6-TAMRA). When the substrate is intact, the 6-TAMRA group quenches the fluorescence of

the 6-FAM group. Upon ribonucleolytic cleavage, fluorescence intensity increases by 180-

fold. Assays were carried out in 2.00 mL of 0.1 M MES-NaOH buffer (pH 6.0) containing

NaCl (0.1 M), substrate (60 nM), and enzyme (0.060–6.25 nM). Reaction progress was

observed by recording fluorescence emission at 515 nm upon excitation at 490 nm. Values of

k_{cat}/K_m were determined by a linear least-squares regression analysis of initial velocity data

using eq 3.1.

$$\frac{k_{cat}}{K_m} = \left(\frac{\Delta F/\Delta t}{F_{max} - F_0} \right) \frac{1}{[E]}$$ (3.1)

In eq 3.1, $\Delta F/\Delta t$ is the slope from the linear regression, F_{max} is the maximal fluorescence

intensity, F_0 is initial fluorescence intensity, and [E] is the total enzyme concentration. F_{MAX}

was determined by adding RNase A (~0.1 μM final concentration) to the reaction after the

correlation coefficient (R^2) for the least squares regression of the initial velocity data was

greater than 0.99.

Ribonuclease inhibitor binding assay. Two assays were used to assess the binding of the

hpRNase variants to RI. The first was a qualitative gel-based assay, and the second was a

quantitative spectrophotometric assay. hpRNase variants were screened for ribonucleolytic

activity in the presence of RI with an agarose gel-based assay as described previously

(Leland *et al.*, 1998), with the following modifications. Each ribonuclease (10 ng) was added

to PBS containing dithiothreitol (10 mM) and RI (0, 20, or 40 units). After a 10-min

incubation on ice, 16S- and 23S-rRNA (4 μg) was added to the assay mixture. The assay

mixture was incubated at 37 °C for 10 min and then prepared for electrophoresis by the

addition of 10 mM Tris-HCl buffer (pH 7.5) containing EDTA (50 mM), glycerol (30% v/v),

xylene cyanol FF (0.25% w/v), and bromphenol blue (0.25% w/v). Finally, the assay

mixtures were subjected to electrophoresis through an agarose gel (1% w/v) containing

ethidium bromide (0.4 µg/mL). The intensity and position of the rRNA band correlates with

the degree of ribonucleolytic activity. As ribonucleolytic activity in an assay mixture

decreases, both the band intensity and its apparent M_r increase.

Values of K_i for the hpRNase variants were determined by using fluorescence

spectroscopy to measure the steady-state rate of 6-FAM–dArU(dA)$_2$–6-TAMRA cleavage in

the presence of increasing concentrations of RI. RI was prepared and quantitated as described

previously (Bretscher *et al.*, 2000; Klink & Raines, 2000). Assays were carried out in 2.00

mL of 0.10 M MES-NaOH buffer (pH 6.0) containing NaCl (0.1 M), dithiothreitol (5 mM),

and substrate (60 nM). After an initial 2–5 min equilibration, ribonuclease was added

(25–750 pM) to the assay mixture and the steady-state rate of substrate cleavage was

recorded. RI was then added to the assay mixture in a step-wise manner. The steady-state rate

was recorded after each addition of RI. Additions of RI were continued until the steady-state

rate was less than 2% of that in the absence of RI. Values of K_i were calculated by fitting the

steady-state rates to an equation that describes inhibition by tight-binding inhibitors (Stone &

Hofsteenge, 1986). In all determinations, the ribonuclease concentration was less than the

value determined for K_i.

Cytotoxicity assay. The effect of hpRNase variants on proliferation of transformed cells

was measured as described previously (Leland *et al.*, 1998) with the following modification.

hpRNase variants were stored in PBS containing human serum albumin (0.1% w/v) and were

sterile-filtered before addition to the cells. (Concentrated ribonuclease solutions, containing

human serum albumin, were sterilized by passage through a 0.45 micron acetate membrane

syringe-tip filter.) After a 44-h incubation with the ribonucleases, cells were treated with

[*methyl-^{3}H*]thymidine for 4 h. Cellular DNA was recovered, and its radioactivity was counted

in a liquid scintillation counter. Results are expressed as the percentage of [*methyl-*

^{3}H]thymidine incorporated into the DNA of cells treated with PBS containing human serum

albumin (0.1% w/v) but no exogenous ribonuclease. Data are the average of triplicate

determinations with each ribonuclease concentration. Cytotoxicity assays were repeated at

least twice with no significant variation in the results.

3.4 Results

Production and purification of hpRNase and its variants. hpRNase and the hpRNase

variants were produced in *E. coli*. All proteins eluted as a single species during cation-

exchange chromatography and migrated as a single band of appropriate M_r during

SDS/PAGE (data not shown). hpRNase and the variants migrated as single bands on

zymogram electrophoresis (Kim & Raines, 1993b; Bravo *et al.*, 1994), indicating that the

preparations were free from contaminating ribonucleolytic activity (data not shown). Our

expression and purification protocol yielded approximately 20 mg of wild-type hpRNase and

5–20 mg of the hpRNase variants per L of *E. coli* growth medium.

Conformational stability. The T_m of hpRNase was 56 °C (Table 3.2). This value is

slightly higher than that determined by Vilanova and coworkers (Canals *et al.*, 1999). The

discrepancy could reflect differences in solution conditions. The T_m of K41R hpRNase was

identical to that of the wild-type enzyme. The ERDD substitutions reduced the T_m by 4 °C

compared to hpRNase. When the K41R and ERDD substitutions were combined in a single

variant, the T_m was lowered by 7 °C. As intended, addition of the Cys4–Cys118 disulfide

bond increased the T_m of the ERDD variant by 5 °C.

Steady-state kinetic parameters. Values of k_{cat}/K_m for hpRNase and its variants were

determined with a fluorogenic ribonuclease substrate (Kelemen *et al.*, 1999). The value of

k_{cat}/K_m for hpRNase was 1.4×10^6 M^{-1}s^{-1} (Table 3.2). Substitution of Lys41 with arginine

(K41R hpRNase) lowered the value of k_{cat}/K_m almost 100–fold. A similar change was

observed when the analogous substitution was made in RNase A (Trautwein *et al.*, 1991;

Bretscher *et al.*, 2000). The amino acid substitutions of ERDD hpRNase did not have a

deleterious effect on ribonucleolytic activity, but instead caused a modest, 2-fold, increase in

the value of k_{cat}/K_m compared to hpRNase. The ERDD substitutions likewise caused a 2-fold

increase in the k_{cat}/K_m value in K41R hpRNase. Addition of the Cys4–Cys118 disulfide bond

reduced the k_{cat}/K_m value for ERDD hpRNase by almost 3-fold to 1.0×10^6 M^{-1}s^{-1}.

Inhibition by ribonuclease inhibitor. An agarose gel-based assay was used as a qualitative

measure of the affinity of RI for the hpRNase variants. hpRNase hydrolyzed rRNA in the

absence of RI, but was inhibited fully by a 2- or 4-fold excess of RI (Figure 3.2). Like that of

wild-type hpRNase, the ribonucleolytic activity of the K41R enzyme was inhibited by RI. In

contrast, incorporation of the ERDD substitutions in wild-type hpRNase or K41R hpRNase,

yielded variants that retained ribonucleolytic activity in the presence of RI. Addition of the

Cys4–Cys118 disulfide bond to ERDD hpRNase (ERDD S–S hpRNase) reduced further

susceptibility to RI.

The interactions between hpRNase variants and RI were quantitated by measuring

cleavage of 6-FAM–dArU(dA)$_2$–6-TAMRA in the presence of increasing concentrations of

RI (Table 3.2). The results of this assay mirror those obtained with the agarose gel-based

assay. Due to the extraordinary tight binding of RI to wild-type hpRNase, it was not possible

to determine a K_i value with this assay. Values of K_i for the interaction between RI and wild-

type hpRNase have been reported to be 2.0×10^{-13} M (Boix *et al.*, 1996) and 5.2×10^{-12} M

(Suzuki *et al.*, 1999). Because the concentration of ribonuclease used in the determination of

these values was greater than the value of K_i, these values provide only an upper limit for the

actual K_i value. Alone, the K41R variation does not disturb significantly RI inhibition,

making it difficult to measure the K_i value with an assay based on ribonucleolytic activity.

The value of K_i for ERDD hpRNase was 2.1×10^{-10} M. Addition of the K41R variation to

ERDD hpRNase increased the K_i by approximately 3-fold. Addition of the Cys4–Cys118

disulfide bond to ERDD hpRNase yields a variant with $K_i = 2.6 \times 10^{-9}$ M. This value of K_i is

10-fold greater than that for ERDD hpRNase.

Cytotoxicity of hpRNase Variants. We tested the effect of wild-type hpRNase and its

variants on cancer cell viability by measuring the ability of cells to incorporate a ^{3}H-labeled

nucleotide (Figure 3.3). At the ribonuclease concentrations used in this assay, wild-type

hpRNase had no effect on cell viability. K41R hpRNase likewise did not affect cell viability.

In contrast, incorporation of the ERDD substitutions resulted in a hpRNase variant with

cytotoxic activity. ERDD hpRNase inhibited proliferation of K–562 cells with an IC_{50} of

7 μM. Incorporation of the K41R substitution into ERDD hpRNase increased the IC_{50} value

to 10 μM. Addition of the Cys4–Cys118 disulfide bond to ERDD hpRNase reduced the IC_{50}

value to 3 μM. The IC_{50} value for ONC was 0.4 μM.

3.5 Discussion

Ribonucleases exert cytotoxicity through a complex mechanism that includes association with the cell surface, internalization, and translocation to the cytosol (Rybak *et al.*, 1991; Newton *et al.*, 1992; Di Donato *et al.*, 1994; Newton *et al.*, 1994; Wu *et al.*, 1995; Leland *et al.*, 1998; Psarras *et al.*, 1998; Piccoli *et al.*, 1999; Suzuki *et al.*, 1999). Once in the cytosol, ribonucleases encounter RI, an extremely potent inhibitor of monomeric mammalian homologs of RNase A. We suspected that hpRNase variants that retain their conformation and ribonucleolytic activity in the presence of RI could destroy cellular RNA and cause cell death.

A cytotoxic hpRNase variant. The value of K_i for the inhibition of hpRNase by RI is a key determinant of cytotoxic activity. To change the K_i for hpRNase, we made four amino acid substitutions in a surface loop to yield ERDD hpRNase (Table 3.1). The ERDD substitutions reduce thermal stability by 4 °C and cause an unexpected 2-fold increase in the value of k_{cat}/K_m compared to hpRNase. Significantly, the ERDD substitutions yield a variant with K_i value of 2.1×10^{-10} M, which is at least 10^3-fold greater than that for hpRNase. This K_i value correlates with a pronounced cytotoxic activity, as ERDD hpRNase is toxic to K-562 cells with an IC_{50} value of 7 μM (Figure 3.3). In contrast, a higher dose of hpRNase has no effect on K-562 cell proliferation. Thus, we conclude that hpRNase has all the necessary features of a cytotoxic ribonuclease except for resistance to RI. hpRNase likely associates with the cell surface and then translocates to the cytosol. If resistant to RI, hpRNase has the conformational stability and ribonucleolytic activity sufficient to cause cell death.

Residues 31–33 of hpRNase comprise a putative nuclear localization signal [NLS (Silver, 1991); Figure 3.1]. This sequence is not conserved in RNase A or ONC, but is present in angiogenin, a homolog that causes neovascularization. Angiogenin is internalized by

subconfluent endothelial cells and accumulates in the nucleus (Moroianu & Riordan, 1994b; Moroianu & Riordan, 1994a; Hu *et al.*, 2000). Nuclear localization appears to be essential for the angiogenic activity of angiogenin—the R33A variant of angiogenin is not localized to the nucleus and is not angiogenic (Moroianu & Riordan, 1994a; Moroianu & Riordan, 1994b). To test if residues 31–33 play a role in the cytotoxicity of hpRNase, we created the R32A and the R33A variants of ERDD hpRNase. The IC_{50} values for both R32A ERDD hpRNase and R33A ERDD hpRNase were identical to that of ERDD hpRNase (data not shown). Thus, the mechanism of ERDD hpRNase cytotoxicity is unlikely to involve nuclear localization.

D'Alessio and coworkers have described a dimeric variant of hpRNase with cytotoxic activity (Piccoli *et al.*, 1999). Interestingly, the dimer was cytotoxic only after it was treated with an aminopeptidase to remove the *N*-terminal methionine residue [Met(−1)] produced by heterologous expression in *E. coli*. The cDNA used to produce hpRNase and its variants described herein also codes for an *N*-terminal methionine. We made no effort to remove [Met(−1)] from hpRNase or its variants. Nonetheless, the ERDD, K41R ERDD, and ERDD S–S variants of hpRNase are potent cytotoxins (Figure 3.3). Thus, it appears that a native *N*-terminus is not necessary for a monomeric variant of hpRNase to be cytotoxic.

Residues 88–90 of hpRNase comprise a consensus Asn–Xaa–Ser/Thr *N*-glycosylation sequence (Imperiali & Hendrickson, 1995)(Figure 3.1). We have shown that replacing residues 86, 88, 89, and 91 yields a variant of hpRNase that evades RI and is cytotoxic (Table 3.2). Likewise, glycosylation of Asn88 may enable hpRNase to evade RI. Interestingly, Asn88 of hpRNase is indeed glycosylated in humans, though only to a minor extent (Ribó *et al.*, 1994). Still, the implications of the existence of an endogenous ribonuclease that evades RI are intriguing.

Effect of replacing Lys41 on cytotoxicity. The K_i value for the inhibition of

ERDD hpRNase by RI is $\geq 5 \times 10^3$-fold less than that estimated for the inhibition of ONC

(Table 3.2). This difference is likely manifested in cytotoxic activity—ONC is almost 20

times more cytotoxic than ERDD hpRNase. We sought to increase ERDD hpRNase

cytotoxicity by incorporating an additional amino acid substitution that would increase

further its K_i value.

Previously, we showed that K41R/G88R RNase A is more cytotoxic than is

G88R RNase A (Bretscher *et al.*, 2000). Based on this result, we anticipated that replacing

Lys41 with an arginine residue in ERDD hpRNase would potentiate the cytotoxic activity of

this variant. Surprisingly, K41R/ERDD hpRNase is not more toxic to K-562 cells than is

ERDD hpRNase (Figure 3.3). This apparent contradiction can be resolved by considering the

conformational stability, the affinity for RI, and the catalytic activity of

K41R/ERDD hpRNase and K41R/G88R RNase A.

The T_m value of K41R/ERDD hpRNase is 49 °C, which is above physiological

temperature. Nonetheless, the transition between the native state and the unfolded state

begins near 37 °C (data not shown). In an unfolded state, K41R/ERDD hpRNase would lack

ribonucleolytic activity and, consequently, cytotoxic activity. Moreover, in an unfolded state,

K41R/ERDD hpRNase would be a substrate for cellular proteases. In contrast, the T_m value

for K41R/G88R RNase A is 63 °C (Bretscher *et al.*, 2000). This variant is significantly less

susceptible to thermal denaturation and subsequent proteolysis than is K41R/ERDD

hpRNase.

In the RI•RNase A complex, RNase A residue Lys41 makes van der Waals contacts with

RI residues Tyr430 and Asp431. The value of K_i measured for the K41R/ERDD variant was

7×10^{-10} M, which is a 3-fold increase compared to the value of K_i measured for ERDD

hpRNase. Replacing Lys41 with an arginine residue likely weakens the interaction with RI

by introducing steric conflicts, or by perturbing Coulombic interactions with Asp431, or

both. The K41R substitution also increases the value of K_i for G88R RNase A (Bretscher *et*

al., 2000). The K_i for K41R/G88R RNase A is, however, 3.2×10^{-9} M, which is almost 5-fold

greater than that for K41R/ERDD hpRNase.

In pancreatic-type ribonucleases, the side chain of Lys41 donates a single hydrogen bond

to the transition state during RNA cleavage (Messmore *et al.*, 1995). When incorporated into

ERDD hpRNase, the K41R substitution reduces the value of k_{cat}/K_m by 60-fold. This decrease

is consistent with an integral role for Lys41 in the hpRNase-catalyzed cleavage of RNA. The

K41R substitution also diminishes the catalytic activity of G88R RNase A. Still, at

5.0×10^5 M^{-1}s^{-1}, the value of k_{cat}/K_m for K41R/G88R RNase A is 10-fold greater than that of

K41R/ERDD hpRNase.

Thus, K41R/ERDD hpRNase is less stable, is more susceptible to inhibition by RI, and is

a worse catalyst of RNA cleavage than is K41R/G88R RNase A. We conclude that the K41R

substitution does not potentiate the cytotoxic activity of ERDD hpRNase because the

favorable change in the K_i value does not compensate for the unfavorable loss of catalytic

activity and conformational stability. In contrast, the K41R substitution in G88R RNase A

increases cytotoxic activity because the change in the K_i value does compensate for the loss

of catalytic activity and does not compromise conformational stability (Bretscher *et al.*,

2000).

Effect of a nonnative disulfide bond on cytotoxicity. As an alternative means to potentiate

the cytotoxicity of hpRNase, we added a nonnative disulfide bond to the ERDD variant. We

had used this strategy previously to increase the cytotoxicity of G88R RNase A (Klink & Raines, 2000). At 3 μM, the IC_{50} value of ERDD S–S hpRNase is nearly 3-fold less than that of ERDD hpRNase (Figure 3.3), and only 8-fold greater than that of ONC (Table 3.2). Again, the change in cytotoxicity is a consequence of changes to conformational stability and affinity for RI.

To create ERDD S–S hpRNase, residues Arg4 and Val118 of ERDD hpRNase were each replaced with a cysteine residue. In the folded protein, the Cys4–Cys118 disulfide bond forms a covalent crosslink between the enzymic N-terminal α-helix and C-terminal β-strand. The T_m of ERDD S–S hpRNase is 5 °C higher than that of ERDD hpRNase (Table 3.2). This increase in conformational stability is identical to that measured when the Cys4–Cys118 disulfide bond was added to G88R RNase A. ERDD S–S hpRNase is less prone to denaturation during the course of a cytotoxicity assay than is ERDD hpRNase. The conformational stability of a protein correlates with its proteolytic susceptibility (Parsell & Sauer, 1989; Kowalski et al., 1998; Klink & Raines, 2000). Thus, the nonnative Cys4–Cys118 disulfide bond enhances the cytotoxicity of ERDD hpRNase by preserving its three-dimensional structure and, hence, its ribonucleolytic activity in the cytosol.

The Cys4–Cys118 disulfide bond made a second, favorable contribution to the cytotoxic activity of the ERDD S–S variant. The K_i value for ERDD S–S hpRNase is 10-fold greater than that of ERDD hpRNase (Figure 3.2 and Table 3.2). The addition of the Cys4–Cys118 disulfide bond to ERDD hpRNase likely causes a subtle reorientation of the N-terminal α-helix and C-terminal β-strand, which disrupts intermolecular contacts with RI and thereby lowers the variant's affinity for RI.

Estimation of cytosolic ribonucleolytic activity. Cytotoxic ribonucleases kill cells because

they are able to degrade RNA in the presence of RI. The amount of ribonucleolytic activity

manifested in the cytosol can be approximated with eq 3.2 (Raines, 1999; Bretscher *et al.*,

2000):

$$\left(k_{cat}/K_m\right)_{cytosol} = \frac{k_{cat}}{K_m\left(1 + \frac{[RI]}{K_i}\right)} \tag{3.2}$$

To calculate $(k_{cat}/K_m)_{cytosol}$, we use the values of k_{cat}/K_m and K_i in Table 3.2 and estimate that

[RI] = 1 μM (Roth, 1967; Blackburn & Moore, 1982; Raines, 1999; Bretscher *et al.*, 2000).

Thus, the values of $(k_{cat}/K_m)_{cytosol}$ for K41R/ERDD hpRNase, ERDD hpRNase, and ERDD

S–S hpRNase are 3×10^1 $M^{-1}s^{-1}$, 6×10^2 $M^{-1}s^{-1}$, and 2.5×10^3 $M^{-1}s^{-1}$, respectively. It is

intriguing that as the value of (k_{cat}/K_m)cytosol increases, the value of IC_{50} decreases.

Prospectus. The hpRNase variants described herein have several distinct advantages

compared to other engineered cytotoxic ribonucleases. First, the cytotoxic hpRNase variants

are derived from a human protein. The amino acid sequences of ERDD hpRNase

($IC_{50} = 7$ μM) and ERDD S–S hpRNase ($IC_{50} = 3$ μM) are 97% and 95% identical to that of

hpRNase. In contrast, the amino acid sequence of ONC is only 31% identical to that of

hpRNase. Hence, the chemotherapeutic efficacy of the hpRNase variants is less likely to be

curtailed by an immune response. Second, the hpRNase variants are toxic to K-562 cells in

the absence of added drugs, such as retinoic acid. The IC_{50} values for ERDD hpRNase and

ERDD S–S hpRNase would likely decrease if administered in combination with small-

molecule chemotherapeutics. Third, the hpRNase variants are small, monomeric proteins and

do not require *in vitro* post-translational modifications. As such, the variants may be incorporated directly into a gene therapy protocol. Thus, the hpRNase variants may have significant promise as chemotherapeutic agents.

3.6 Acknowledgements

Table 3.1   Amino acid substitutions made in human pancreatic ribonuclease

hpRNase Residue	Substitution in hpRNase	Corresponding RNase A Residue[a]	Secondary Structure[b]	RI contact[c]
Arg4	R4C	Ala4	α-helix	none
Lys41	K41R	Lys41	active-site	Tyr430, Asp431
Leu86	L86E	Glu86	β-strand	Lys316
Asn88	N88R	Gly88	surface loop	Trp257, Trp259, Tyr433
Gly89	G89D	Ser89	surface loop	Glu202, Trp257, Trp259
Arg91	R91D	Lys91	surface loop	Trp257, Glu283, Trp314
Val118	V118C	Val118	β-strand	none

[a] From Figure 3.1.

[b] From the structure of crystalline RNase A (Wlodawer et al., 1988).

[c] From the structure of the crystalline RI•RNase A complex (Kobe & Deisenhofer, 1995; Kobe & Deisenhofer, 1996).

Table 3.2 Biochemical and biophysical parameters of human pancreatic ribonuclease, its variants, and Onconase™

Ribonuclease	T_m^a (°C)	k_{cat}/K_m^b (10^6 M⁻¹s⁻¹)	K_i^c (10^{-10} M)	IC_{50}^d (μM)
hpRNase	56	1.4 ± 0.1	–	–
K41R hpRNase	56	0.022 ± 0.06	ND	–
ERDD hpRNase	52	2.7 ± 0.3	2.1 ± 0.2	7
K41R ERDD hpRNase	49	0.048 ± 0.001	7 ± 2	10
ERDD S–S hpRNase	57	1.0 ± 0.1	26 ± 8	3
Onconase	90	0.0013 ± 0.0001	≥10^4	0.4

[a] T_m values (± 2 °C) for hpRNase and the hpRNase variants in PBS were determined by UV spectroscopy. The T_m value for onconase is from ref (Leland et al., 1998) and was determined by CD spectroscopy.

[b] k_{cat}/K_m values (± SE) are for catalysis of 6-FAM~dArUdAdA~6-TAMRA cleavage at pH 6.0 and 25 °C.

[c] K_i values (± SE) for the hpRNase variants are for inhibition of catalysis of 6-FAM~dArUdAdA~6-TAMRA cleavage at pH 6.0 and 25 °C by ribonuclease inhibitor. The K_i value for onconase is from ref. (Boix et al., 1996) and is an estimate based on the IC_{50} for inhibition.

[d] IC_{50} values are for the toxicity to K-562 cells (Figure 3.3).

ND: not determined

Figure 3.1   Amino acid sequences of ribonuclease A, human pancreatic ribonuclease, and

Onconase™.

Sequences were aligned using the PILEUP program, Version 9, from the

Genetics Computer Group (Madison, WI) with Gap Weight 1.00 and Gap

Length Weight 0.100. Residues are numbered according to RNase A.

Residues conserved among all three ribonucleases are boxed. RNase A

residues that contact RI in the RI•RNase A complex are white on black (Kobe

& Deisenhofer, 1995). The three residues most important for catalysis by

RNase A, as well as the corresponding residues in hpRNase and ONC, are

highlighted in blue. Cysteine residues are highlighted in yellow.

	1	10	20	30	40
RNase A (Bos taurus)	K E T A A A K F E R Q H M D S S T S A A S S S N Y C N Q M M K S R N L T K D R C K P				
hpRNase (human pancreas)	K E S R A K K F Q R Q H M D S D S S P S S S S T Y C N Q M M R R R N M T Q G R C K P V				
Onconase (Rana pipiens)	- Q D W L T - F Q K K H I T N T R D V D - - - - - C D N I M - S T N L - - F H C K D K				

	50	60	70	80
RNase A (Bos taurus)	N T F V H E S L A D V Q A V C S Q K N V A C K N G Q T N C Y Q S Y S T M S I T D C R I			
hpRNase (human pancreas)	N T F V H E P L V D V Q N V C F Q E K V T C K N G Q G N C Y K S N S S M H I T D C R L			
Onconase (Rana pipiens)	N T F I Y S R P E P V K A I C - K G I I A S K N V L T T - - - - - S E F Y L S D C N V			

	90	100	110	120	124
RNase A (Bos taurus)	T G S S K Y P N C A Y K T T Q A N K H I I V A C I G N P Y V P V F D A S V - - - -				
hpRNase (human pancreas)	T N G S R Y P N C A Y R T S P K E R H I I V A C E G S P Y V P V F D A S V E D S T				
Onconase (Rana pipiens)	T - - S R - P - C K Y K L K K S T N K F C V T C E N Q A - - P V F - V G V G S C -				

89

Figure 3.2   Agarose gel-based assay for ribonuclease inhibition by ribonuclease inhibitor.

Inhibition of ribonucleases (10 ng) was assessed by visualizing cleavage of

16S- and 23S-rRNA in the absence or presence of RI (20 or 40 units; one unit

of RI is defined as the amount of RI required to inhibit 5 ng of RNase A by

50%). Because the gel was run for only a short period of time, the 16S- and
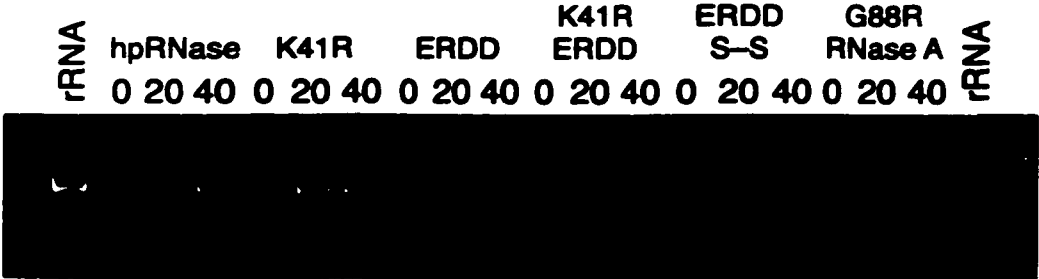
23S-rRNAs are not well resolved.

Figure 3.3   Proliferation of K-562 cells cultured in the presence of ribonucleases.

K-562 cell proliferation was measured by incorporation of [*methyl-*

^3H]thymidine into cellular DNA after a 44-h incubation with the

ribonucleases. Values reported are the mean of three cultures and are

expressed as the percentage of control cultures which lacked exogenous

ribonucleases.
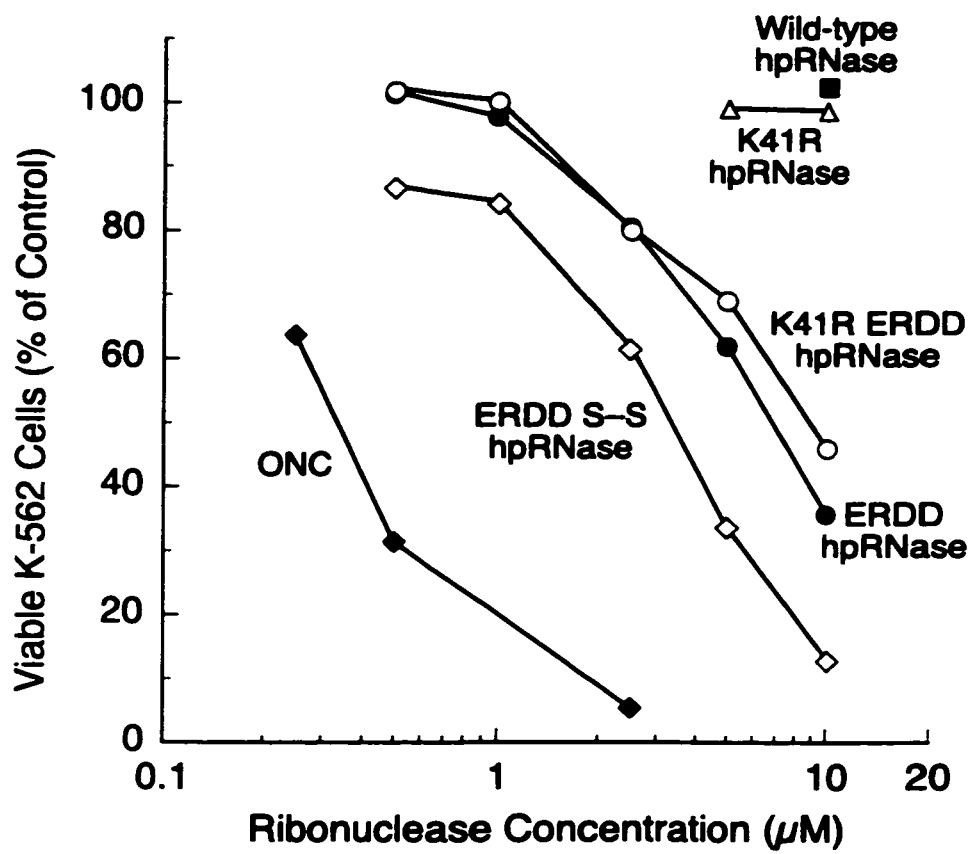
Chapter Four

A synapomorphic disulfide bond is critical for the conformational stability and cytotoxicity of an amphibian ribonuclease

This chapter has been submitted to *FEBS Letters* as:

Leland, P. A., Staniszewski, K. E., Kim, B. -M., and Raines, R. T. (2000) A synapomorphic disulfide bond is critical for the conformational stability and cytotoxicity of an amphibian ribonuclease. *FEBS Lett.*

4.1 Abstract

Onconase™ (ONC) is a homolog of ribonuclease A (RNase A) that has unusually high conformational stability and is toxic to human cancer cells *in vitro* and *in vivo*. ONC and its amphibian homologs have a *C*-terminal disulfide bond, which is absent in RNase A. Replacing this cystine with a pair of alanine residues greatly decreases the conformational stability of ONC. In addition, the C87A/C014A variant is 10-fold less toxic for human leukemia cells. These data indicate that the synapomorphic disulfide bond of ONC is an important determinant of its cytotoxicity.

4.2 Introduction

Onconase™ (ONC) is a ribonuclease that is present in the oocytes and early embryos of the Northern leopard frog (*Rana pipiens*) (Youle & D'Alessio, 1997; Irie *et al.*, 1998). ONC was discovered based on its potent anti-cancer activity (Darzynkiewicz *et al.*, 1988) and is currently being tested in Phase III human clinical trails for treatment of malignant mesothelioma, an asbestos-related lung cancer.

The amino acid sequence of ONC is 30% identical to that of bovine pancreatic ribonuclease A (RNase A; EC 3.1.27.5) (Ardelt *et al.*, 1991), the defining member of the pancreatic-type ribonuclease superfamily (Beintema *et al.*, 1988). The catalytic triad of residues characteristic of pancreatic-type ribonucleases (His12, Lys41, and His119 in RNase A) is conserved in ONC as His10, Lys31, and His97. ONC also retains three of the four disulfide bonds common to the pancreatic-type ribonucleases (Figure 4.1) (Wlodawer *et al.*, 1988; Mosimann *et al.*, 1994). In addition, ONC has a synapomorphic[2] disulfide bond between residues 87 and 104. The Cys87–Cys104 disulfide bond in ONC tethers its C-terminal residue to a central β-strand, and appears to be unique to the amphibian homologs of RNase A (Beintema *et al.*, 1988; Irie *et al.*, 1998).

ONC has unusually high conformational stability (Leland *et al.*, 1998). Here, we determine the contribution of the Cys87–Cys104 disulfide bond to the conformational stability of ONC. Specifically, we replace the half-cystines at residues 87 and 104 with a pair of alanine residues. We show that this variant of ONC (C87A/C104A ONC) has substantially

---

[2] Synapomorphic: *shared derived characteristic*; A characteristic feature present in a subset of homologous proteins. For example, amphibian ribonucleases, including ONC, can be distinguished from other pancreatic-type ribonucleases by their C-terminal disulfide bond.

less conformational stability than does the wild-type enzyme. In addition, we show that removal of the Cys87–Cys104 disulfide bond causes a significant decrease in cytotoxic activity.

4.3 Experimental Procedures

Materials. *E. coli* strain BL21(DE3) was from Novagen (Madison, WI). Enzymes used for DNA manipulation were from Promega (Madison, WI) or New England Biolabs (Beverly, MA). Oligonucleotides used for site-directed mutagenesis were from Integrated DNA Technologies (Coralville, IA). The substrate 6-carboxyfluorescein–dArUdAdA–6-carboxytetramethylrhodamine [6-FAM–dArU(dA)$_2$–6-TAMRA] was from Integrated DNA Technologies. Ribonuclease inhibitor (RI) was from Promega. K-562 cells were from the American Type Culture Collection (Manassas, VA). [*Methyl*-^{3}H]thymidine was from DuPont/NEN (Boston, MA). Phosphate buffered-saline (PBS) contained (in 1 liter) 0.20 g of KCl, 0.20 g of KH$_2$PO$_4$, 8.0 g of NaCl, and 2.16 g of Na$_2$HPO$_4$•7H$_2$O. All other chemicals and reagents were of commercial grade or better and were used without further purification.

Production of ribonucleases. Plasmid pONC directs the expression of wild-type ONC in *E. coli* (Leland *et al.*, 1998). Oligonucleotide-mediated site-directed mutagenesis of plasmid pONC was used to replace Cys87 and Cys104 with a pair of alanine residues. The integrity of the C87A/C104A ONC cDNA was confirmed by dye terminator cycle sequencing using a BigDye cycle sequencing kit (Perkin Elmer, Norwalk, CT) and an ABI 377XL Automated DNA Sequencer at the University of Wisconsin Biotechnology Center.

Wild-type ONC was produced, folded, and purified as described previously (Leland *et al.*, 1998). The concentration of ONC was determined by UV spectroscopy using an extinction coefficient of $\varepsilon_{280} = 0.87$ mL mg^{-1} cm^{-1}, which was calculated by using the method of Pace and coworkers (Pace *et al.*, 1995). The C87A/C104A variant of ONC was produced, folded, and purified using methods identical to those described for wild-type ONC (Leland *et al.*, 1998). Removal of a disulfide bond in ONC is expected to change the extinction coefficient by less than 1%, compared to that of the wild-type protein (Pace *et al.*, 1995). Hence, the concentration of C87A/C104A ONC was also determined using an extinction coefficient of $\varepsilon_{280} = 0.87$ mL mg^{-1} cm^{-1}. MALDI-TOF mass spectrometry was performed on a Bruker Biflex III instrument at the University of Wisconsin–Madison Biotechnology Center.

Circular dichroism spectroscopy. Circular dichroism (CD) spectra of ONC and C87A/C104A ONC (0.2 mg/mL in PBS) were collected at 25°C on an Aviv Model 202 SF CD spectrometer (Lakewood, NJ) equipped with an Aviv temperature controller. Raw data were converted to molar elipticity ($[\Theta]$) by using a mean residue mass of 110 Da.

Determination of conformational stability. The conformational stability of ONC was determined previously by using CD spectroscopy (Leland *et al.*, 1998). The conformational stability of C87A/C104A ONC was also determined by using CD spectroscopy to monitor the change in molar elipticity at 204 nm ($[\Theta_{204}]$) with increasing temperature. The temperature of an C87A/C104A ONC solution (0.2 mg/mL in PBS) was increased from 35°C to 85°C in 2°C-increments. The decrease in elipticity at 204 nm (Θ_{204}) was recorded after a 3-min equilibration at each temperature. CD data were fitted to a two-state model for denaturation (Pace *et al.*, 1989). The melting temperature (T_m) is the temperature at the midpoint of thermal denaturation curve.

Assay for ribonucleolytic activity. Ribonucleolytic activity was measured at (23 ± 2)°C in

2.00 mL of 0.10 M MES-NaOH buffer (pH 6.0) containing NaCl (0.10 M),

6-FAM~dArU(dA)$_2$~6-TAMRA (60 nM), enzyme (100–340 nM) and RI (0.1–0.3 nM).

Fluorescence was measured with a QuantaMaster 1 photon-counting fluorescence

spectrometer from Photon Technology International (South Brunswick, NJ) using excitation

and emission wavelengths of 495 nm and 515 nm, respectively. Values of k_{cat}/K_M were

determined by a linear least-squares regression analysis of initial velocity data using eq. 4.1:

$$k_{cat}\Big/K_m = \left(\frac{\Delta F\big/\Delta t}{F_{max} - F_0}\right)\frac{1}{[E]}$$ (4.1)

In eq. 4.1, $\Delta F/\Delta t$ is the slope from the linear regression, F_{max} is the maximal fluorescence

intensity, F_0 is the initial fluorescence intensity, and [E] is the enzyme concentration. F_{max}

was determined by adding RNase A (~0.1 μM final concentration) to the reaction after

completing the least-squares regression of the initial velocity data.

Determination of cytotoxic activity. The effect of ONC and C87A/C104A ONC on the

proliferation of a human leukemia cell line (K-562) was measured as described previously

(Leland *et al.*, 1998). Data represent the average of quadruplicate samples within an

individual assay. Results from two independent cytotoxicity assays did not deviate

significantly.

4.4 Results

Production and characterization of ribonucleases. Wild-type ONC and C87A/C104A

ONC were produced in *E. coli* with isolated yields of 25 and 15 mg per liter of culture,

respectively. Our yield of wild-type ONC is comparable to other methods for expression and

purification of the enzyme (Notomista *et al.*, 1999). Both proteins migrate as a single band of

appropriate M_r during SDS/PAGE (data not shown). Analysis of an equimolar mixture of

wild-type and C87A/C104A ONC with MALDI mass spectrometry gave two peaks with a

difference of 61 Da, consistent with the change in molecular mass expected for the

C87A/C104A substitution (data not shown). The CD spectra of wild-type and C87A/C104A

ONC do, however, differ (Figure 4.2). Notably, the molar elipticity of C87A/C104A ONC

becomes positive at a lower wavelength than does the signal of wild-type ONC. This change

is consistent with accumulation of random secondary structure, potentially at the expense of

β-sheet, in the C87A/C104A variant of ONC (Woody, 1995).

Contribution of the Cys87–Cys104 disulfide bond to conformational stability. ONC has

remarkable conformational stability—its T_m is 90°C. Previously, we suggested that the high

conformational stability of ONC, compared to that of RNase A (T_m of 62°C), is due a

disulfide bond between ONC residues 87 and 104 (Leland *et al.*, 1998). Cytotoxic

ribonucleases from the oocytes of *Rana japonica* (Japanese rice paddy frog) and

Rana catesbeiana (Bullfrog) each retain a disulfide bond analogous to the Cys87–Cys104

pairing in ONC (Titani *et al.*, 1987; Kamiya *et al.*, 1990; Chang *et al.*, 1998). Significantly,

the *R. catesbeiana* and *R. japonica* ribonucleases also have high conformational stability

(T_m > 75°C) (Okabe *et al.*, 1991).

The T_m of C87A/C104A ONC was measured by using CD spectroscopy to record the

change in molar elipticity at 204 nm with increasing temperature. As shown in Figure 2 and

listed in Table 4.1, the Cys87–Cys104 disulfide bond does contribute significantly to the

conformational stability of ONC. Indeed, the T_m of the C87A/C104 variant of ONC is 62°C,

which is almost 30°C lower than that of the wild-type enzyme.

Contribution of the Cys87–Cys104 disulfide bond to ribonucleolytic activity. The

ribonucleolytic activity of ONC is less than that of RNase A. Nevertheless, ribonucleolytic

activity is necessary for the cytotoxic activity of ONC (Wu *et al.*, 1993). The contribution of

the Cys87–Cys104 disulfide bond to ribonucleolytic activity was determined in MES-NaOH

buffer (pH 6.0) containing NaCl and RI. Because RI binds to RNase A with extraordinarily

high affinity ($K_d = 4.4 \times 10^{-14}$ M (Lee *et al.*, 1989)) but is a weak inhibitor of ONC (estimated

$K_i \geq 10^{-6}$ M (Boix *et al.*, 1996)), addition of small amount of RI ($\leq 3 \times 10^{-10}$ M) to the assay is

an effective method to eliminate any trace contaminating ribonucleolytic activity from

pancreatic-type ribonucleases without inhibiting the catalytic activity of ONC. Indeed,

addition of RI to a rabbit reticulocyte lysate does not change the ability of ONC to inhibit

protein synthesis (Newton *et al.*, 1997).

As reported in Table 4.1, ONC cleaves a tetranucleotide substrate with a k_{cat}/K_M value of

2.2×10^2 M^{-1}s^{-1}. This value is slightly lower than that reported previously (Bretscher *et al.*,

2000). This difference is likely due to contaminating ribonucleolytic activity in previous

assays, which is eliminated by addition of RI to the assays described herein. At

0.6×10^2 M^{-1}s^{-1}, the value of k_{cat}/K_M for C87A/C104A ONC is only 4-fold lower than that of

the wild-type enzyme.

Contribution of the Cys87–Cys104 disulfide bond to cytotoxicity. The effect of ONC and

the C87A/C104A variant on the viability of a human leukemic cell line was tested by

measuring incorporation of a ^{3}H-labeled nucleotide into DNA after a 44-h incubation with

the ribonucleases. As shown in Figure 4.3 and listed in Table 4.1, ONC inhibited

proliferation of K-562 cells with an IC_{50} of 0.2 μM. Deletion of the Cys87–Cys104 disulfide

bond reduced substantially the cytotoxic activity of ONC. At 2 μM, the IC_{50} value for

C87A/C104A ONC was 10-fold higher than that of the wild-type enzyme.

4.5 Discussion

ONC kills cells by cleaving RNA, a cytosolic molecule (Wu *et al.*, 1993). Changes that

compromise ribonucleolytic activity within the cytosol should also compromise cytotoxic

activity. For example, alkylation of the active-site histidine residues yields an ONC

derivative that lacks catalytic activity and is ineffective as a cytotoxin (Wu *et al.*, 1993).

Additionally, the Met(−1) variant of ONC is an inefficient catalyst and a weak cytotoxin

(Boix *et al.*, 1996; Newton *et al.*, 1997). The value of k_{cat}/K_M of C87A/C104A ONC is 4-fold

lower than that of the wild-type enzyme (Table 4.1). This change may reduce the cytotoxic

potency of this variant. Deletion of the Cys87–Cys104 disulfide bond could also decrease

cytotoxicity by a second mechanism.

ONC likely encounters proteases while routing to the cytosol, or within the cytosol itself.

The high conformational stability of ONC may limit susceptibility to cellular proteases and

thus allow for accumulation of ribonucleolytic activity in the cytosol. CD spectra indicate

that C87A/C104A ONC contains more random secondary structure than does wild-type ONC

(Figure 4.2), a difference that is consistent with the loss of a covalent crosslink. Additionally, the conformational stability of the C87A/C104A variant is lowered significantly compared to that of the wild-type enzyme (Figure 4.2; Table 4.1). These changes may render the variant more susceptible to attack by endopeptidases. If so, a higher concentration of enzyme would be necessary to deliver sufficient ribonucleolytic activity to kill the cell.

In addition to defining secondary structure and enhancing conformational stability, the C-terminal disulfide bond of ONC may limit the susceptibility of ONC to carboxypeptidases. In this respect, it is intriguing that the N-terminal residue in ONC, as well as that in the R. catesbeiana and R. japonica ribonucleases, is pyroglutamate (which forms from the N-terminal glutamine residue (Awade et al., 1994)). This cyclic residue could confer resistance to exopeptidases that would otherwise act at the N-terminus of wild-type ONC and the C87A/C104A variant. The C-terminus of the variant is, however, unobstructed and could be a substrate for carboxypeptidases.

Recently, we used a cytotoxic RNase A variant to define the relationship between ribonuclease stability and cytotoxic activity (Klink & Raines, 2000). By removing a native disulfide bond, or by incorporating a nonnative disulfide bond in a cytotoxic RNase A variant, we created a family of cytotoxins with differing conformational stabilities. Significantly, as the conformational stability of the variants increases, their cytotoxicity also increases. Concomitantly, increased conformational stability correlates with reduced susceptibility to proteolysis. Thus, the ribonucleolytic activity and, consequently, the cytotoxicity, of ribonucleases appear to be dependent on proteolytic susceptibility. Ribonucleases with high conformational stability retain catalytic activity within the cytosol for a greater period of time and therefore, are more effective cytotoxins.

Conclusions. The Cys87–Cys104 disulfide bond of ONC is present in monomeric

cytotoxic homologs of ONC, but absent in monomeric homologs that lack cytotoxicity. We

find that this disulfide bond makes a substantial contribution to the conformational stability

of ONC. A variant lacking this disulfide bond is 10-fold less toxic for human leukemia cells.

We conclude that the Cys87–Cys104 disulfide bond is an important determinant of the

cytotoxicity of ONC.

4.6 Acknowledgements

Table 4.1   Biochemical and biophysical parameters of Onconase™ and its

C87A/C104A variant

Onconase™	T_m^a (°C)	k_{cat}/K_M^b (10² M⁻¹s⁻¹)	IC_{50}^c (μM)
Wild-type	90 ± 2	2.2 ± 0.1	0.2
C87A/C104A	62 ± 2	0.6 ± 0.1	2.0

[a] Values of T_m (± SE) were determined by circular dichroism

spectroscopy (Figure 4.2).

[b] Values of k_{cat}/K_M values (±S.E.) are for catalysis of

6-FAM~dArU(dA)₂~6-TAMRA cleavage at pH 6.0 and 23°C in

the presence of RI (0.1–0.3 nM), which inhibits any contaminating

pancreatic-type ribonucleases.

[c] Values of IC_{50} are for toxicity to human leukemia cell strain

K–562 (Figure 4.3).

Figure 4.1   Connectivity of the disulfide bonds in Onconase™ (104 residues) and

ribonuclease A (124 residues).

The secondary structural context of each half-cystine residue is indicated by H

(α-helix), S (β-sheet), or L (loop). The N-terminal residue of Onconase™ is a
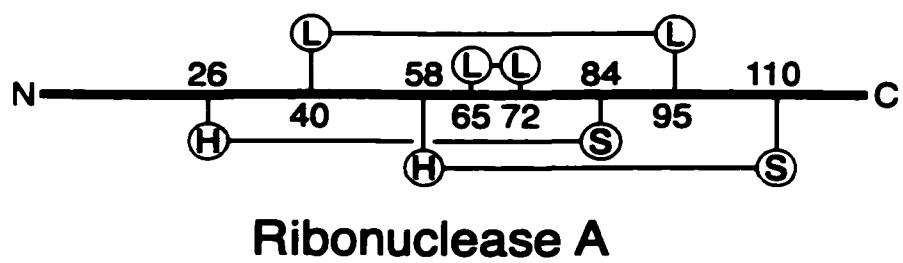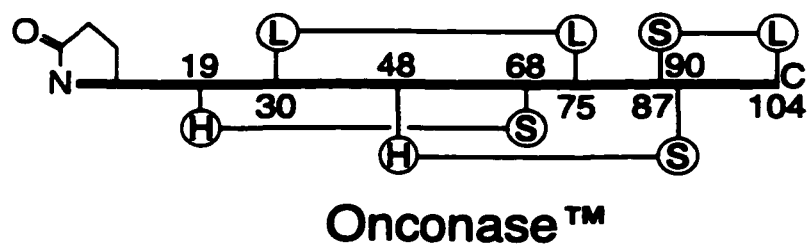
pyroglutamate.

Onconase™

Ribonuclease A

Figure 4.2.   Conformation and conformational stability of wild-type Onconase™ and the

C87A/C104A variant in phosphate-buffered saline.

(A) Circular dichroism spectrum of wild-type Onconase™ (solid line) and

C87A/C104A Onconase (broken line) at 25 °C. Inset: spectra normalized

using the molar elipticity at 210 nm as a reference. (B) Thermal unfolding of

wild-type Onconase™ and the C87A/C104A variant monitored by circular

dichroism spectroscopy at 204 nm. Data for wild-type Onconase™ are from

ref. (Leland et al., 1998).
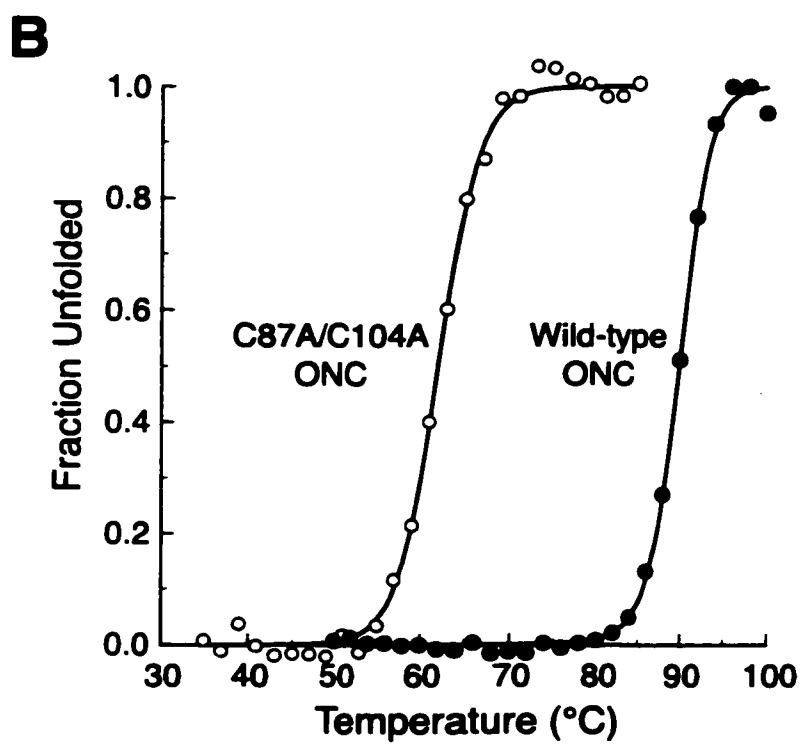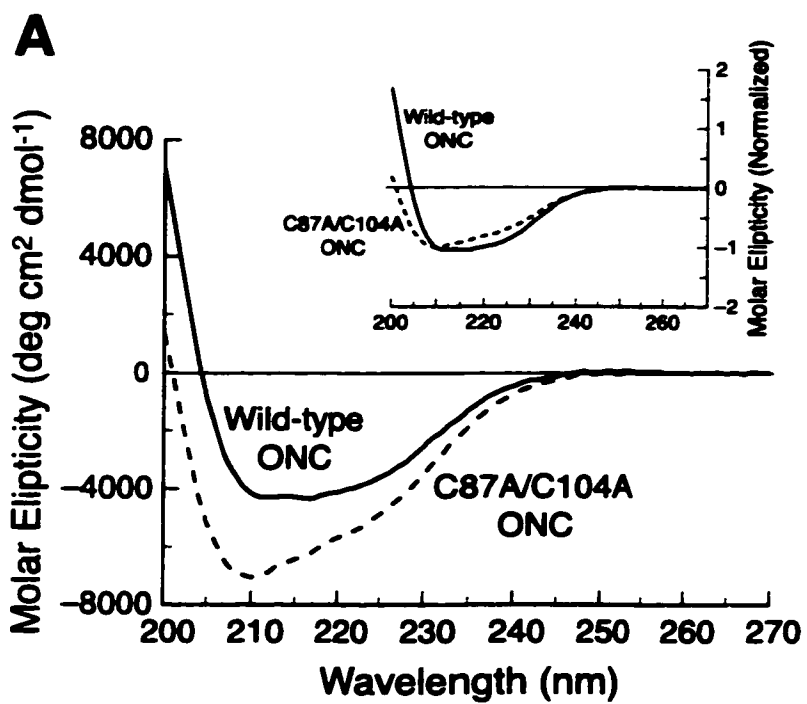
Figure 4.3   Proliferation of human leukemia cell strain K-562 in the presence of wild-type

Onconase™ and the C87A/C104A variant.

Cell proliferation was measured by incorporation of [*methyl*-^{3}H]thymidine

into cellular DNA after a 44-h incubation with the ribonucleases. Values are

the mean of four cultures and are expressed as the percentage of control

cultures lacking exogenous ribonucleases. The standard error of each point is

<11%.
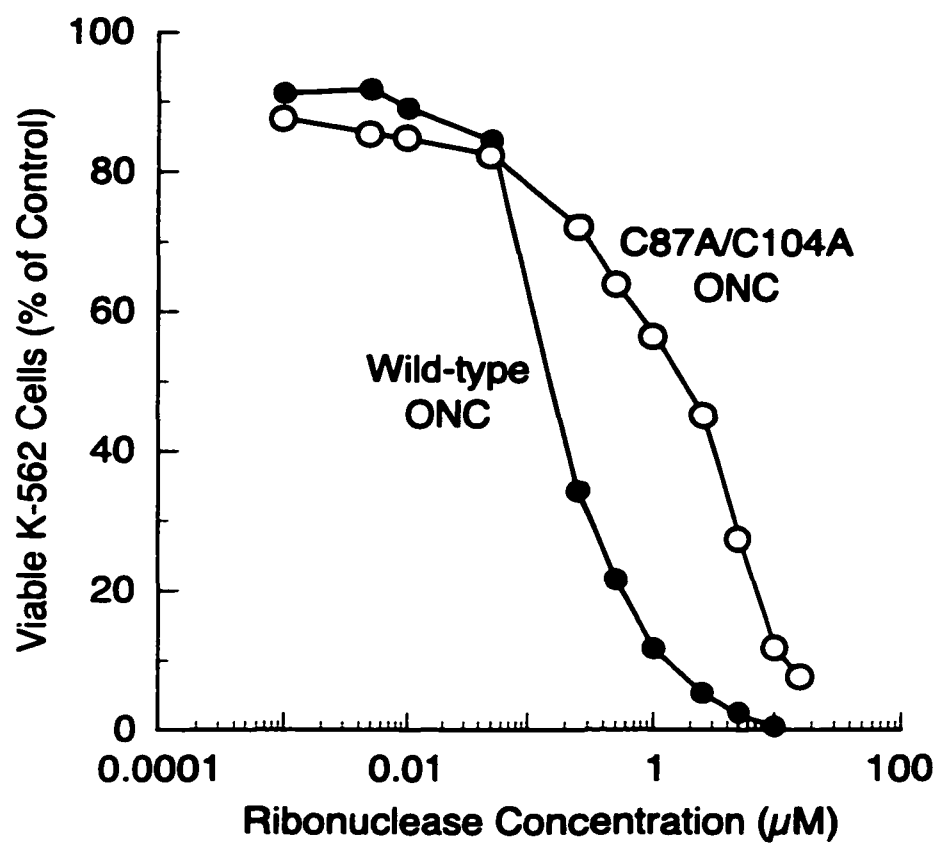
Chapter Five

The Ribonucleolytic Activity of Angiogenin

5.1 Abstract

Angiogenin (ANG), a homolog of bovine pancreatic ribonuclease A (RNase A), promotes the growth of new blood vessels. The biological activity of ANG is dependent on its ribonucleolytic activity, which surprisingly is 10^4- to 10^6-fold lower than that of RNase A. Here, the efficient heterologous production of human ANG in *Escherichia coli* is achieved by replacing two sequences of rare codons with codons favored by *E. coli*. Hypersensitive fluorogenic substrates are used to determine steady-state kinetic parameters for catalysis by ANG in continuous assays. The ANG pH–rate profile is a classic bell-shaped curve, with $pK_1 = 5.0$ and $pK_2 = 7.0$. The ribonucleolytic activity of ANG is highly sensitive to Na^+ concentration. A decrease in Na^+ concentration from 0.25 M to 0.025 M causes a 170-fold increase in the value of k_{cat}/K_M. Likewise, the binding of ANG to a tetranucleotide substrate analog is dependent on $[Na^+]$. ANG cleaves a dinucleotide version of the fluorogenic substrates with a k_{cat}/K_M value of 61 $M^{-1}sec^{-1}$. When the substrate is extended from two nucleotides to four or six nucleotides, values of k_{cat}/K_M increase 5- and 12-fold, respectively. Together, these data provide a systematic evaluation of substrate binding and turnover by ANG.

5.2 Introduction

Angiogenin (ANG) is a 14.1-kDa protein that promotes angiogenesis—the growth of new capillaries from an existing capillary network (Riordan, 1997). ANG was first isolated from the conditioned media of a human adenocarcinoma and later identified as a component of normal human plasma (Fett *et al.*, 1985; Shapiro *et al.*, 1987). Determination of the amino acid sequence revealed that ANG is a member of the bovine pancreatic ribonuclease A (RNase A) family of enzymes (Strydom *et al.*, 1985).

Like RNase A, ANG catalyzes hydrolysis of the $P-O^{5'}$ bond in RNA. The ribonucleolytic activity of ANG has been reported to be 10^4- to 10^6-fold lower than that of RNase A, but nevertheless is necessary for angiogenic activity (Riordan, 1997). As a consequence of its low ribonucleolytic activity, ANG has typically been assayed in a discontinuous manner. The effects of pH and salt concentration on catalysis by ANG have not been analyzed in detail.

Recently, we described a hypersensitive assay for ribonucleolytic activity based on the relief of fluorescence quenching (Kelemen *et al.*, 1999). We showed that ANG cleaves a tetranucleotide version of these substrates with a k_{cat}/K_M value of $3.3 \times 10^2 \ M^{-1}sec^{-1}$. This value is more than 10-fold greater than those reported for other ANG substrates. Moreover, this value of k_{cat}/K_M was determined with a continuous assay.

Here, we show that expression in *Escherichia coli* of the cDNA for human ANG is limited by codon usage. We overcome this limitation by replacing several rare codons with the corresponding codons favored by *E. coli*. We then used our hypersensitive assay to characterize in detail the ribonucleolytic activity of ANG. First, we determine the pH–rate profile for ANG. Next, we measure the effect of salt concentration on catalysis by ANG.

Finally, we measure the effect of substrate length on the ribonucleolytic activity of ANG. In

addition to assays of catalytic activity, we measure the effect of salt concentration on the

binding of ANG to a single-stranded nucleic acid. Our data provide a comprehensive picture

of substrate binding and turnover by ANG.

5.3 Experimental Procedures

Materials: *E. coli* strain DH5α was from Life Technologies (Gaithersburg, MD). *E. coli*

strain BL21(DE3) and the pET22b(+) expression vector were from Novagen (Madison, WI).

Enzymes used for DNA manipulation were from Promega (Madison, WI) or New England

Biolabs (Beverly, MA). Poly(cytidylic acid) [poly(C)] was from Midland Certified Reagent

(Midland, TX). The fluorogenic ribonuclease substrates (Table 5.1) were from Integrated

DNA Technologies. All other chemicals and reagents were of commercial grade or better and

were used without further purification.

DNA oligonucleotides for the PCR, site-directed mutagenesis, and DNA sequencing were

from Integrated DNA Technologies (Coralville, IA) or Life Technologies. The PCR reactions

was performed with reagents from PanVera (Madison, WI). DNA was sequenced with a

Sequenase 2.0 kit from United States Biochemicals (Cleveland, OH) or with a BigDye cycle

sequencing kit (Perkin Elmer, Norwalk, CT) and a ABI 377XL Automated DNA Sequencer

at the University of Wisconsin–Madison Biotechnology Center.

UV absorbance measurements were made on a Cary Model 3 spectrophotometer or a

Cary 50 Bio spectrophotometer (Varian, Palo Alto, CA). Fluorescence-based assays for

ribonucleolytic activity were performed with a QuantaMaster 1 Photon Counting

Fluorometer equipped with sample stirring (Photon Technology International, South

Brunswick, NJ).

Construction of the pANG plasmid. A cDNA coding for human ANG was the generous

gift of Promega. The ANG cDNA was amplified with the PCR and oligonucleotides PAL1

(5′-CCACCGACC<u>CATATG</u>CAGGATAACTCCAGGTACACACAC-3′) and PAL2a

(5′-CCAGGGGCC<u>CTCGAG</u>TTACGGACGACGGAAATTGACTG-3′). Oligonucleotide

PAL1 incorporated an *Nde*I site (underlined) and, consequently, a Met(−1) in the 5′ end of

the cDNA. The catalytic and biological activities of Met(−1) ANG are indistinguishable from

those of native ANG (Shapiro *et al.*, 1988). PAL2a incorporates an *Xho*I site (underlined)

immediately 3′ to the UAA termination codon. The amplified cDNA fragment was purified

with a Wizard PCR purification kit (Promega) and digested with *Nde*I and *Xho*I. The digest

product was band-purified and then ligated to the band-purified *Nde*I-*Xho*I fragment of

pET22B(+). The integrity of the ANG cDNA was confirmed with sequencing.

The ANG cDNA contains two prominent runs of codons that occur with low frequency in

the *E. coli* genome. To optimize bacterial expression of ANG, these rare codons were

replaced with high frequency *E. coli* codons by using site-directed mutagenesis.

Oligonucleotide PAL5 (5′-TGAGGTCAG<u>GCC*GCGA*CGGC</u>GCATGATGCTTTCA-3′) was

used to replace the rare arginine codons 31–33 ([31]AGG, [32]AGA, and [33]CGG) with preferred

codons for arginine ([31]CGC, [32]CGU, and [33]CGC; reverse complements in italics) and to

incorporate a silent *Bgl*I site (underlined). Oligonucleotide PAL6 (5′-AGAAGACTTGCT

AATGC<u>GCAGG</u>TTTTC*GCG*GTGAGGGTTTCCA-3′) was used to replace the rare codons

of Arg66, Leu69, Arg70, and Ile71 ([66]AGA, [69]CUA, [70]AGA, [71]AUA) with preferred codons

for these amino acids ([66]CGC, [69]CUG, [70]CGC, and [71]AUU; reverse complements in italics)

and to incorporate a silent *BspMI* site (underlined). Following mutagenesis, the integrity of the ANG cDNA was confirmed by sequencing. The pET22B(+)-based vector carrying the optimized ANG cDNA was named pANG and was used exclusively for expression of wild-type ANG.

Expression of ANG from the pET-22b(+)-based vectors was quantitated with SDS–PAGE. Cells (1 mL) from a 20 mL culture were collected immediately prior to and 2 h after induction with IPTG. Pelleted cells were resuspended in 0.2 mL of 0.05 M Tris-HCl buffer (pH 6.8) containing DTT (0.1 M), SDS (2% w/v), bromphenol blue (0.1% w/v), and glycerol (10% v/v). Samples were boiled for 15 min, loaded on to a polyacrylamide (15% w/v) gel, and subjected to electrophoresis. The ANG induction bands were quantitated with ImageQuant™ software from Molecular Dynamics. Pre-induction samples were used to subtract the contribution of bands that comigrated with ANG. A high M_r band was used to normalize the induction bands for differences in loading.

Angiogenin Production and Purification. ANG was overexpressed and purified using methods described previously, with the following modifications (Leland *et al.*, 1998). Following expression in *E. coli* strain BL21(DE3) and cell lysis with a French pressure cell, inclusion bodies (containing ANG) were recovered by centrifugation and resuspended in 20 mM Tris-HCl buffer, pH 8.0, containing guanidine-HCl (7 M), DTT (10 mM), and EDTA (10 mM). The inclusion bodies were solubilized and denatured by stirring at room temperature for 2 h. The protein solution was then diluted 10-fold with 20 mM AcOH, centrifuged to remove precipitant, and dialyzed overnight versus 20 mM AcOH. Material that precipitated during dialysis was removed by centrifugation. Folding of ANG was initiated by drop-wise addition into 0.10 M Tris-HCl buffer (pH 7.8) containing L-Arg (0.5 M), reduced

glutathione (3 mM), and oxidized glutathione (0.6 mM) at 4 °C. High concentrations of L-

Arg appear to suppress aggregation by enhancing the stability of partially structured folding

intermediates (De Bernardez-Clark *et al.*, 1999). ANG was then concentrated by

ultrafiltration and applied to a Superdex G-75 gel filtration FPLC column (Pharmacia,

Pisataway, NJ) equilibrated in 50 mM sodium acetate buffer (pH 5.0), containing NaCl (0.10

M) and NaN_3 (0.02% w/v). Fractions corresponding to monomeric ANG were pooled and

applied to a Mono S cation-exchange FPLC column (Pharmacia). ANG was eluted from the

column with a linear gradient of NaCl (0.52–0.62 M) in 20 mM sodium phosphate buffer (pH

7.2).

Trace amounts of any contaminating ribonucleases were removed from ANG by

chromatography on a dedicated HiTrap SP cation-exchange column using a LKB peristaltic

pump (Pharmacia). All buffers were made with DEPC-treated ddH_2O. Initially, the column

was equilibrated with 50 mM sodium phosphate buffer (pH 7.0). The system was then

flushed with 20 mL of 50 mM sodium phosphate buffer (pH 7.0) containing NaCl (1.0 M)

and again equilibrated with 50 mM sodium phosphate buffer (pH 7.0). ANG (5 mg) in

50 mM sodium phosphate buffer (pH 7.0) was loaded onto the column. The loaded column

was washed with 20 mL of 50 mM sodium phosphate buffer (pH 7.0) and then with 35 mL of

50 mM sodium phosphate (pH 7.0) containing NaCl (0.30 M). ANG was eluted from the

column with 40 mL of 50 mM sodium phosphate buffer (pH 7.0) containing NaCl (1.0 M).

The sample was dialyzed exhaustively against ddH_2O, concentrated, and aliquoted into 1.7

mL siliconized tubes. Zymogram electrophoresis was used to confirm that final preparations

were ANG were free from contaminating ribonucleolytic activity (Blank *et al.*, 1982; Ribó *et*

al., 1991; Kim & Raines, 1993b; delCardayré et al., 1995). ANG concentration was

determined by UV spectroscopy with an extinction coefficient of ε_{280} = 0.85 mL mg^{-1} cm^{-1}.

Steady-state kinetics. All assays of ribonucleolytic activity were performed in a 2 mL

final volume with stirring at (25 ± 2) °C. Buffer systems, substrate concentration, and

enzyme concentration varied between the assays and are described below. Fluorogenic

substrates were used to measure *s*teady-state kinetic parameters (Kelemen et al., 1999). The

substrates consist of a single ribonucleotide embedded within a series of

deoxyribonucleotides (Table 5.1). The 5' end of each substrate is labeled with 6-

carboxyfluorescein (6-FAM) and the 3' end is labeled with 6-carboxytetramethylrhodamine

(6-TAMRA; substrates 1-4) or 4-((4-(dimethylamino)phenyl)azo)benzoic acid (4-DABCYL;

substrate 5). When the substrate is intact, 6-TAMRA or 4-DABCYL quenches the

fluorescence of 6-FAM. Ribonucleolytic cleavage manifests 6-FAM fluorescence. Cleavage

of the fluorogenic substrates was observed by recording fluorescence emission at 515 nm

with excitation at 490 nm. Values of k_{cat}/K_M were determined by a linear least-squares

regression analysis of the initial fluorescence change using eq (5.1).

$$\frac{k_{cat}}{K_m} = \left(\frac{\Delta F/\Delta t}{F_{max} - F_0} \right) \frac{1}{[E]} \qquad (5.1)$$

In eq 5.1, $\Delta F/\Delta t$ is the slope from the linear regression analysis, F_{max} is the maximal

fluorescence intensity, F_0 is the initial fluorescence intensity, and [E] is the total enzyme

concentration. F_{max} was determined by adding RNase A (~0.1 μM final concentration) to the

reaction mixture after the correlation coefficient (R^2) for the regression analysis of the initial velocity data was greater than 0.99.

pH–rate profiles for catalysis by ANG. Reactions for determination of the ANG pH–rate profile were performed in a three-component buffer system containing acetate (0.05 M), MES (0.05 M), and Tris (0.10 M) (Ellis & Morrison, 1982). The buffer pH was adjusted with HCl or NaOH as required. This buffer system maintains a constant ionic strength (I = 0.1 M) from pH = 4.0 to pH = 8.0. In addition to the buffer system, reactions mixtures contained NaCl (0.1 M), substrate 5 (20 nM), and ANG (470 nM). Substrate 5 (Table 5.1) uses 6-DABCYL as the quenching group. Unlike 6-TAMRA, 6-DABCYL is chemically stable at acidic pH and is therefore better suited for the determination of pH-rate profiles. Data for RNase A and ANG were fitted to eq 5.2, which describes the participation of two titratable residues in catalysis:

$$\left(k_{cat}\Big/K_M\right)_{obs} = \frac{\left(k_{cat}\Big/K_M\right)_{INT}}{\dfrac{[H^+]}{K_1} + 1 + \dfrac{K_2}{[H^+]}} \tag{5.2}$$

In eq 5.2, $(k_{cat}/K_M)_{obs}$ is the observed k_{cat}/K_M, $(k_{cat}/K_M)_{INT}$ is the intrinsic value of k_{cat}/K_M, K_1 is the acidity constant for the first titratable residue, and K_2 is the acidity constant for the second titratable residue. The value of $(k_{cat}/K_M)_{obs}$ at each pH was determined using eq 5.1 as described above.

Salt–rate profile for catalysis by ANG. Reactions for determination of the effect of [Na$^+$] on ANG catalysis were performed in 1 mM Bis-Tris buffer (pH 6.0) containing NaCl

(0.025–0.25 M), substrate **2** (6 nM), and ANG (47 nM). Values of k_{cat}/K_M were determined at

seven Na^+ concentrations. At $[Na^+]$ less than 0.01 M, the value of K_M for ANG acting on

substrate **2** is comparable to the concentration of the substrate used in these determinations.

With this condition, it is not feasible to measure accurate values of k_{cat}/K_M. We used eq 5.3

(Park & Raines, 2000a) to describe the dependence of catalysis by ANG on Na^+.

$$\left(\frac{k_{cat}}{K_M}\right)_{obs} = \left(\frac{k_{cat}}{K_M}\right)^{\Theta} [Na^+]^n \qquad (5.3)$$

In eq 5.3, $(k_{cat}/K_M)_{obs}$ is the observed k_{cat}/K_M at each Na^+ concentration, $(k_{cat}/K_M)^{\Theta}$ is the value

of k_{cat}/K_M when $[Na^+] = 1.0$ M, and n describes the dependence of catalysis on $[Na^+]$. This

equation is analogous to an equation used by Record and coworkers to describe the effect of

$[Na^+]$ on the binding of DNA ligands to proteins (Record et al., 1976). These authors show

that the slope of a $\log[K_d]$ versus $\log[Na^+]$ plot provides a quantitative measure of the number

of ion pairs formed between a DNA ligand and a protein. Their analysis is, however, limited

to the interactions between polyelectrolytes (>18 DNA monomer units) and proteins (Zhang

et al., 1996). Substrate **2**, which was used to determine the ANG salt–rate profile, is a

tetranucleotide (Table 5.1). Therefore, the value of n calculated using eq 5.3 does not provide

a quantitative measure of the number of ion pairs between ANG and substrate **2**.

Nonetheless, comparison of the values of n determined for ANG and those calculated for

other pancreatic-type ribonucleases under similar conditions provides a measure of the

relative importance of Coulombic interactions on catalysis.

Substrate dependence of catalysis by ANG. Substrates **1–4** (Table 5.1), which include

three, five, seven, or nine phosphoryl groups, respectively, were used to measure the effect of

substrate length on ANG catalysis. Reactions were performed in 0.10 M MES-NaOH buffer

(pH 6.0) containing NaCl (0.10 M), substrate (4–60 nM), and ANG (470 nM) at (25 ± 2) °C.

Values of k_{cat}/K_M were calculated using eq 5.1 and are the average of duplicate or triplicate

determinations for each substrate.

Fluorescence Anisotropy. Fluorescence anisotropy was used to measure the binding

affinity of single-stranded DNA, which serves as a substrate analog, to ANG. Here, we used

a tetranucleotide with a 5′ fluorescein label [Fl~d(AUAA)]. The concentration of

Fl~d(AUAA) was 5 nM. Fluorescence anisotropy was measured at (25 ± 2) °C in 0.01 M

MES–NaOH buffer (pH 6.0) containing NaCl (0.02 or 0.10 M) as described previously

(Fisher *et al.*, 1998b). Data collected at 0.10 M NaCl were fitted to eq 5.4.

$$A = \frac{\Delta A \cdot [\text{Ang}]}{K_d + [\text{Ang}]} + A_{min} \tag{5.4}$$

In eq 5.4, A is the measured fluorescence anisotropy, ΔA is the total change in anisotropy,

and A_{min} is the anisotropy of the unbound tetranucleotide (Fisher *et al.*, 1998b). Eq 5.4

describes binding at a single specific site. Yet, at 0.02 M NaCl and high [ANG], the substrate

analog also binds nonspecifically to ANG. Therefore, data collected at 0.02 M NaCl were

fitted to eq 5.5, which includes a term ($K_{ns}\cdot[\text{ANG}]$) to describe the nonspecific binding.

$$A = \frac{\Delta A \cdot [\text{Ang}]}{K_d + [\text{Ang}]} + A_{\text{min}} + K_{ns} \cdot [\text{Ang}] \tag{5.5}$$

5.4 Results

Production and purification of ANG. Our initial attempts to produce and purify human

ANG from a pET-22b(+)-based vector yielded less than 2 mg of protein per L of *E. coli*

growth medium. Analysis with SDS–PAGE showed that the low yield was due to poor

expression of the ANG cDNA in *E. coli* (Figure 5.1). The ANG mRNA has multiple

occurrences of codons that are disfavored by *E. coli*. In two instances, these rare codons are

sequential. The codons for Arg31, Arg32, Arg33 occur with a frequency of less than five per

1000 codons (Wada *et al.*, 1991). When these rare codons are replaced with the arginine

codons favored by *E. coli*, expression of ANG increases by 4.0-fold (Figure 5.1). The codons

for Arg66, Leu69, Arg70, Ile71 occur with a frequency of less than four per 1000 codons.

When these rare codons are exchanged for the corresponding favored codons, expression of

ANG increases by 2.2-fold compared to that with the native cDNA. Finally, when both sets

of codon substitutions are incorporated in a single cDNA, the expression level is 4.2-fold

greater than that with the native ANG cDNA. This new cDNA was named pANG and used

exclusively for production of ANG.

After induction of expression with IPTG, ANG accumulated in inclusion bodies of the

E. coli cells. The inclusion bodies were reduced, denatured, folded, and applied to a gel

filtration column. Monomeric ANG represented the major peak on the chromatogram. The

gel filtration fractions were then applied to a cation-exchange column. ANG eluted as a

defined peak. Preparations used to measure kinetic parameters were applied to a second

cation-exchange column to remove any trace contaminating ribonucleases. Following

chromatography, ANG migrates as a single band of appropriate M_r during SDS–PAGE and

as a single band during zymogram electrophoresis, indicating that the preparations are free

from contaminating ribonucleolytic activity (data not shown). Our expression and

purification protocol yields approximately 20 mg of ANG per L of E. coli growth medium.

   pH–rate profiles for catalysis by ANG. The ANG pH–rate profile was determined by

measuring k_{cat}/K_M values for substrate 5 as a function of pH. The k_{cat}/K_M values were fitted to

eq. 5.2 which describes catalysis by an enzyme with two titratable active-site residues, where

one residue must be protonated and the second must be deprotonated for catalysis to occur.

Like that determined previously for RNase A (Witzel, 1963; del Rosario & Hammes, 1969;

Park et al., 2000), the ANG pH–rate profile is bell-shaped with a maximum near pH = 6

(Figure 5.2). But unlike that of RNase A, the ANG pH–rate profile has a wide plateau. The

values of the ANG acid dissociation constants pK_1 and pK_2 are 5.0 and 7.0, respectively.[3] The

value of the ANG pH-independent k_{cat}/K_M is 220 $M^{-1}sec^{-1}$.

   Salt dependence of catalysis by ANG. The effect of salt on catalysis by ANG was

determined by measuring k_{cat}/K_M values for substrate 2 as a function of Na^+ concentration in

1 mM BisTris-HCl (pH 6.0). A low buffer concentration was used to minimize inhibition

caused by any low-level contaminants in the buffer. The effects of such contaminants is

minimal at high salt concentrations, but can be pronounced at low salt concentration (Park &

Raines, 2000b). The k_{cat}/K_M values for ANG-catalyzed cleavage of substrate 2 increase from

---

[3] The error on the pK values, determined by curve fitting, is < 1%. Errors determined from duplicate experiments are closer to 6%. We therefore assume that the error on the pK values to be 6%.

71 M^{-1}sec^{-1} at 0.25 M NaCl to 1.2 × 10^4 M^{-1}sec^{-1} at 0.025 M NaCl (Figure 5.3). The value of

n, which is calculated using eq 5.3, is 2.3 ± 0.1.

Substrate dependence of catalysis by ANG. To measure the effect of substrate length on

ANG catalysis, we used a family of hypersensitive nucleotide substrates (Table 5.1). As

reported, the values of k_{cat}/K_M for RNase A acting on substrates 1–4 range from 2.5 × 10^7 M$^-$

^{1}sec^{-1} for substrate 1 to 4.8 × 10^7 M^{-1}sec^{-1} for substrate 4, a modest 2-fold change [Figure 5.4,

(Kelemen *et al.*, 1999)]. In contrast, the range of k_{cat}/K_M values for ANG catalyzed cleavage

of substrates 1–4 is significantly larger (Figure 5.4, Table 5.1). Substrate 1 has the lowest

value of k_{cat}/K_M at 61 M^{-1}sec^{-1}. ANG acts on substrate 2 with k_{cat}/K_M equal to 310 M^{-1}sec^{-1}, a 5-

fold increase relative to the value measured for substrate 1. The k_{cat}/K_M value for substrate 3,

a hexanucleotide, at 720 M^{-1}sec^{-1} is 12-fold greater than that measured for substrate 1. The

value of k_{cat}/K_M for substrate 4, which contains eight nucleotides, is 740 M^{-1}sec^{-1} and is within

error of that measured for substrate 3.

Binding of a DNA oligonucleotide to ANG. Fluorescence anisotropy was used to measure

the effect of Na$^+$ on the binding of a substrate analog to ANG. The fluorescein-labeled DNA

oligonucleotide Fl–d(AUAA) had been used previously to measure the binding of single-

stranded nucleic acid to RNase A and several variants (Fisher *et al.*, 1998a; Fisher *et al.*,

1998b; Fisher *et al.*, 1998c). As reported, the value of K_d for the Fl–d(AUAA)•RNase A

complex is strongly dependent on [Na$^+$] (Fisher *et al.*, 1998a; Fisher *et al.*, 1998b; Fisher *et

al.*, 1998c). Similarly, the interaction between ANG and the Fl–d(AUAA) oligonucleotide is

dependent on [Na$^+$]. At 0.024 M Na$^+$, Fl–d(AUAA) forms a complex with ANG that has a K_d

value of 6.6 μM. Increasing the [Na$^+$] weakens binding significantly—at 0.142 M Na$^+$, the

value of K_d for the ANG• Fl–d(AUAA) complex is 490 μM.

5.5 Discussion

Angiogenin production and purification. The pancreatic-type ribonucleases are highly

amenable to heterologous production in *E. coli.* Previously, we used the T7 RNA polymerase

expression system (Studier *et al.,* 1990) to produce RNase A (delCardayré *et al.,* 1995),

bovine seminal ribonuclease (Kim & Raines, 1993a), human pancreatic ribonuclease (Leland

et al., 2000), and Onconase™ (Leland *et al.,* 1998). This system has consistently yielded ≥20

mg/L of fully active ribonuclease.

Surprisingly, when we attempted to use the T7 RNA polymerase system for the

heterologous production of ANG, it was not possible to purify any significant quantity of

ANG. Because the T7 RNA polymerase system produces mRNA with high efficiency, we

suspected that inefficient translation was limiting the production of ANG. Analysis with the

program RNA FOLD (Genetics Computer Group, Madison WI) indicated that the start codon

and Shine-Delgarno sequence were accessible to the translation machinery (data not shown).

Inspection of the cDNA for human ANG revealed, however, two prominent sequences of

codons that are disfavored by *E. coli.* The effect of rare codons on the production of foreign

proteins in *E. coli* is highly variable and is largely dependent on their context within the

mRNA. The rare AGA and AGG arginine codons are often associated with errors that cause

premature termination of translation (Spanjaard & van Duin, 1988; Kane *et al.,* 1992;

Rosenberg *et al.,* 1993).

When the AGG and AGA codons for Arg31 and Arg32, as well as the rare CGG codon

for Arg33, are replaced with the corresponding high-use codons, expression of ANG

increases dramatically (Figure 5.1). Likewise, when the sequence of rare codons from amino

acid 66 to amino acid 71, which includes two AGA arginine codons, is replaced with the

corresponding favored codons, expression of ANG increases. Combination of both sets of

codon substitutions into a single cDNA results in a modest increase in production of ANG,

compared to that supported by the cDNA with codon substitutions restricted to amino acids

31–33. The codon-optimized cDNA consistently yields > 20 mg of pure ANG per L of

starting culture. Shapiro and coworkers have also described the production of ANG from a

synthetic cDNA in *E. coli* (Shapiro *et al.*, 1988). Their isolated yields of ANG, however, are

limited to 2 mg per L of growth medium. More recently, Kim and coworkers described a

system for secretion of ANG from *E. coli* with isolated yields of 40 mg per L of growth

medium (Yoon *et al.*, 1999). Surprisingly, this system requires that cells are grown for 72 h

after induction of ANG expression. These authors do not, however, measure the

ribonucleolytic activity of the purified enzyme.

pH–rate profile for catalysis by ANG. The ANG pH-rate profile is a classic bell-shaped

curve (Figure 5.2). The pH dependence of catalysis is consistent with a mechanism in which

two residues, one protonated and the other deprotonated, effect catalysis. By analogy to the

RNase A transphosphorylation reaction, ANG residue His13 likely acts as a base to abstract a

proton from the 2'-oxygen, and thereby facilitates its attack on the phosphorus atom. ANG

residue His114 acts as an acid that protonates the 5'-oxygen to facilitate its displacement

(Raines, 1998). As expected from this mechanism, the H13A and the H114A variants of

ANG are ineffective catalysts (Shapiro & Vallee, 1989). Hydrolysis of the 2',3'-cyclic

phosphodiester likely occurs in a separate process that resembles the reverse of the

transphosphorylation reaction (Thompson *et al.*, 1994).

Unlike the RNase A pH–rate profile, the ANG pH-rate profile has an obvious plateau

(Figure 5.2). Accordingly, the pK_a values calculated for the active-site histidines of ANG are

separated by two pH units, with $pK_1 = 5.0$ and $pK_2 = 7.0$. The acid dissociation constants

determined in the same manner for RNase A differ by only 0.4 pH units, with $pK_1 = 6.0$ and

$pK_2 = 6.4$ (Park et al., 2000). Because pK_1 and pK_2 are macroscopic parameters, it is not

possible to assign a pK value to an active-site histidine. The pK_a values for the active-site

histidine residues of ANG and RNase A have been measured using NMR spectroscopy. In

RNase A, His12 is slightly more acidic than is His119 (Markley, 1975; Quirk & Raines,

1999). This situation favors a protonation state that is appropriate for catalysis of the

transphosphorylation reaction. Surprisingly, the pK_a values of the active-site histidine

residues in Ang are inverted—His114 is more acidic than is His13 (Lequin et al., 1997).

Salt–rate profile for catalysis by ANG. The ribonucleolytic activity of ANG is strongly

dependent on [Na^+] (Figure 5.3). This result emphasizes that Coulombic interactions within

the phosphoryl group binding sites of ANG are important for substrate binding. Consistent

with this conclusion, Shapiro and coworkers have shown than the K_i values of 3',5'-ADP and

5'-ADP are 6-fold lower than that of 5'-AMP (Russo et al., 1996). Similarly, addition of a 3'

phosphoryl group to CpA increases its K_i value 9-fold (Russo et al., 1996).

When the chemical step is rate limiting in catalysis, the value of n in eq. 5.3 is

proportional to the extent of Coulombic interactions between the enzyme and the substrate in

its transition state (Park & Raines, 2000a). The very low k_{cat} measured for CpA cleavage by

ANG suggests that ANG catalysis is limited by chemistry (Russo et al., 1994). The value of

n for ANG is 2.3 when catalysis is measured using substrate 2. The salt-rate profile for wild-

type RNase A is not appropriate to compare with that of ANG because chemistry is only

partially rate-limiting for RNase A (Park & Raines, 2000a). Rather, the Coulombic

interactions between RNase A and substrate 2 are best described by the salt-rate profile of

K41R RNase A (Park & Raines, 2000a). The K41R substitution in RNase A does not change

the Coulombic interactions between the enzyme and the substrate, but diminishes turnover

such that chemistry is rate limiting (Messmore et al., 1995). The value of n for K41R

RNase A is 2.7 when catalysis is measured using substrate 2 (Park & Raines, 2000a). RNase

A residues Lys7, Arg10, and Lys66 interact with the phosphoryl groups of a bound substrate

(Fisher et al., 1998b). When each of these amino acids are changed to Ala, the value of n is

reduced to 1.4 (Park & Raines, 2000a). Thus, the n values for ANG and K41R RNase A are

similar, indicating that the Coulombic interactions between RNase A and substrate 2 appear

to be largely conserved in ANG.

Kinetic and structural studies, as well as comparisons to RNase A, have been used to

define the phosphoryl group binding sites of ANG. In RNase A, four enzymic subsites [P(-1),

P0, P1, and P2] interact with the phosphoryl groups of a bound substrate (Raines, 1998). The

P1 subsite is the active site where cleavage of the $P-O^{5'}$ bond occurs. The P0 and P2 subsites

bind the phosphoryl groups on the 5' side and 3' side of the scissile phosphodiester bond,

respectively. The P(-1) subsite of RNase A, which binds the second phosphoryl group on the

5' side of the scissile phosphodiester bond, was described only recently (Fisher et al., 1998a).

The ANG P1 subsite is similar to that of RNase A (Acharya et al., 1994; Leonidas et al.,

1999). Kinetic studies support the presence of a P2 subsite in ANG (Russo et al., 1996). The

amino acid residues that contribute to the P2 subsite of ANG are, however, distinct from

those that contribute to the analogous subsite of RNase A (Leonidas et al., 1999). ANG

appears to lack a P0 subsite (Russo et al., 1996). Removal of the three C-terminal residues of

ANG (Arg121, Arg122, Pro 123) reduces cleavage of dinucleotide substrates by 10-fold but does not change significantly catalysis of polynucleotide cleavage, indicating that these residues may constitute a peripheral subsite (Russo *et al.*, 1996; Shapiro, 1998).

Binding of a DNA oligonucleotide to ANG. Previously, we showed that fluorescence anisotropy is a suitable technique to assay complex formation between RNase A and a substrate analog (Fisher *et al.*, 1998a; Fisher *et al.*, 1998b; Fisher *et al.*, 1998c). Here, we have used this technique to quantitate substrate binding to ANG. The affinity of ANG for the Fl–d(AUAA) oligonucleotide is dependent on [Na^+]. A 6-fold change in [Na^+] caused a 75-fold change in the K_d values. The value of K_d determined for ANG•Fl–d(AUAA) complex at 0.142 M Na^+ (K_d = 490 μM) is not significantly greater than that reported previously for RNase A and an identical oligonucleotide (K_d = 88 μM) (Fisher *et al.*, 1998c). Moreover, the dependence of the K_d values on [Na^+] for RNase A is notably similar to that measured for ANG—an 8-fold change in [Na^+] results in a 100-fold decrease in the value of K_d for the RNase A• Fl–d(AUAA) complex (Fisher *et al.*, 1998c). These data show that substrate binding by ANG is not compromised dramatically compared to that by RNase A. This conclusion is consistent with the small difference in the values of *n* calculated using the salt-rate profiles of ANG and K41R RNase A.

Substrate Length Dependence. Catalysis by ANG shows a strong dependence on the length of the substrates (Figure 5.4). This result emphasizes the significance of peripheral subsites in catalysis by ANG. As described above, catalysis by ANG appears to be limited by chemistry. As the length of the substrate molecule increases, the binding energy also increases. Greater binding energy, in turn, results in uniformly greater stabilization of all enzyme-bound species, including the rate-limiting transition state (Albery & Knowles, 1976).

Ultimately, the greater binding energy afforded by a longer substrate is manifested as greater

catalytic activity. Although substrate 4 is two nucleotides longer than is substrate 3, the

values of k_{cat}/K_M are approximately equal. Apparently, the additional nucleotides of substrate

4, compared to substrate 3, are unable to participate in interactions that enhance catalysis.

Unlike ANG, RNase A does not discriminate between substrates 1–4 (Figure 5.4).

Catalysis by RNase A is not limited by chemistry alone (Park & Raines, 2000a). Therefore,

the effects of enhanced binding energy provided by a longer substrate on RNase A catalysis

are more difficult to interpret (Park & Raines, 2000a).

Conclusions. A distinctive property of ANG is its markedly low ribonucleolytic activity

compared to that of RNase A. The properties of the active-site histidine residues, phosphoryl

group binding sites, and nucleobase binding sites likely contribute to the low catalytic

activity of ANG. Our data, however, suggest that these features cannot account in total for

the difference in catalytic activity between ANG and RNase A. What then is the basis of the

inefficiency of ANG as a catalyst of RNA cleavage? It is possible that the orientation of the

catalytic residues of ANG (His13, Lys41, His114) is not optimal for cleavage of the

substrates commonly used for measurement of ribonucleolytic activity. Recently, Acharya,

Shapiro, and coworkers described the structure of crystalline ANG at 1.8 Å resolution

(Leonidas *et al.*, 1999). In their comparison of the ANG structure to that of the

RNase A•uridine vanadate complex, these authors noted subtle changes to the positions of

the ANG active-site residues compared to their RNase A counterparts.

The physiological substrate of ANG is still unknown. It is unlikely that ANG has a

specific recognition sequence for catalysis. Instead, the target may have a specific secondary

structure, such as a hairpin or a pseudo-knot, or may be part of a protein•nucleic acid

complex. The poor catalytic activity of ANG may have evolved to maximize specificity for the target substrate. Identification of the physiological substrate is essential for the complete description of the molecular mechanism of angiogenesis by ANG.

5.6 Acknowledgement.

Table 5.1 Parameters for cleavage of fluorogenic substrates by angiogenin.

substrate		phosphoryl groups	k_{cat}/K_M $(M^{-1}sec^{-1})^a$
1	6-FAM~rUdA~6-TAMRA	3	61 ± 4
2	6-FAM~(dA)rU(dA)$_2$~6-TAMRA	5	310 ± 10
3	6-FAM~(dA)$_2$rU(dA)$_3$~6-TAMRA	7	720 ± 30
4	6-FAM~(dA)$_3$rU(dA)$_4$~6-TAMRA	9	740 ± 30
5	6-FAM~(dA)rU(dA)$_2$~4-DABCYL	5	200 ± 20

[a]Values (±SE) of k_{cat}/K_M were obtained in 0.10 M MES-NaOH buffer (pH 6.0) containing

NaCl (0.10 M) except the value for substrate 5 which was obtained in 0.05 M acetate,

0.05 M MES, 0.1 M Tris buffer (pH 6.0) containing NaCl (0.10 M)

Figure 5.1   Results from SDS–PAGE of *Escherichia coli* lysates harboring a pET-22b(+)-

based plasmid that directs the expression of human angiogenin.

Cell lysates were prepared immediately prior to addition of IPTG (–) and 2 h

after addition of IPTG (+). M_r standards are shown. Angiogenin migrates as a

14.1-kDa band, which is marked with an arrow. Wild-type (*wt*) is from the

human cDNA for angiogenin. In *PAL5*, the disfavored codons for Arg31,

Arg32, and Arg33 are replaced with the corresponding codons favored by

E coli. In *PAL6*, the disfavored codons for Arg66, Leu69, Arg70, and Ile71 in

are replaced with the corresponding codons favored by *E. coli*. In *PAL5+6*,

both sets of codon substitutions are incorporated in the same angiogenin
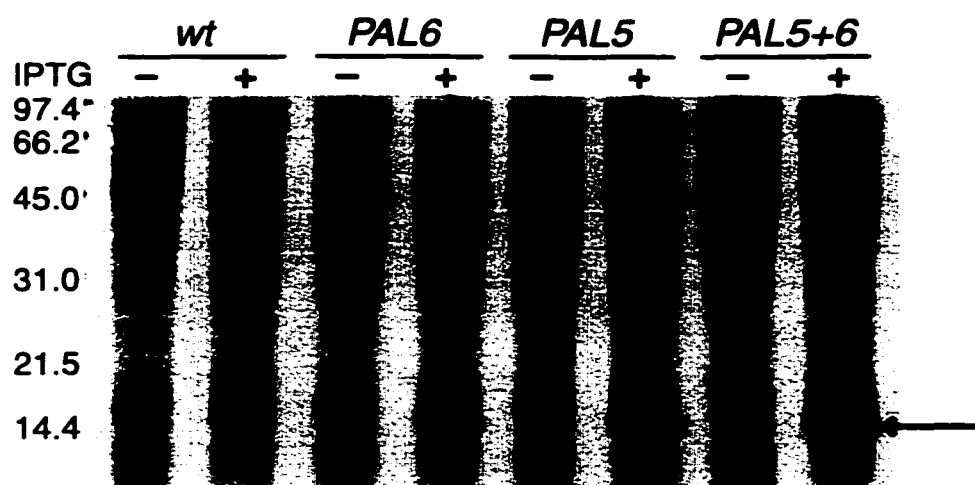
cDNA.

Figure 5.2.   Dependence of k_{cat}/K_M values for catalysis by angiogenin and ribonuclease A

on pH.

Values for angiogenin (O) were determined at 25 °C in a three-component

buffer system (0.05 M acetate, 0.05 M MES, 0.10 M Tris) containing NaCl

(0.10 M). Values of k_{cat}/K_M for cleavage of substrate 5 at each pH were

calculated using eq 5.1 and fitted to eq 5.2. Values for ribonuclease A (●) are

from (Park et al., 2000) and were determined at 25 °C in sodium citrate (pH

3.22), sodium succinate (pH 3.84 and 4.97), MES-NaOH (pH 5.99), MOPS-

NaOH (7.04), Tris-HCl (pH 7.97), CHES-NaOH (pH 9.14) and CAPS-NaOH

(pH 10.0). All buffers were used at 0.10 M and contained NaCl (0.10 M),

substrate 5 (5-80 nM), and RNase A (0.1-200 nM).
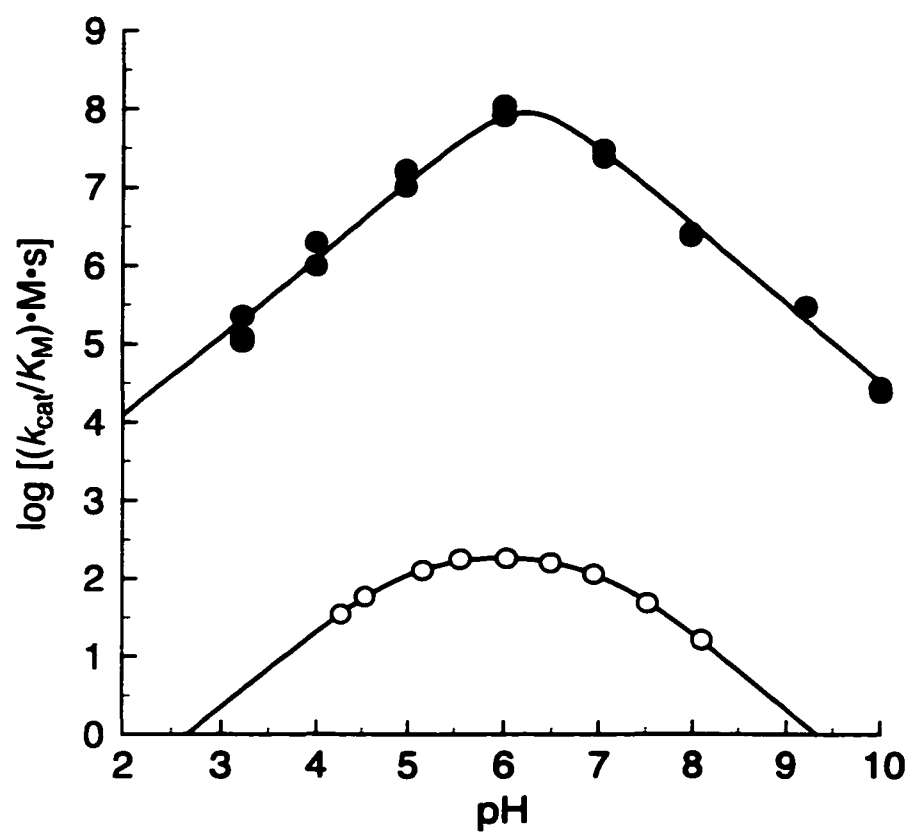
Figure 5.3   Dependence of k_{cat}/K_M values for catalysis by angiogenin and ribonuclease A

on Na^+ concentration.

Determinations were made at 25 °C in 1 mM Bis-Tris buffer (pH 6.0)

containing NaCl (0.025–0.25 M for angiogenin and 0.001–1.0 M for

ribonuclease A). Values of k_{cat}/K_M for cleavage of substrate 2 by angiogenin

(O) at each $[Na^+]$ were calculated using eq 5.1 and fitted to eq 5.3. Data for

the Na^+ dependence of catalysis by ribonuclease A (●) are from (Park &

Raines, 2000a).
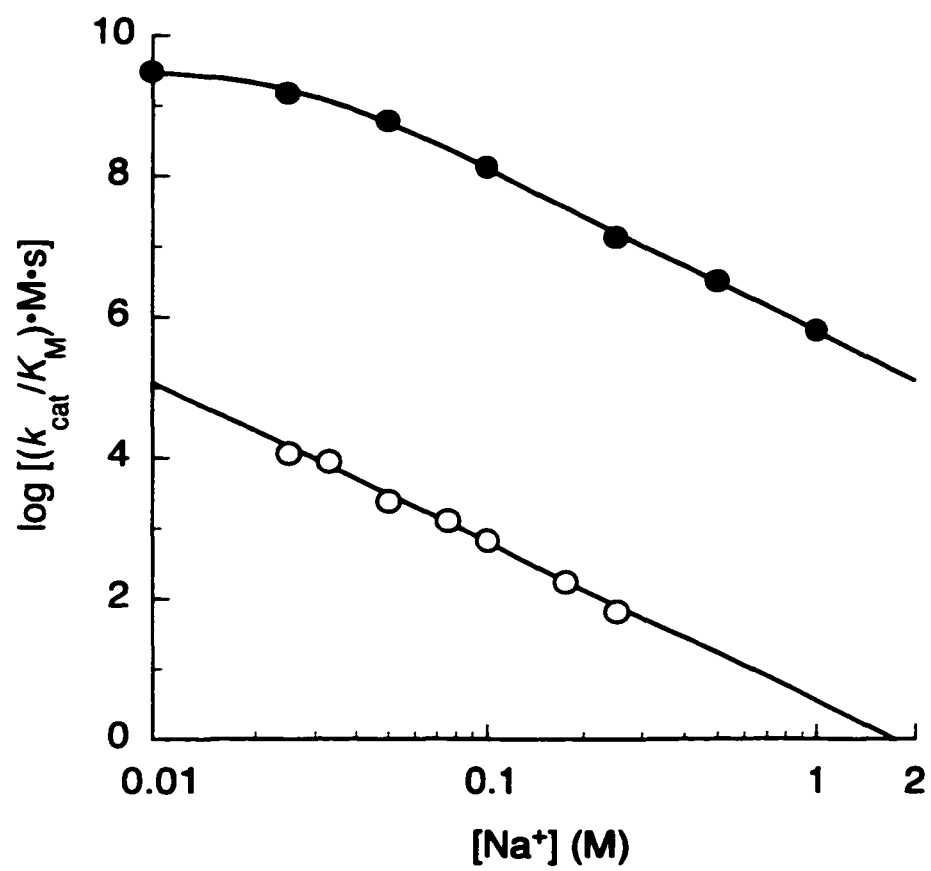
Figure 5.4.   Dependence of k_{cat}/K_M values for catalysis by angiogenin and ribonuclease A

on substrate length.

Values of k_{cat}/K_M are relative to that determined for cleavage of the

dinucleotide substrate 1, which contains three phosphoryl groups, and are the

average of duplicate or triplicate determinations. Cleavage of the nucleotide

substrates by angiogenin (open bars) was measured at 25 °C in 0.10 M MES-

NaOH buffer (pH 6.0) containing NaCl (0.10 M). Values of k_{cat}/K_M for

ribonuclease A (filled bars) are from (Kelemen *et al.*, 1999) and were

determined with 1–200 pM enzyme and solution conditions identical to those

described for angiogenin.
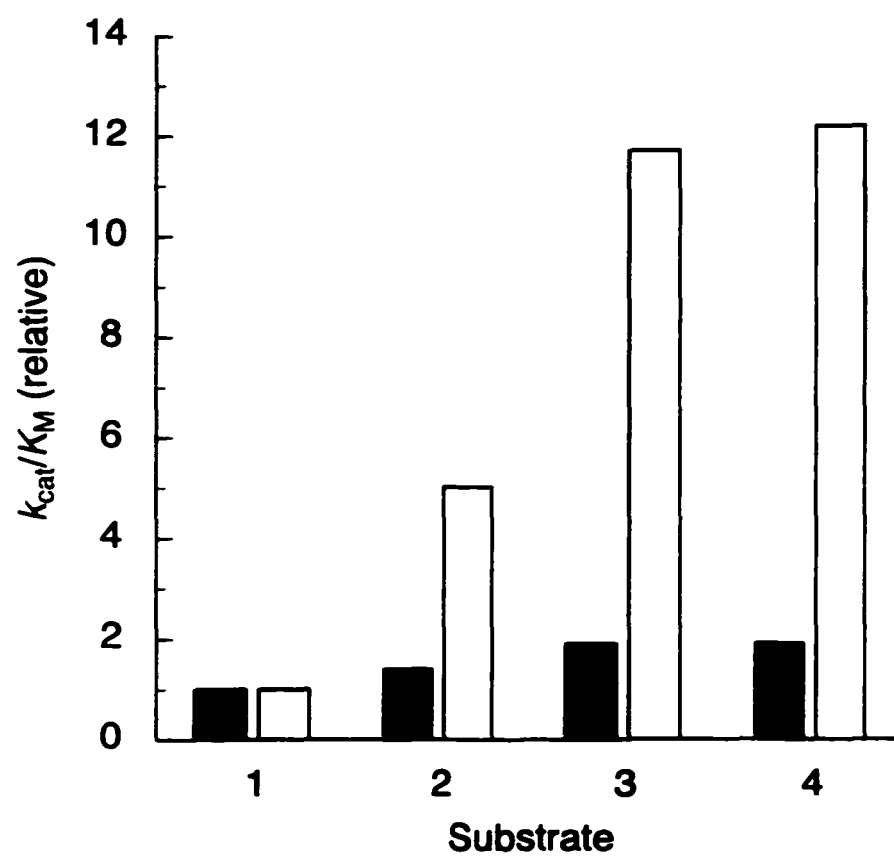
Chapter Six

References

Acharya, K. R., Shapiro, R., Allen, S. C., Riordan, J. F. & Vallee, B. L. (1994). Crystal structure of human angiogenin reveals the structural basis for its functional divergence from ribonuclease. *Proc. Natl. Acad. Sci. U.S.A.* **91**, 2915-2919.

Acharya, K. R., Shapiro, R., Riordan, J. F. & Vallee, B. L. (1995). Crystal structure of bovine angiogenin at 1.5-Å resolution. *Proc. Natl. Acad. Sci. U.S.A.* **92**, 2949-2953.

Albery, W. J. & Knowles, J. R. (1976). Evolution of enzyme function and the development of catalytic efficiency. *Biochemistry* **15**, 5631-5640.

Anfinsen, C. B. (1973). Principles that govern the folding of protein chains. *Science* **181**, 223-230.

Ardelt, W., Mikulski, S. M. & Shogen, K. (1991). Amino acid sequence of an anti-tumor protein from *Rana pipiens* oocytes and early embryos. *J. Biol. Chem.* **266**, 245-251.

Awade, A. C., Cleuziat, P., Gonzales, T. & Robert-Baudouy, J. (1994). Pyrrolidone carboxyl peptidase (Pcp): an enzyme that removes pyroglutamic acid (pGlu) from pGlu-peptides and pGlu-proteins. *Proteins* **20**, 34-51.

Barnard, E. A. (1969). Biological function of pancreatic ribonuclease. *Nature* **221**, 340-344.

Beintema, J. J., Schüller, C., Irie, M. & Carsana, A. (1988). Molecular evolution of the ribonuclease superfamily. *Prog. Biophys. Molec. Biol.* **51**, 165-192.

Blackburn, P. (1979). Ribonuclease Inhibitor from Human Placenta: Rapid Purification and Assay. *J. Biol. Chem.* **254**, 12484-12487.

Blackburn, P. & Moore, S. (1982). Pancreatic ribonuclease. *The Enzymes* **XV**, 317-433.

Blank, A., Sugiyama, R. H. & Dekker, C. A. (1982). Activity staining of nucleolytic enzymes after SDS-PAGE: Use of aqueous isopropanol to remove detergent from gels. *Anal. Biochem.* **120**, 267-275.

Blázuez, M., Fominaya, J. M. & Hofsteenge, J. (1996). Oxidation of sulfhydryl groups of ribonuclease inhibitor in epithelial cells is sufficient for its intracellular degradation. *J. Biol. Chem.* **271**, 18638-18642.

Boix, E., Wu, Y., Vasandani, V. M., Saxena, S. K., Ardelt, W., Ladner, J. & Youle, R. J. (1996). Role of the N terminus in RNase A homologues: differences in catalytic activity, ribonuclease inhibitor interaction and cytotoxicity. *J. Mol. Biol.* **257**, 992-1007.

Bravo, J., Fernández, E., Ribó, M., de Llorens, R. & Cuchillo, C. M. (1994). A versatile negative-staining ribonuclease zymogram. *Anal. Biochem.* **219**, 82-86.

Bretscher, L. E., Abel, R. L. & Raines, R. T. (2000). A ribonuclease A variant with low catalytic activity but high cytotoxicity. *J. Biol. Chem.* **275**, 9893-9896.

Cafaro, B., De Lorenzo, C., Piccoli, R., Bracale, A., Mastronicola, M. R., Di Donato, A. & D'Alessio, G. (1995). The antitumor action of seminal ribonuclease and its quaternary conformations. *FEBS Lett.* **359**, 31-34.

Canals, A., Ribó, M., Benito, A., Bosch, M., Mombelli, E. & Vilanova, M. (1999). Production of engineered human pancreatic ribonucleases, solving expression and purification problems, and enhancing thermostability. *Protein Express. Purif.* **17**, 169-181.

Chang, C.-F., Chen, C., Chen, Y.-C., Hom, K., Huang, R. F. & Huang, T. H. (1998). The solution structure of a cytotoxic ribonuclease from the oocytes of *Rana catesbeiana* (Bullfrog). *J. Mol. Bio.* **283**, 231-244.

Cleland, W. W. (1979). Statistical analysis of enzyme kinetic data. *Methods Enzymol.* **63**, 103-138.

Crick, F. H. C. (1952). Is α-keratin a coiled coil? *Nature* **170**, 882-883.

D'Alessio, G., Di Donato, A., Mazzarella, L. & Piccoli, R. (1997). Seminal ribonuclease: the importance of diversity. In *Ribonucleases: Structures and Functions* (D'Alessio, G. & Riordan, J. F., eds.), pp. 383-423. Academic Press, New York.

Darzynkiewicz, Z., Carter, S. P., Mikulski, S. M., Ardelt, W. J. & Shogen, K. (1988). Cytostatic and cytotoxic effect of Pannon (P-30 Protein), a novel anticancer agent. *Cell Tissue Kinet.* **21**, 169-182.

De Bernardez-Clark, E., Schwarz, E. & Rudolph, R. (1999). Inhibition of aggregation side reactions during *in vitro* protein folding. *Methods Enzymol.* **309**, 217-236.

del Rosario, E. J. & Hammes, G. G. (1969). Kinetic and equilibrium studies of the ribonuclease-catalyzed hydrolysis of uridine 2',3'-cyclic phosphate. *Biochemistry* **8**, 1884-1889.

delCardayré, S. B. & Raines, R. T. (1994). Stuctural determinants of enzymatic processivity. *Biochemistry* **33**, 6031-6037.

delCardayré, S. B., Ribó, M., Yokel, E. M., Quirk, D. J., Rutter, W. J. & Raines, R. T. (1995). Engineering ribonuclease A: production, purification, and characterization of wild-type enzyme and mutants at Gln11. *Protein Engng.* **8**, 261-273.

Di Donato, A., Cafaro, V. & D'Alessio, G. (1994). Ribonuclease A can be transformed into a dimeric ribonuclease with antitumor activity. *J. Biol. Chem.* **269**, 17394-17396.

Eberhardt, E. S., Wittmayer, P. K., Templer, B. M. & Raines, R. T. (1996). Contribution of a tyrosine side chain to ribonuclease A catalysis and stability. *Protein Sci.* **5**, 1697-1703.

Ellis, K. J. & Morrison, J. F. (1982). Buffers of constant ionic strength for studying pH-dependent processes. *Methods Enzymol.* **87**, 405-425.

Fett, J. W., Strydom, D. J., Lobb, R. R., Alderman, E. M., Bethune, J. L., Riordan, J. F. & Vallee, B. L. (1985). Isolation and characterization of angiogenin, an angiogenic protein from human carcinoma cells. *Biochemistry* **24**, 5480-5486.

Fisher, B. M., Grilley, J. E. & Raines, R. T. (1998a). A new remote subsite in ribonuclease A. *J. Biol. Chem.* **273**, 34134-34138.

Fisher, B. M., Ha, J.-H. & Raines, R. T. (1998b). Coulombic forces in protein-RNA interactions: binding and cleavage by ribonuclease A and variants at Lys7, Arg10 and Lys66. *Biochemistry* **37**, 12121-12132.

Fisher, B. M., Schultz, L. W. & Raines, R. T. (1998c). Coulombic effects of remote subsites on the active site of ribonuclease A. *Biochemistry* **37**, 17386-17401.

Folkman, J. & Klagsbrun, M. (1987). Angiogenic factors. *Science* **235**, 442-447.

Fredman, P. (1993). Glycosphingolipid tumor agents. *Adv. Lipid Res.*(213-234).

Futami, J., Seno, M., Ueda, M., Tada, H. & Yamada, H. (1999). Inhibition of cell growth by a fused protein of human ribonuclease 1 and human basic fibroblast growth factor. *Protein Eng.* **12**, 1013-1019.

Gill, S. C. & von Hippel, P. H. (1989). Calculation of protein extinction coefficients from amino acid sequence data. *Anal. Biochem.* **182**, 319-326.

Harper, J. W. & Vallee, B. L. (1989). A covalent angiogenin/ribonuclease hybrid with a fourth disulfide bond generated by regional mutagenesis. *Biochemistry* **28**, 1875-1884.

Hofsteenge, J. (1997). Ribonuclease inhibitor. In *Ribonucleases: Structures and Functions* (D'Alessio, G. & Riordan, J. F., eds.), pp. 621-658. Academic Press, New York.

Hu, G.-F., Chang, S.-I., Riordan, J. F. & Vallee, B. L. (1991). An angiogenin-binding protein from endothelial cells. *Proc. Natl. Acad. Sci. U.S.A.* **88**, 2227-2231.

Hu, G.-F., Xu, C. & Riordan, J. F. (2000). Human angiogenin is rapidly translocated to the nucleus of human umbilical vein endothelial cells and binds to DNA. *J. Cellular Biochem.* **76**, 452-462.

Huang, H.-C., Wang, S.-C., Leu, Y.-J., Lu, S.-C. & Liao, Y.-D. (1998). The *Rana catesbeiana rcr* gene encoding a cytotoxic ribonuclease. *J. Biol. Chem.* **273**, 6395-6401.

Imperiali, B. & Hendrickson, T. L. (1995). Asparagine-linked glycosylation: specificity and function of oligosaccharyl transferase. *Bioorg. Med. Chem.* **3**, 1565-1578.

Irie, M., Nitta, K. & Nonaka, T. (1998). Biochemistry of frog ribonucleases. *Cell. Mol. Life Sci.* **54**, 775-784.

Juan, G., Ardelt, B., Li, X., Mikulski, S. M., Shogen, K., Ardelt, W., Mittelman, A. & Darzynkiewicz, Z. (1998). G_1 arrest of U937 cells by onconase is associated with suppression of cyclin D3 expression, induction of p16[INK4A], p21[WAF1/CIP1] and p27[KIP] and decreased pRb phosphorylation. *Leukemia* **12**, 1241-1248.

Kabsch, W. (1988). Evaluation of single-crystal x-ray diffraction data from a position-sensitive detector. *J. Appl. Crystallogr.* **21**, 916-924.

Kamiya, Y., Oyama, F., Oyama, R., Sakakibara, F., Nitta, K., Kawauchi, H., Takayanagi, Y. & Titani, K. (1990). Amino acid sequence of a lectin from Japanese frog (*Rana japonica*) eggs. *J. Biochem. (Tokyo)* **108**, 139-143.

Kane, J. F., Violand, B. N., Curran, D. F., Staten, N. R., Duffin, K. L. & Bogosian, G. (1992). Novel in-frame two codon translation hop during synthesis of bovine placental lactogen in a recombinant strain of *Escherichia coli*. *Nucleic Acids Res.* **20**, 6707-6712.

Kawanomoto, M., Motojima, K., Sasaki, M., Hattori, H. & Goto, S. (1992). cDNA cloning and sequence of rat ribonuclease inhibitor, and tissue distribution of mRNA. *Biochem. Biophys. Acta* **1129**, 335-338.

Kelemen, B. R., Klink, T. A., Behlke, M. A., Eubanks, S. R., Leland, P. A. & Raines, R. T. (1999). Hypersensitive substrate for ribonucleases. *Nucleic Acids Res.* **27**, 3696-3701.

Kim, J.-S. & Raines, R. T. (1993a). Bovine seminal ribonuclease produced from a synthetic gene. *J. Biol. Chem.* **268**, 17392-17396.

Kim, J.-S. & Raines, R. T. (1993b). Ribonuclease S-peptide as a carrier in fusion proteins. *Protein Sci.* **2**, 348-356.

Kim, J.-S., Soucek, J., Matousek, J. & Raines, R. T. (1995a). Catalytic activity of bovine seminal ribonuclease is essential for its immunosuppressive and other biological activities. *Biochem. J.* **308**, 547-550.

Kim, J.-S., Soucek, J., Matousek, J. & Raines, R. T. (1995b). Mechanism of ribonuclease cytotoxicity. *J. Biol. Chem.* **270**, 31097-31102.

Kim, J.-S., Soucek, J., Matousek, J. & Raines, R. T. (1995c). Structural basis for the biological activities of bovine seminal ribonuclease. *J. Biol. Chem.* **270**, 10525-10530.

Klink, T. A. & Raines, R. T. (2000). Conformational stability is a determinant of ribonuclease A cytotoxicity. *J. Biol. Chem.* **in press**.

Klink, T. A., Woycechowsky, K. J., Taylor, K. M. & Raines, R. T. (2000). Contribution of disulfide bonds to the stability of ribonuclease A. *Eur. J. Biochem.* **267**, 566-572.

Kobe, B. & Deisenhofer, J. (1993). Crystal structure of porcine ribonuclease inhibitor, a protein with leucine-rich repeats. *Nature* **366**, 751-756.

Kobe, B. & Deisenhofer, J. (1995). A structural basis of the interactions between leucine-rich repeats and protein ligands. *Nature* **374**, 183-186.

Kobe, B. & Deisenhofer, J. (1996). Mechanism of ribonuclease inhibition by ribonuclease inhibitor protein based on the crystal structure of its complex with ribonuclease A. *J. Mol. Biol.* **264**, 1028-1043.

Kowalski, J. M., Parekh, R. N. & Wittrup, K. D. (1998). Secretion efficiency in *Saccharomyces cerevisiae* of bovine pancreatic trypsin inhibitor mutants lacking disulfide bonds is correlated with thermodynamic stability. *Biochemistry* **37**, 1264-1273.

Kraulis, P. J. (1991). MOLSCRIPT: a program to produce both detailed and schematic plots of protein structures. *J. Appl. Crystallogr.* **24**, 946-950.

Kunkel, T. A., Roberts, J. D. & Zakour, R. A. (1987). Rapid and efficient site-specific mutagenesis without phenotypic selection. *Methods Enzymol.* **154**, 367-382.

Kurachi, K., Davie, E. W., Strydom, D. J., Riordan, J. F. & Vallee, B. L. (1985). Sequence of the cDNA and gene for angiogenin, a human angiogenesis factor. *Biochemistry* **24**, 5494-5499.

Lavie, Y., Cao, H., Bursten, S. L., Giuliano, A. E. & Cabot, M. C. (1996). Accumulation of glucosylceramides in multidrug-resistant cancer cells. *J. Biol. Chem.* **271**, 19530-19536.

Lee, F. S., Shapiro, R. & Vallee, B. L. (1989). Tight-binding inhibition of angiogenin and ribonuclease A by placental ribonuclease inhibitor. *Biochemistry* **28**, 225-230.

Lee, F. S. & Vallee, B. L. (1989). Binding of placental ribonuclease inhibitor to the active site of angiogenin. *Biochemistry* **28**, 3556-3561.

Lee, F. S. & Vallee, B. L. (1993). Structure and action of mammalian ribonuclease (angiogenin) inhibitor. *Progress Nucl. Acid Res. Molec. Biol.* **44**, 1-30.

Leland, P. A., Schultz, L. W., Kim, B.-M. & Raines, R. T. (1998). Ribonuclease A variants with potent cytotoxic activity. *Proc. Natl. Acad. Sci. U.S.A.* **98**, 10407-10412.

Leland, P. A., Staniszewski, K. E., Kim, B.-M. & Raines, R. T. (2000). Endowing human pancreatic ribonuclease with cytotoxic activity. *in preparation for Cancer Res.*

Leonidas, D. D., Shapiro, R., Allen, S. C., Subbarao, G. V., Veluraja, K. & Acharya, K. R. (1999). Refined crystal structures of native human angiogenin and two active site variants: Implications for the unique functional properties of an enzyme involved in neovascularisation during tumour growth. *J. Mol. Biol.* **285**, 1209-1233.

Lequin, O., Thüring, H., Robin, M. & Lallemand, J.-Y. (1997). Three-dimensional solution structure of human angiogenein determined by ^{1}H,^{15}N-NMR spectroscopy. *Eur. J. Biochem.* **250**, 712-726.

Lewis, M., Hunt, L. & Barker, W. (1989). Striking sequence similarity among sialic acid-binding lectin, pancreatic ribonucleases and angiogenin: possible structural and functional relationships. *Protein Sequences Data Anal.* **2**, 101-105.

Liao, Y.-D., Huang, H.-C., Chan, H.-J. & Kuo, S.-J. (1996). Large-scale preparation of a ribonuclease from *Rana catesbeiana* (bullfrog) oocytes and characterization of its specific cytotoxic activity against tumor cells. *Protein Express. Purif.* **7**, 194-202.

Lin, J.-J., Newton, D. L., Mikulski, S. M., Kung, H.-F., Youle, R. J. & Rybak, S. M. (1994). Characterization of the mechanism of cellular and cell free protein synthesis inhibition by an anti-tumor ribonuclease. *Biochem. Biophys. Res. Comm.* **204**, 156-162.

Lodish, H., Baltimore, D., Berk, A., Zipursky, S. L., Matsudaira, P. & Darnell, J. (1995). *Molecular Cell Biology*, Scientific American Books, New York.

Markley, J. L. (1975). Correlation proton magnetic resonance studies at 250 MHz of bovine pancreatic ribonuclease. I. Reinvestigation of the histidine peak assignment. *Biochemistry* **14**, 3546-3553.

Mastronicola, M. R., Piccoli, R. & D'Alessio, G. (1995). Key extracellular and intracellular steps in the antitumor action of seminal ribonuclease. *Eur. J. Biochem.* **230**, 242-249.

Matousek, J., Kim, J.-S., Soucek, J., Rihà, J., Ribò, M., Leland, P. A. & Raines, R. T. (1997). Ribonucleases endowed with specific toxicity for spermatogenic layers. *Comp. Biochem. Physiol.* **118B**, 881-888.

Matousek, J., Soucek, J., Rîha, J., Zankel, T. R. & Benner, S. A. (1995). Immunosuppressive activity of angiogenin in comparison with bovine seminal ribonuclease and pancreatic ribonuclease. *Comp. Biochem. Physiol.* **112B**, 235-241.

Matousek, J., Soucek, J., Stratil, A. & Vallee, B. L. (1992). Immunosuppressive activity of angiogenin. *Anim. Genet.* **Suppl. 23**, 46.

Merritt, E. A. & Murphy, M. E. P. (1994). Raster3D Version 2.0, a program for photorealistic molecular graphics. *Acta Crystallogr., Sect. D* **50**, 869-873.

Messmore, J. M., Fuchs, D. N. & Raines, R. T. (1995). Ribonuclease A: revealing structure – function relationships with semisynthesis. *J. Am. Chem. Soc.* **117**, 8057-8060.

Mikulski, S. M., Ardelt, A., Shogen, K., Bernstein, E. H. & Menduke, H. (1990a). Striking increase of survival of mice bearing M109 madison carcinoma treated with a novel protein from amphibian embryos. *J. Natl. Cancer Inst.* **82**, 151-152.

Mikulski, S. M., Chun, H. G., Mittelman, A., Panella, T., Puccio, C. A., Shogen, K. & Constanzi, J. J. (1995). Relationship between response rate and median survival in patients with advanced non-small cell lung cancer: comparison of ONCONASE® with other anticancer agents. *Int. J. Oncol.* **6**, 889-897.

Mikulski, S. M., Grossman, A. M., Carter, P. W., Shogen, K. & Costanzi, J. J. (1993). Phase I human clinical trial of ONCONASE (P-30 Protein) administered intravenously on a weekly schedule in cancer patients with solid tumors. *Int. J. Oncol.* **3**, 57-64.

Mikulski, S. M., Viera, A., Ardelt, W., Menduke, H. & Shogen, K. (1990b). Tamoxifen and trifluoroperazine (Stelazine) potentiate cytostatic/cytotoxic effects of P-30 protein, a novel protein possessing anti-tumor activity. *Cell Tissue Kinet.* **23**, 237-246.

Mikulski, S. M., Viera, A. & Shogen, K. (1992). In vitro synergism between a novel amphibian oocytic ribonuclease (ONCONASE) and tamoxifen, lovastatin and cisplatin, in human OVCAR-3 ovarian carcinoma cell line. *Int. J. Oncol.* **1**, 779-785.

Montecucco, C., Papini, E. & Schiavo, G. (1994). Bacterial toxins penetrate cells via a four-step mechanism. *FEBS Lett.* **346**, 92-98.

Moroianu, J. & Riordan, J. F. (1994a). Identification of the nucleolar targeting signal of human angiogenin. *Biochem. Biophys. Res. Comm.* **203**, 1765-1772.

Moroianu, J. & Riordan, J. F. (1994b). Nuclear translocation of angiogenin in proliferating endothelial cells is essential to its angiogenic activity. *Proc. Natl. Acad. Sci.* **92**, 1677-1681.

Mosimann, S. C., Ardelt, W. & James, M. N. G. (1994). Refined 1.7 Å X-ray crystallographic structure of P-30 protein, an amphibian ribonuclease with anti-tumor activity. *J. Mol. Biol.* **236**, 1141-1153.

Murthy, B. S., De Lorenzo, C., Piccoli, R., D'Alessio, G. & Sirdeshmukh, R. (1996). Effects of protein RNase inhibitor and substrate on the quaternary structures of bovine seminal RNase. *Biochemistry* **35**, 3880-3885.

Murthy, B. S. & Sirdeshmukh, R. (1992). Sensitivity of monomeric and dimeric forms of bovine seminal ribonuclease to human placental ribonuclease inhibitor. *Biochem. J.* **281**, 343-348.

Neumann, U. & Hofsteenge, J. (1994). Interaction of semisynthetic variants of RNase A with ribonuclase inhibitor. *Protein Sci.* **3**, 248-256.

Newton, D. L., Ilercil, O., Laske, D. W., Oldfield, E., Rybak, S. M. & Youle, R. J. (1992). Cytotoxic ribonuclease chimeras. Targeted tumoricidal activity *in vitro* and *in vivo*. *J. Biol. Chem.* **267**, 19572-19578.

Newton, D. L., Nicholls, P. J., Rybak, S. M. & Youle, R. J. (1994). Expression and characterization of recombinant human eosinophil-derived neurotoxin and eosinophil-derived neurotoxin-anti-transferrin receptor sFv. *J. Biol. Chem* **269**, 26739-26745.

Newton, D. L., Xue, Y., Boque, L., Wlodawer, A., Kung, H. F. & Rybak, S. M. (1997). Expression and characterization of a cytotoxic human-frog chimeric ribonuclease: potential for cancer therapy. *Protein Eng.* **10**, 463-470.

Newton, D. L., Xue, Y., Olson, K. A., Fett, J. W. & Rybak, S. M. (1996). Angiogenin single-chain immunofusions: influence of peptide linkers and spacers between fusion protein domains. *Biochemistry* **35**(2), 545-553.

Nitta, K., Oyama, F., Oyama, R., Sekiguchi, K., Kawauchi, H., Takayanagi, Y., Hakomori, S.-I. & Titani, K. (1993). Ribonuclease activity of sialic acid-binding lectin from *Rana catesbeiana* eggs. *Glycobiology* **3**, 37-45.

Nitta, K., Ozaki, K., Ishikawa, M., Furusawa, S., Hosono, M., Kawauchi, H., Sasaki, K., Takayanagi, Y., Tsuiki, S. & Hakomori, S. (1994). Inhibition of cell proliferation by *Rana catesbeiana* and *Rana japonica* lectins belonging to the ribonuclease superfamily. *Cancer Res.* **54**, 920-927.

Nitta, K., Takayanagi, G., Kawauchi, H. & Hakomori, S. (1987). Isolation and characterization of *Rana catesbeiana* lectin and demonstration of lectin-binding glycoprotein of rodent and human cell membranes. *Cancer Res.* **47**, 4877-4883.

Notomista, E., Cafaro, V., Fusiello, R., Bracale, A., D'Alessio, G. & Di Donato, A. (1999). Effective expression and purification of recombinant onconase, an antitumor protein. *FEBS Lett* **463**, 211-215.

Okabe, Y., Katayama, N., Iwama, M., Watanabe, H., Ohgi, K., Irie, M., Nitta, K., Kawauchi, H., Takayanagi, Y., Oyama, F., Titani, K., Abe, Y., Okazaki, T., Inokuchi, N. & Koyama, T. (1991). Comparative base specificity, stability, and lectin activity of two lectins from *Rana catesbeiana* and *R. japonica* and liver ribonuclease from *R. catesbeiana*. *J. Biochem.* **109**, 786-790.

Pace, C. N., Shirley, B. A. & Thomson, J. A. (1989). Measuring the conformational stability of a protein. In *Protein Structure* (Creighton, T. E., ed.), pp. 311-330. IRL Press, New York.

Pace, C. N., Vajdos, F., Fee, L., Grimsley, G. & Gray, T. (1995). How to measure and predict the molar absorption coefficient of a protein. *Protein Sci.* **4**, 2411-2423.

Papageorgiou, A., Shapiro, R. & Acharya, K. (1997). Molecular recognition of human angiogenin by placental ribonuclease inhibitor—an X-ray crystallographic study at 2.0 Å resolution. *EMBO J.* **16**, 5162-5177.

Park, C. & Raines, R. T. (2000a). Dissecting energetics of ribonuclease A catalysis by salt-rate profiles. *in preparation for Biochemistry*.

Park, C. & Raines, R. T. (2000b). Origin of the 'inactivation' of ribonuclease A at low salt concentration. *FEBS Lett.* **468**, 199-202.

Park, C., Kelemen, B. R., Raines, R. T. (2000). The role of active-site histidine residues in substrate binding by ribonuclease A. *in preparation for Biochemistry*.

Parsell, D. A. & Sauer, R. T. (1989). The structural stability of a protein is an important determinant of its proteolytic susceptibility in *Escherichia coli*. *J. Biol. Chem.* **264**, 7590-7595.

Pelham. H. R. B., Roberts, L. M. & Lord, J. M. (1992). Toxin entry: how reversible is the secretory pathway? *Trends Cell Biol.* **2**, 183-185.

Piccoli, R., Di Gaetano, S., De Lorenzo, C., Grauso, M., Monaco, C., Spalletti-Cernia, D., Laccetti, P., Cinátl, J., Matousek, J. & D'Alessio, G. (1999). A dimeric mutant of human pancreatic ribonuclease with selective cytotoxicity toward malignant cells. *Proc. Natl. Acad. Sci. U.S.A.* **96**, 7768-7773.

Polakowski, I. J., Lewis, M. K., Muthukkaruppan, V., Erdman, B., Kubai, L. & Auerbach, R. (1993). A ribonuclease inhibitor expresses anti-angiogenic properties and leads to reduced tumor growth in mice. *Am. J. Pathol.* **143**, 507-517.

Psarras, K., Ueda, M., Yamamura, T., Ozawa, S., Kitajima, M., Aiso, S., Komatsu, S. & Seno, M. (1998). Human pancreatic RNase1-human epidermal growth factor fusion: an entirely human 'immunotoxin analog' with cytotoxic properties against squamous cell carcinomas. *Protein Eng.* **11**, 1285-1292.

Quirk, D. J. & Raines, R. T. (1999). His ... Asp catalytic dyad of ribonuclease A: histidine pKa values in the wild-type, D121N, and D121A enzymes. *Biophys. J.* **76**, 1571-1579.

Radzicka, A. & Wolfenden, R. (1988). Comparing the polarities of the amino acids: side-chain distribution coefficients between the vapor phase, cyclohexane, 1-octanol, and neutral aqueous solution. *Biochemistry* **27**, 1664-1670.

Raines, R. T. (1998). Ribonuclease A. *Chem. Rev.* **98**, 1045-1065.

Raines, R. T. (1999). Ribonuclease A: from model system to cancer chemotherapeutic. In *Enzymatic Mechanisms* (Frey, P. A. & Northrop, D. B., eds.), pp. 235-249. IOS Press, Washington, DC.

Raines, R. T., Toscano, M. P., Nierengarten, D. M., Ha, J. H. & Auerbach, R. (1995). Replacing a surface loop endows ribonuclease A with angiogenic activity. *J. Biol. Chem.* **270**, 17180-17184.

Record, M. T., Jr., Lohman, T. M. & de Haseth, P. (1976). Ion effects on ligand – nucleic acid interactions. *J. Mol. Biol.* **107**, 145-158.

Ribó, M., Beintema, J. J., Osset, M., Fernández, E., Bravo, J., de Llorens, R. & Cuchillo, C. M. (1994). Heterogeneity in the glycosylation pattern of human pancreatic ribonuclease. *Biol. Chem. Hoppe-Seyler* **375**, 357-363.

Ribó, M., Fernández, E., Bravo, J., Osset, M., Fallon, M. J. M., de Llorens, R. & Cuchillo, C. M. (1991). Purification of human pancreatic ribonuclease by high performance liquid chromatography. In *Structure, Mechanism and Function of Ribonucleases* (de Llorens, R., Cuchillo, C. M., Nogués, M. V. & Parés, X., eds.), pp. 157-162. Universitat Autónoma de Barcelona, Bellaterra, Spain.

Riordan, J. F. (1997). Structure and function of angiogenin. In *Ribonucleases: Structures and Functions* (D'Alessio, G. & Riordan, J. F., eds.), pp. 445-489. Academic Press, New York.

Rosenberg, A. H., Goldman, E., Dunn, J. J., Studier, F. W. & Zubay, G. (1993). Effects of consecutive AGG codons on translation in *Escherichia coli*, demonstrated with a versatile codon test system. *J. Bacteriol.* **175**, 716-722.

Roth, J. S. (1962). Further studies on ribonuclease inhibitor. *Biochem. Biophys. Acta* **61**, 903-915.

Roth, J. S. (1967). Some observations on the assay and properties of ribonucleases in normal and tumor tissues. *Methods Cancer Res.* **3**, 153-242.

Russo, N., Acharya, K. R., Vallee, B. L. & Shapiro, R. (1996). A combined kinetic and modeling study of the catalytic center subsites of human angiogenin. *Proc. Natl. Acad. Sci. U.S.A.* **93**, 804-808.

Russo, N., Shapiro, R., Acharya, K. R., Riordan, J. F. & Vallee, B. L. (1994). Role of glutamine-117 in the ribonucleolytic activity of human angiogenin. *Proc. Natl. Acad. Sci. U.S.A.* **91**, 2920-2924.

Rybak, S. M. & Newton, D. L. (1999). Natural and engineered cytotoxic ribonucleases: therapeutic potential. *Exp. Cell Res.* **253**, 325-335.

Rybak, S. M., Pearson, J. W., Fogler, W. E., Volker, K., Spence, S. E., Newton, D. L., Mikulski, S. M., Ardelt, A., Riggs, C. W., Kung, H.-F. & Longo, D. L. (1996). Enhancement of vincristine cytotoxicity in drug-resistant cells by simultaneous treatment with onconase, an antitumor ribonuclease. *J. Natl. Cancer Inst.* **88**, 747-753.

Rybak, S. M., Saxena, S. K., Ackerman, E. J. & Youle, R. J. (1991). Cytotoxic potential of ribonuclease and ribonuclease hybrid proteins. *J. Biol. Chem.* **266**, 21202-21207.

Sakakibara, F., Kawauchi, H., Takayanagi, G. & Ise, H. (1979). Egg lectin of *Rana japonica* and its receptor glycoprotein of Ehrlich tumor cells. *Cancer Res.* **39**, 1347-1352.

Saxena, S. K., Gravell, M., Wu, Y.-N., Mikulski, S. M., Shogen, K., Ardelt, W. & Youle, R. J. (1996). Inhibition of HIV-1 production and selective degradation of viral RNA by an amphibian ribonuclease. *J. Biol. Chem.* **271**, 20783-20788.

Saxena, S. K., Rybak, S. M., Winkler, G., Meade, H. M., McGray, P., Youle, R. J. & Ackerman, E. J. (1991). Comparison of RNases and toxins upon injection into *Xenopus* oocytes. *J. Biol. Chem.* **266**, 21208-21214.

Sela, M., Anfinsen, C. B. & Harrington, W. F. (1957). The correlation of ribonuclease activity with specific aspects of tertiary structure. *Biochim. Biophys. Acta* **26**, 502-512.

Shapiro, R. (1998). Structural features that determine the enzymatic potency and specificity of human angiogenin: threonine-80 and residues 58-70 and 116-123. *Biochemistry* **37**, 6847-6856.

Shapiro, R., Fox, E. A. & Riordan, J. F. (1989). Role of lysines in human angiogenin: chemical modification and site-directed mutagenesis. *Biochemistry* **28**, 1726-1732.

Shapiro, R., Harper, J. W., Fox, E. A., Jansen, H.-W., Hein, F. & Uhlmann, E. (1988). Expression of Met(-1) angiogenin in *Escherichia coli*: conversion to the authentic <Glu-1 protein. *Anal. Biochem.* **175**, 450-461.

Shapiro, R., Strydom, D. J., Olson, K. A. & Vallee, B. L. (1987). Isolation of angiogenin from normal human plasma. *Biochemistry* **26**, 5141-5146.

Shapiro, R. & Vallee, B. L. (1989). Site-directed mutagenesis of histidine-13 and histidine-114 of human angiogenin. Alanine derivatives inhibit angiogenin-induced angiogenesis. *Biochemistry* **28**, 7401-7408.

Silver, P. A. (1991). How Proteins Enter the Nucleus. *Cell* **64**, 489-497.

Smith, M. R., Newton, D. L., Mikulski, S. M. & Rybak, S. M. (1999). Cell cycle-related differences in susceptibility of NIH/3T3 cells to ribonucleases. *Exp. Cell. Res.* **247**, 220-232.

Sorrentino, S. (1998). Human extracellular ribonucleases: multiplicity, molecular diversity and catalytic properties of the major RNase types. *Cell. Mol. Life Sci.* **54**, 785-794.

Sorrentino, S. & Libonati, M. (1994). Human pancreatic-type and nonpancreatic-type ribonucleases: A direct side-by-side comparison of their catalytic properties. *Arch. Biochem. Biophys.* **312**, 340-348.

Spanjaard, R. A. & van Duin, J. (1988). Translation of the sequence AGG-AGG yields 50% ribosomal frame shift. *Proc. Natl. Acad. Sci. U.S.A.* **85**, 7967-7971.

Stone, S. R. & Hofsteenge, J. (1986). Kinetics of the inhibition of thrombin by hirudin. *Biochemistry* **25**, 4622-4628.

Strydom, D. J., Fett, J. W., Lobb, R. R., Alderman, E. M., Bethune, J. L., Riordan, J. F. & Vallee, B. L. (1985). Amino acid sequence of human tumor derived angiogenin. *Biochemistry* **24**, 5486-5494.

Studier, F. W., Rosenberg, A. H., Dunn, J. J. & Dubendorff, J. W. (1990). Use of T7 RNA polymerase to direct expression of cloned genes. *Methods Enzymol.* **185**, 60-89.

Suwa, T., Ueda, M., Jinno, H., Ozawa, S., Kitagawa, Y., Ando, N. & Kitajima, M. (1999). Epidermal growth factor receptor-dependent cytotoxic effect of anti- EGFR antibody-ribonuclease conjugate on human cancer cells. *Anticancer Res.* **19**, 4161-4165.

Suzuki, H., Parente, A., Rarina, B., Greco, L., La Montagna, R. & Leone, E. (1987). Complete amino-acid sequence of bovine seminal ribonuclease, a dimeric protein from seminal plasma. *Biol. Chem. Hoppe-Seyler* **368**, 1305-1312.

Suzuki, M., Saxena, S. K., Boix, E., Prill, R. J., Vasandani, V. M., Ladner, J. E., Sung, C. & Youle, R. J. (1999). Engineering receptor-mediated cytotoxicity into human ribonucleases by steric blockade of inhibitor interaction. *Nature Biotechnol.* **17**, 265-270.

Thompson, J. E., Venegas, F. D. & Raines, R. T. (1994). Energetics of catalysis by ribonucleases: fate of the 2',3'-cyclic intermediate. *Biochemistry* **33**, 7408-7414.

Titani, K., Takio, K., Kuwada, M., Nitta, K., Sakakibara, F. & Kawauchi, H. (1987). Amino acid sequence of sialic acid binding lectin from frog (*Rana catesbeiana*). *Biochemistry* **26**, 2194-2198.

Trautwein, K., Holliger, P., Stackhouse, J. & Benner, S. A. (1991). Site-directed mutagenesis of bovine pancreatic ribonuclease: lysine-41 and aspartate-121. *FEBS Lett.* **281**, 275-277.

Vicentini, A. M., Kieffer, B., Mathies, R., Meyhack, B., Hemmings, B. A., Stone, S. R. & Hofsteenge, J. (1990). Protein chemical and kinetic characterization of recombinant porcine ribonuclease inhibitor expressed in *Saccharomyces cerevisiae*. *Biochemistry* **29**, 8827-8834.

Wada, K., Wada, Y., Doi, H., Ishibashi, F., Gojobori, T. & Ikemura, T. (1991). Codon usage tabulated from the GenBank genetic sequence data. *Nucleic Acids Res.* **19**, 1981-1986.

Witzel, H. (1963). The function of the pyrimidine base in the ribonuclease reaction. *Progr. Nucleic Acid Res.* **2**, 221-258.

Wlodawer, A., Anders, L. A., Sjölin, L. & Gilliland, G. L. (1988). Structure of phosphate-free ribonuclease A refined at 1.26 Å. *Biochemistry* **27**, 2705-2717.

Woody, R. W. (1995). Circular Dichroism. *Methods Enzymol.* **246**, 34-71.

Wu, Y., Mikulski, S. M., Ardelt, W., Rybak, S. M. & Youle, R. J. (1993). A cytotoxic ribonuclease. *J. Biol. Chem.* **268**, 10686-10693.

Wu, Y., Saxena, S. K., Ardelt, W., Gadina, M., Mikulski, S. M., De Lorenzo, V., D'Alessio, G. & Youle, R. J. (1995). A study of the intracellular routing of cytotoxic ribonucleases. *J. Biol. Chem.* **270**, 17476-17481.

Yoon, J. M., Kim, S. H., Kwon, O. B., Han, S. H. & Kim, B. K. (1999). High level expression of soluble angiogenin in *Escherichia coli*. *Biochem. Mol. Bio. Int.* **47**, 267-273.

Youle, R. J. & D'Alessio, G. (1997). Antitumor RNases. In *Ribonucleases: Structures and Functions* (D'Alessio, G. & Riordan, J. F., eds.), pp. 491-514. Academic Press, New York.

Youle, R. J., Newton, D., Wu, Y.-N., Gadina, M. & Rybak, S. M. (1993). Cytotoxic ribonucleases and chimeras in cancer therapy. *Crit. Rev. Therapeutic Drug Carrier Systems* **10**, 1-28.

Youle, R. J., Wu, Y.-N., Mikulski, S. M., Shogen, K., Hamilton, R. S., Newton, D., D'Alessio, G. & Gravell, M. (1994). RNase inhibition of human immunodeficiency virus infection of H9 cells. *Proc. Natl. Acad. Sci. U. S. A.* **91**, 6012-6016.

Zhang, W., Bond, J. P., Anderson, C. F., Lohman, T. M. & Record, M. T. (1996). Large electrostatic differences in the binding thermodynamics of a cationic protein to oligomeric and polymeric DNA. *Proc. Natl. Acad. Sci. U.S.A.* **93**, 2511-2516.